

Alma Mater Studiorum – Università di Bologna

DOTTORATO DI RICERCA IN  
MECCANICA E SCIENZE AVANZATE DELL'INGEGNERIA

Ciclo XXVIII

**Settore Concorsuale di afferenza:** 09/A1 Ingegneria Aeronautica, Aerospaziale e Navale

**Settore Scientifico disciplinare:** ING-IND/05 Impianti e Sistemi Aerospaziali

DESIGN AND IMPLEMENTATION OF SOFTWARE SOLUTIONS FOR  
SATELLITE GROUND SEGMENT,  
WITH APPLICATION TO THE ESEO MISSION

**Presentata da: Marco Bosco**

**Coordinatore Dottorato**

**Prof. Vincenzo Parenti Castelli**

**Relatore**

**Prof. Paolo Tortora**

**Esame finale anno 2016**

*Hope for the best,  
but prepare for the worst.*



## Sommario

Titolo: Progettazione e Sviluppo di Soluzioni Software per il Segmento di Terra di Satelliti, con Applicazione alla Missione ESEO.

Il successo di una missione spaziale dipende non solo dalla buona progettazione e realizzazione del segmento spaziale (piattaforma e payloads) e dalla riuscita del lancio. Infatti, il segmento di terra è fondamentale per poter operare il satellite e quindi portare a termine con successo la missione. Questo lavoro di tesi si concentra proprio sul segmento di terra ed in particolare sulla progettazione e lo sviluppo di soluzioni software necessarie per le varie funzionalità svolte dal segmento di terra.

La prima parte di questo lavoro, che è stata svolta nel primo, secondo e nella prima parte del terzo anno di dottorato, si concentra sul progetto ESEO (European Student Earth Orbiter), una missione microsattellitare sponsorizzata dall'Education Office dell'Agenzia Spaziale Europea (ESA). ESEO sarà lanciato nel 2017 in orbita bassa con lo scopo di scattare immagini della Terra, misurare livelli di radiazione e testare tecnologie spaziali per future missioni satellitari. Lo scopo educativo di questo progetto è quello di fornire agli studenti universitari la possibilità di lavorare in un vera missione satellitare, formandoli per la loro carriera nell'industria spaziale. Il laboratorio di Microsatelliti e Sistemi Spaziali dell'Università di Bologna è coinvolto in questo progetto per lo sviluppo del centro di controllo missione, della stazione di terra primaria per la ricezione dei dati di telemetria e l'invio dei comandi e del ricevitore GPS di bordo. L'oggetto di questo dottorato è stata la progettazione e lo sviluppo dei primi due elementi partendo dall'esperienza acquisita dal laboratorio durante le operazioni del microsattellite ALMASat-1 lanciato nel Febbraio 2012 a bordo del Vega maiden flight. Nel corso di questo lavoro, la stazione di terra è stata ampiamente rinnovata con l'introduzione di una software-defined radio (SDR) e lo sviluppo di nuovo software. Per il centro di controllo missione, si è sviluppato in LabVIEW un sistema di monitoraggio e controllo per ESEO connesso ad un database appositamente progettato in MySQL per la gestione dei dati di telemetria e dei comandi durante le operazioni del satellite. Inoltre è stata instaurata una rete di stazioni di terra che comprende le stazioni di Vigo e Monaco per poter operare al meglio la missione ESEO garantendo una ridondanza a terra per comunicare con il satellite. I requisiti e il design dettagliato del segmento di terra, la descrizione dell'interfaccia di comunicazione tra satellite e terra così

come la descrizione del database e delle procedure operazionali sono riportate nella documentazione tecnica che è stata preparata per la preliminary design review (PDR) e critical design review (CDR) del progetto ESEO superate rispettivamente nel Novembre 2013 e Luglio 2015.

Durante il terzo anno, da Maggio a Ottobre 2015, è stata svolto un tirocinio presso EUMETSAT (European Organisation for the Exploitation of Meteorological Satellites) durante il quale si sono sviluppate delle soluzioni software per le stazioni di terra utilizzate per operare satelliti meteorologici in orbita bassa, come Metop e NOAA, e in orbita geostazionaria, come la famiglia dei satelliti Meteosat. In particolare, tre diverse applicazioni sono state sviluppate, testate e rese operative. La prima attività ha riguardato l'integrazione di un sistema di generazione automatica di reports periodici contenenti grafici e tabelle che illustrano alcuni parametri selezionati delle stazioni di terra collocate a Svalbard ed utilizzate per inviare comandi e ricevere telemetria e dati scientifici dai satelliti Metop-A, Metop-B e NOAA-19. Questa applicazione si è rivelata particolarmente utile per gli ingegneri delle operazioni per individuare problemi relativi a queste stazioni. La seconda attività è consistita nello sviluppo di un'applicazione per il calcolo e la visualizzazione dei passaggi dei satelliti in orbita bassa al di sopra di una rete di stazioni di terra. Questa applicazione basata sulla propagazione delle TLE consente di aggiungere una maschera d'orizzonte per ogni antenna, calcolare e risolvere conflitti tra passaggi di più satelliti sulla stessa stazione e calcolare le orbite cieche dei satelliti NOAA per garantire il supporto dalle stazioni EUMETSAT di Svalbard quando possibile. Infine, l'ultima attività ha riguardato lo sviluppo di un simulatore del sistema di monitoraggio e controllo delle stazioni di terra che saranno utilizzate per il programma Meteosat Third Generation (MTG). Il simulatore riproduce tutte le funzionalità svolte dal sistema: autenticazione, richiesta dei parametri di telemetria, registrazione a eventi, richiesta della schedula, invio di comandi immediati e time-tagged.

# Table of Contents

|   |      |
|---|------|
| Sommario.....   | I    |
| List of Figures.....                                      | V    |
| List of Tables.....                                       | VIII |
| List of Acronyms.....                                     | IX   |
| 1. Introduction.....                                      | 1    |
| 1.1 Background and Motivation.....                        | 2    |
| 1.2 Thesis Outline.....                                   | 3    |
| 2. Ground Systems and Operations.....                     | 5    |
| 2.1 Ground segment engineering process.....               | 7    |
| 2.2 Differences with small spacecraft ground systems..... | 9    |
| 3. The European Student Earth Orbiter Project.....        | 11   |
| 3.1 Telecommunication System.....                         | 14   |
| 3.1.1 Space-to-Ground communication protocol.....         | 15   |
| 3.1.2 Link budget.....                                    | 18   |
| 3.2 Ground Segment.....                                   | 22   |
| 3.2.1 Forli Ground Station.....                           | 26   |
| 3.2.1.1 Satellite Tracking Software.....                  | 32   |
| 3.2.1.2 Software Defined Radio implementation.....        | 34   |
| 3.2.1.3 Compatibility Tests.....                          | 39   |
| 3.2.2 Spacecraft Monitoring and Control.....              | 41   |
| 3.2.2.1 Database definition.....                          | 45   |
| 3.2.2.2 Automatic procedures.....                         | 47   |
| 3.2.2.3 Telemetry Visualisation and Analysis Tool.....    | 48   |
| 3.2.2.4 Users' Requests.....                              | 49   |
| 3.2.3 Spacecraft Simulator.....                           | 50   |
| 3.2.4 Code review.....                                    | 51   |
| 4. EUMETSAT Ground Station Software Solutions.....        | 53   |
| 4.1 Ground Station Analysis and Reporting Tool.....       | 54   |
| 4.1.1 Motivations and Background.....                     | 54   |
| 4.1.2 Reports generation.....                             | 56   |
| 4.1.3 Database definition.....                            | 57   |
| 4.1.4 Reports content.....                                | 57   |
| 4.1.5 Repeat cycle analysis.....                          | 61   |
| 4.1.6 Code verification and results validation.....       | 63   |
| 4.2 Satellite Passes And Conflicts Engine.....            | 64   |

|         |  |     |
|---------|--|-----|
| 4.2.1   | Applications .....                             | 64  |
| 4.2.2   | Graphical User Interface .....                 | 67  |
| 4.2.2.1 | Error handling .....                           | 70  |
| 4.2.3   | Results .....                                  | 71  |
| 4.2.4   | Validation .....                               | 75  |
| 4.3     | Ground Station Centralised M&C Simulator ..... | 78  |
| 4.3.1   | Data Flows .....                               | 78  |
| 4.3.2   | Device Simulator .....                         | 80  |
| 4.3.3   | Simulator .....                                | 82  |
| 4.3.4   | Testing .....                                  | 86  |
| 5.      | Conclusions .....                              | 90  |
|         | Appendix A .....                               | 92  |
|         | Appendix B .....                               | 94  |
|         | Appendix C .....                               | 95  |
|         | Appendix D .....                               | 97  |
|         | Appendix E .....                               | 99  |
|         | Bibliography .....                             | 100 |
|         | Acknowledgments .....                          | 103 |

## List of Figures

|  |    |
|--|----|
| Figure 1. Schematic of typical space system, with the emphasis on software elements [1]                                  | 1  |
| Figure 2. Ground segment systems [4]   | 5  |
| Figure 3. Generic ground segment example [3]   | 7  |
| Figure 4. ESEO University Network and roles  | 11 |
| Figure 5. ESEO maximum revisit time (in days) for the observed points  | 13 |
| Figure 6. ESEO platform  | 13 |
| Figure 7. Bit operations and frame detection (downlink)  | 17 |
| Figure 8. RSSI (dBm) average interference world plot between 6/8/2014 and 11/8/2014                                      | 18 |
| Figure 9. Theoretical Noncoherent BFSK BER curve   | 20 |
| Figure 10. Detail of the visibility circles of Forlì, Munich and Vigo stations (5°, 10°, 15° and 20° minimum elevations) | 23 |
| Figure 11. ESEO Ground Segment   | 24 |
| Figure 12. ESEO Ground Segment detailed block diagram  | 26 |
| Figure 13. Forlì Ground Station configuration for ALMASat-1 mission  | 27 |
| Figure 14. ALMASat-1 Ground Station  | 27 |
| Figure 15. Septum dish feed mounted on a 3m parabolic dish by RF Hamdesign   | 27 |
| Figure 16. VSWR plot for the RX port of the septum dish feed by RF Hamdesign   | 27 |
| Figure 17. S-band parabolic dish antenna and VHF/UHF Yagi antenna  | 28 |
| Figure 18. Mission control room  | 28 |
| Figure 19. USRP N210 by Ettus Research   | 29 |
| Figure 20. SBX daughterboard by Ettus Research   | 29 |
| Figure 21. USRP block diagram  | 30 |
| Figure 22. VHF/UHF ground station  | 31 |
| Figure 23. S-band ground station   | 32 |
| Figure 24. Computation of azimuth and elevation from ground station to satellite   | 33 |
| Figure 25. Gpredict satellite tracking software  | 33 |
| Figure 26. LabVIEW block diagram of the signal acquisition loop of the SDR software                                      | 34 |
| Figure 27. SDR software GUI  | 35 |
| Figure 28. GFSK signal time plot   | 36 |
| Figure 29. GFSK signal waterfall plot  | 36 |
| Figure 30. Non-coherent BFSK signal  | 37 |
| Figure 31. GFSK signal spectrum  | 40 |
| Figure 32. SDR Test setup  | 40 |
| Figure 33. SDR software for testing purposes   | 41 |
| Figure 34. Spacecraft Monitoring and Control GUI   | 42 |
| Figure 35. AOCS Telemetry display  | 44 |
| Figure 36. AOCS Telecommands display   | 44 |
| Figure 37. Uplink chain flowchart  | 45 |
| Figure 38. Downlink chain flowchart  | 45 |
| Figure 39. Telemetry Visualisation and Analysis Tool   | 48 |
| Figure 40. TM Scrollable display and statistical analysis  | 48 |

|   |    |
|---|----|
| Figure 41. TM Graphical display .....   | 48 |
| Figure 42. Lifecycle for each individual payload request at MCC .....   | 50 |
| Figure 43. S/C simulator block diagram .....  | 51 |
| Figure 44. Software Engineering Process .....   | 52 |
| Figure 45. The Metop satellites are operated via two CDAs collocated in Svalbard, Norway and linked to the operational ground segment in Darmstadt via fibre-optic and satellite communications links ..... | 53 |
| Figure 46. TMPropagator client, CDA1 mimic display .....  | 55 |
| Figure 47. GSAR reports web calendar interface .....  | 56 |
| Figure 48. Reports generation flowchart .....   | 56 |
| Figure 49. CDA tracked passes counter .....   | 57 |
| Figure 50. CDA2 Antenna Azimuth, 21/10/2015 .....   | 58 |
| Figure 51. CDA2 Antenna Elevation, 21/10/2015 .....   | 58 |
| Figure 52. CDA2 Antenna Tilt, 21/10/2015 .....  | 58 |
| Figure 53. CDA2 Antenna Tilt movements, 21/10/2015 .....  | 58 |
| Figure 54. CDA2 devices status, 21/10/2015 .....  | 59 |
| Figure 55. CDA2 ACU status, 21/10/2015 .....  | 59 |
| Figure 56. CDA2 tracked passes with FD information (S/C, orbit, AOS time) and TM data (BTSE, corrected, uncorrected and received frames), 21/10/2015 .....  | 60 |
| Figure 57. CDA2 TM data during M02 pass, orbit 46725 .....  | 60 |
| Figure 58. CDA high level block diagram .....   | 61 |
| Figure 59. Metop-A S-band $E_bN_0$ repeat cycle comparison .....  | 63 |
| Figure 60. <i>TMPropagator</i> GRD, CDA tracking receiver levels .....  | 64 |
| Figure 61. GSAR, CDA tracking receiver levels .....   | 64 |
| Figure 62. Antarctic Data Acquisition service. © EUMETSAT .....   | 65 |
| Figure 63. Fairbanks horizon mask .....   | 66 |
| Figure 64. Wallops horizon mask .....   | 66 |
| Figure 65. Svalbard CDAs nominal pass planning .....  | 67 |
| Figure 66. SPACE graphical user interface .....   | 68 |
| Figure 67. Satellite pass events .....  | 70 |
| Figure 68. Visibility passes list .....   | 71 |
| Figure 69. Visibility passes summary .....  | 71 |
| Figure 70. Satellites passes duration over CDA1 during one day .....  | 72 |
| Figure 71. Satellites passes maximum elevation over CDA1 during one day .....   | 72 |
| Figure 72. Satellites passes conflicts table .....  | 73 |
| Figure 73. One-day conflict-free schedule for Metop-A, Metop-B, NOAA19 over Fairbanks, McMurdo and Svalbard .....   | 73 |
| Figure 74. Conflict-free passes percentage over Fairbanks for Metop-A, Metop-B and NOAA19 .....   | 74 |
| Figure 75. Pass details: Metop-A over CDA1, orbit 45500, sampling time 30 seconds ..  | 74 |
| Figure 76. Predicted azimuth and elevation on a time axis .....   | 75 |
| Figure 77. Predicted azimuth and elevation on a polar plot .....  | 75 |
| Figure 78. Doppler corrected downlink frequency for Metop-A pass over CDA1, orbit 45500 .....   | 75 |

|   |    |
|---|----|
| Figure 79. HL and LL M&C connection .....                           | 79 |
| Figure 80. Kinds of data streams exchanged over the interface ..... | 80 |
| Figure 81. Definition of a device mechanism .....                   | 82 |
| Figure 82. Device Simulator Editor .....                            | 84 |
| Figure 83. Device Simulator Runtime Configuration window .....      | 87 |
| Figure 84. Device Simulator Status window .....                     | 88 |
| Figure 85. Telemetry points messages table .....                    | 88 |
| Figure 86. Events messages history .....                            | 89 |
| Figure 87. Time-tagged commands inserted in the schedule.....       | 89 |
| Figure 88. Acknowledgement messages history.....                    | 89 |

## List of Tables

|   |    |
|---|----|
| Table 1. Ground segment phases .....  | 7  |
| Table 2. Technical documentation required for ground segment and operations.....  | 8  |
| Table 3. Fundamental differences between a small spacecraft ground system and classical ground systems for large spacecraft [5] ..... | 10 |
| Table 4. ESEO orbital parameters .....  | 12 |
| Table 5. U frame structure .....  | 15 |
| Table 6. S frame structure.....   | 15 |
| Table 7. I frame structure.....   | 16 |
| Table 8. UHF downlink budget at 9.6 kbps .....  | 20 |
| Table 9. UHF uplink budget at 9.6 kbps .....  | 21 |
| Table 10. Statistics of contact durations with the stations (5° minimum elevation).....   | 23 |
| Table 11. ICOM IC-910H frequency coverage in Italy .....  | 28 |
| Table 12. VHF/UHF ground station components .....   | 31 |
| Table 13. S-band ground station components.....   | 32 |
| Table 14. Different values of the SDR fetch size, time and rate .....   | 37 |
| Table 15. SDR settings for bit rate equal to 9.6 kbps .....   | 38 |
| Table 16. SDR settings for bit rate equal to 4.8 kbps. ....   | 38 |
| Table 17. Packet Error Rate for different Signal-to-Noise Ratio values in downlink testing .....                                      | 41 |
| Table 18. ESEO equipment/payloads .....   | 46 |
| Table 19. CDA's devices status .....  | 59 |
| Table 20. Metop and NOAA satellites frequencies .....   | 61 |
| Table 21. Metop repeat cycle values.....  | 62 |
| Table 22. IJPS satellites .....   | 65 |
| Table 23. Ground Stations location .....  | 65 |
| Table 24. TLE set format definition .....   | 69 |
| Table 25. Errors between results given by <i>pyephem</i> and EUMETSAT FD team.....  | 76 |
| Table 26. Errors between results given by <i>pyorbital</i> and EUMETSAT FD team. ....   | 76 |
| Table 27. Exchanged messages between HL and LL M&C .....  | 83 |
| Table 28. Simulator periodic macros .....   | 85 |
| Table 29. Simulator packet-triggered macros.....  | 86 |

## List of Acronyms

|                            |   |
|----------------------------|---|
| <b>ACU</b>                 | Antenna Control Unit  |
| <b>AIT</b>                 | Assembly Integration Test   |
| <b>AITV</b>                | Assembly Integration Test Verification                                  |
| <b>AMGS</b>                | Alma Mater Ground Station   |
| <b>AND</b>                 | Alpha Numeric Display   |
| <b>AOS</b>                 | Acquisition of Signal   |
| <b>BER</b>                 | Bit Error Rate  |
| <b>BTSE</b>                | Back To Search Event  |
| <b>CCSDS</b>               | Consultative Committee for Space Data Standardisation                   |
| <b>CDA</b>                 | Command and Data Acquisition  |
| <b>CDR</b>                 | Critical Design Review  |
| <b>CRC</b>                 | Cyclic Redundancy Check   |
| <b>CSV</b>                 | Comma Separated Values  |
| <b>DB</b>                  | Database  |
| <b>DOM</b>                 | Document Object Model   |
| <b>DS</b>                  | Device Simulator  |
| <b><math>E_bN_0</math></b> | Energy per bit to Noise power spectral density ratio                    |
| <b>ECSS</b>                | European Cooperation for Space Standardisation                          |
| <b>EGSE</b>                | Electrical Ground System Equipment                                      |
| <b>EPS</b>                 | Eumetsat Polar System   |
| <b>ESA</b>                 | European Space Agency   |
| <b>ESEO</b>                | European Student Earth Orbiter  |
| <b>EUMETSAT</b>            | European Organisation for the Exploitation of Meteorological Satellites |
| <b>FD</b>                  | Flight Dynamics   |
| <b>FDS</b>                 | Flight Dynamics System  |
| <b>FFT</b>                 | Fast Fourier Transform  |
| <b>FOS</b>                 | Flight Operations System  |
| <b>FRT</b>                 | First Receive Time  |
| <b>FSK</b>                 | Frequency Shift Keying  |
| <b>GEO</b>                 | Geostationary Earth Orbit   |
| <b>GRD</b>                 | Graphical Display   |
| <b>GS</b>                  | Ground Segment  |
| <b>GSN</b>                 | Ground Stations Network   |
| <b>HDRFEP</b>              | High Rate Demodulator and Front End Processor                           |
| <b>HK</b>                  | HouseKeeping  |
| <b>HPC</b>                 | High Priority Command   |
| <b>HTML</b>                | Hyper Text Markup Language  |
| <b>ICD</b>                 | Interface Control Document  |
| <b>IJPS</b>                | Initial Joint Polar System  |
| <b>LEO</b>                 | Low Earth Orbit   |

|                 |   |
|-----------------|---|
| <b>LEOP</b>     | Launch and Early Orbit Phase                    |
| <b>LOS</b>      | Loss of Signal                                  |
| <b>LRT</b>      | Last Receive Time                               |
| <b>M01</b>      | Metop-B   |
| <b>M02</b>      | Metop-A   |
| <b>MCC</b>      | Mission Control Centre                          |
| <b>MCS</b>      | Mission Control System                          |
| <b>M&amp;C</b>  | Monitoring & Control                            |
| <b>MTG</b>      | Meteosat Third Generation                       |
| <b>N18</b>      | NOAA 18   |
| <b>N19</b>      | NOAA 19   |
| <b>NOAA</b>     | National Oceanic and Atmospheric Administration |
| <b>NORAD</b>    | North American Aerospace Defence Command        |
| <b>OBDH</b>     | On Board Data Handling                          |
| <b>ORR</b>      | Operational Readiness Review                    |
| <b>PDR</b>      | Preliminary Design Review                       |
| <b>PMCS</b>     | Polar Monitoring and Control System             |
| <b>RF</b>       | Radio Frequency                                 |
| <b>RR</b>       | Requirements Review                             |
| <b>S/C</b>      | Spacecraft                                      |
| <b>SNR</b>      | Signal-to-Noise Ratio                           |
| <b>SS</b>       | Space Segment                                   |
| <b>STFT</b>     | Short-Time Fourier Transform                    |
| <b>TC</b>       | Telecommand                                     |
| <b>TLE</b>      | Two Line Elements                               |
| <b>TM</b>       | Telemetry                                       |
| <b>TMTC</b>     | Telemetry and Telecommand                       |
| <b>TT&amp;C</b> | Telemetry, Tracking and Command                 |
| <b>UDP</b>      | User Datagram Protocol                          |
| <b>USRP</b>     | Universal Software Radio Peripheral             |
| <b>UTC</b>      | Coordinated Universal Time                      |
| <b>VI</b>       | Virtual Instrument                              |
| <b>VSWR</b>     | Voltage Standing Wave Ratio                     |
| <b>XML</b>      | eXtensive Markup Language                       |
| <b>XSD</b>      | XML Schema Definition                           |
| <b>XSL</b>      | eXtensive Stylesheet Language                   |

# 1. Introduction

A space system is composed of three segments: space, ground and launch. The space segment comprises of spacecraft and payloads whilst the ground segment comprises of all of the ground facilities needed to operate the mission. Software is pervasive throughout the whole ‘product tree’ of any space mission: Figure 1 shows a typical space system schematically, with emphasis on the software elements. The space segment has on-board computers, data-handling systems, attitude and orbit control systems, all of which contain software. The ground segment has mission control systems, simulators, flight-dynamics systems, mission-analysis tools, communications networks and ground-station data systems such as telemetry and telecommand processors, as well as ‘downstream processing’ systems for payload data. These all contain software, often of considerable complexity. Developing and maintaining this software in a disciplined way is a key to the success of any space mission [1].

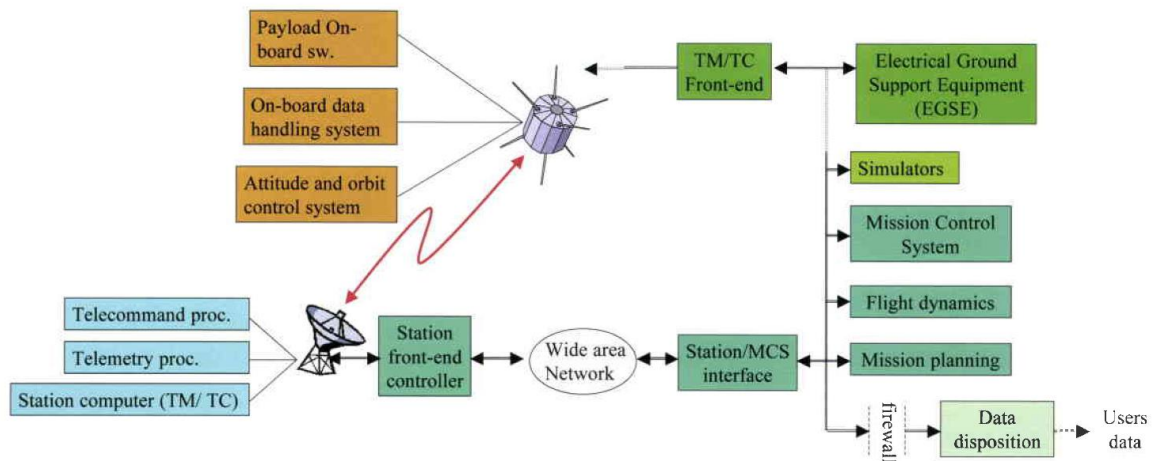


Figure 1. Schematic of typical space system, with the emphasis on software elements [1]

This thesis presents the software solutions designed and implemented for the ground segment of a microsatellite mission named ESEO and for the ground stations of EUMETSAT, the European Organisation for the Exploitation of Meteorological Satellites. The implemented solutions cover almost all the functionalities required to operate successfully a satellite mission:

- Signal acquisition/transmission, signal demodulation/modulation, frame detection in a software-defined radio (SDR) environment.

- Satellite monitoring and control: telecommand packing and encoding, telemetry unpacking and calibration, command stack, automatic procedures, telemetry limit processing and display.
- Telemetry and telecommand archiving.
- Satellite tracking based on two line elements TLE.
- Satellite simulator and TMTC front-end.
- Ground station performance analysis and reporting
- Computation of satellite passes over a ground station network and conflict-free schedule generation.
- Ground station monitoring and control.

## **1.1 Background and Motivation**

In December 2013, ALMASpace S.r.l., a former spin-off of the Microsatellite and Space Systems Lab (now merged into the SITAEEL company), was awarded a contract relative to the invitation to tender (ITT) from the European Space Agency (ESA) for the phases C0/C1/D/E1 of the European Student Earth Orbiter (ESEO) project. Whilst ALMASpace is the prime contractor, the University of Bologna is a subcontractor, responsible for the on-board GPS receiver, the primary TMTC ground station, the mission control centre and the organisation of lectures and internships for the students of the ESEO University network. Regarding the ground segment and operations, the contract signed between ESTEC and ALMASpace S.r.l. list the following main requirements [2]:

- The ESEO ground segment architecture shall consist of a Mission Control Centre in order to perform telemetry, telecommand and control functions, and one or more Ground Stations located in Europe in order to perform TMTC radio communications with the ESEO satellite.
- The ESEO ground segment shall allow payload operators access to their payload data via internet.
- The ESEO ground segment shall allow payload operators to submit request for their payload operations and associated telecommands via internet to the Mission Control Centre for processing.
- The ESEO ground station(s) shall communicate with the ESEO satellite over VHF (30-300 MHz), UHF (300-1000 MHz), or S-band (2-4 GHz) in either radio amateur

or regulated bands. Frequency shall be allocated by IARU (in case of radio amateur bands) or ITU (in case of regulated bands).

- The ESEO ground segment and satellite shall be operated by students to the maximum extent possible, and mission operations shall be supported by the System Prime Contractor staff.

This was the motivation for the major part of the work done during the PhD course and described in this thesis. Moreover, we wanted to improve the theoretical and practical knowledge at our lab about the ground segment and operations for satellite missions. A first experience of the design of a ground station and performance of operations was gained during the ALMASat-1 mission launched in 2012 on-board the Vega Maiden Flight.

## 1.2 Thesis Outline

The thesis is organised as follows:

**Chapter 2. Ground Systems and Operations.** This section explains which are the components of the ground segment and what is needed to successfully operate a satellite mission. We also list the main differences between the ground segment for large and small satellites.

**Chapter 3. European Student Earth Orbiter Project.** The design and the development of the ground segment for this microsatellite mission is widely discussed in this section. After a first description of the ESEO project with particular attention to the telecommunication system, the main topics of this chapter are the Forlì ground station and the ESEO Monitoring and Control system.

**Chapter 4. EUMETSAT Ground Station Software Solutions.** During an internship at EUMETSAT, some innovative software solutions have been implemented to improve ground stations operations. This section describes three software applications: the ground station analysis and reporting tool, the satellite passes and conflicts engine and the ground station centralised M&C simulator.

**Chapter 5. Conclusion.** In this final chapter, we draw the conclusion from the work done during the PhD course and we provide recommendations for future work.

## 2. Ground Systems and Operations

The success of a space mission depends not only on a properly designed and built space segment (SS) and the successful launch via a launch segment. It also depends on the ground segment (GS) and successful mission operations, carried out by a team of experts using the infrastructure and processes of the mission's GS. Its organization and design as well as the assembly, integration, test, and verification (AITV) are therefore equally important as the respective activities of the space and launch segment. A GS thereby comprises a ground system, i.e., infrastructure, hardware, software, and processes, and a team that conducts the necessary operations on the space segment [3].

The Mission success is defined as the achievement of the target mission objectives as expressed in terms of the quantity, quality and availability of delivered mission products and services (e.g. communication services, science data and space samples) within a given cost envelope.

The ground systems, as shown in Figure 2, usually consists of the following main elements:

- Mission control system (MCS)
- Electrical ground support equipment (EGSE)
- Ground station system (GSTS)
- Ground communication subnet (GCS)

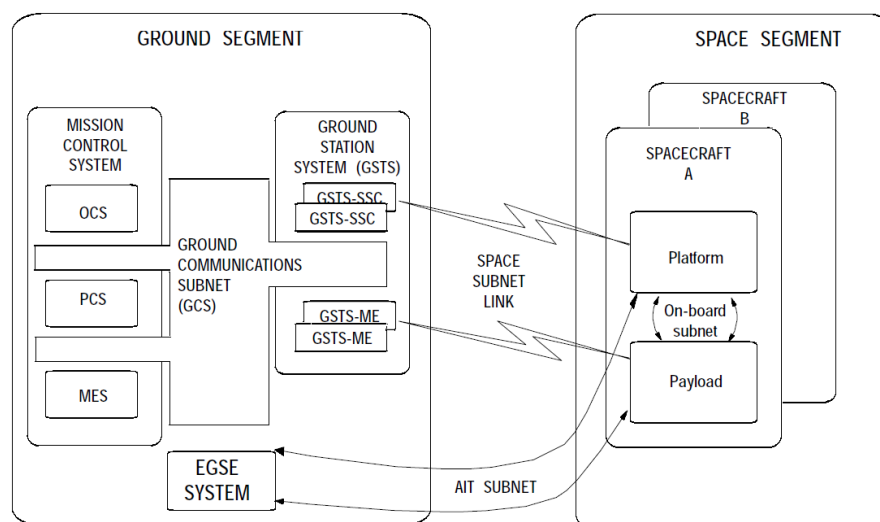


Figure 2. Ground segment systems [4]

The MCS shall comprise all the elements required to control the mission and to exploit its products. It is composed of the following elements:

- Operations control system (OCS), mainly supporting planning, monitoring and control, and performance evaluation of the platform elements of the space segment (SS). It also includes the flight dynamics support element, which may be considered as a system in its own right, named flight dynamics system (FDS)
- Payload control system (PCS), providing the same functions as the OCS but dedicated to the control of the payload elements of the SS.
- Mission exploitation system (MES), supporting the users of the mission products in establishing high-level production plan and in providing them with mission products and with all data required for their planning and utilization.

Depending on the type of the mission, often OCS and PCS are grouped in the same system. The EGSE system shall be part of the overall ground support equipment (GSE), supporting the verification of the SS during assembly, integration and test (AIT).

The GSTS shall constitute the direct interface with the SS while in-orbit and with the MCS. It provides support functions for controlling the SS elements and exploiting the mission products. It consists of the following instances:

- GSTS-SSC: for the ground station system in support of SS control (i.e. providing telemetry, telecommand and tracking services) for both the platform and the payload.
- GSTS-ME: for the ground station system in support of mission exploitation; e.g. for transmission and reception of payload service data such as telecommunications signal, Earth images, science data.

The GCS shall connect all operational ground facilities. The GCS constitutes the ground part of the end-to-end data path.

A generic example of a GS, its subsystems, and the data flows between them is shown in Figure 3. It comprises a GSN of three ground stations and a MCC. The main systems of the MCC are the Ground Data System (GDS), the Flight Dynamics System (FDS), and the Flight Operations System (FOS).

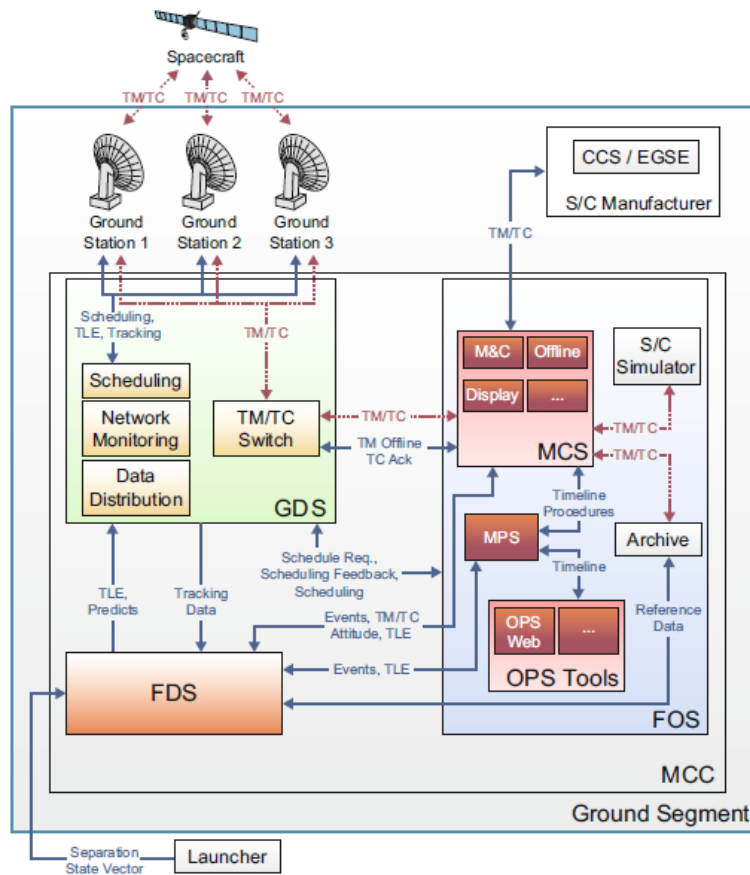


Figure 3. Generic ground segment example [3]

## 2.1 Ground segment engineering process

The ground engineering processes are partitioned in phases and each phase ends with a formal review, as shown in Table 1.

Table 1. Ground segment phases

| Phase            | O/A                              | B                     | C                  | D                            | E                    | F        |
|------------------|----------------------------------|-----------------------|--------------------|------------------------------|----------------------|----------|
| <b>Objective</b> | Mission analysis and feasibility | GS preliminary design | GS detailed design | GS production and validation | Operations execution | Disposal |
| <b>Reviews</b>   | RR                               | PDR                   | CDR                | ORR                          | IOQR, IOOR           | MCOR     |
| <b>Focus</b>     | System definition                |                       | GS implementation  |                              | Operations           |          |

During the project, it is requested to prepare some technical documentation describing the architecture of the ground segment, requirements, the communication interface with the S/C and the operations (Table 2).

**Table 2. Technical documentation required for ground segment and operations**

| Title  | Purpose   | Content  |
|--|---|--|
| Ground Segment & Operations Requirements Document  | To specify the requirements for the ground segment and mission operations in terms of functionality, performance, detailed interface requirements and verification requirements | Ground segment & operations requirements in terms of: <ul style="list-style-type: none"> <li>• Functional requirements</li> <li>• performance requirements</li> <li>• operations and logistic support</li> <li>• internal and external interfaces</li> <li>• re-use of generic infrastructure elements (e.g. software systems, ground station equipment)</li> <li>• maintainability of hardware and software</li> <li>• location of main facilities failure case operations and recovery</li> <li>• system and network management</li> <li>• configuration management</li> </ul> |
| Ground Segment Design Definition File              | To describe the characteristics of the detailed design of the ground segment throughout the project   | The document shall contain a description of the detailed design including: <ul style="list-style-type: none"> <li>• Product and Function Trees</li> <li>• Hardware and software description and performance</li> <li>• Schematics</li> <li>• Ground segment architecture diagrams</li> <li>• Software architecture diagrams</li> <li>• Electrical and data interfaces between the ground segment elements</li> <li>• On-board software verification facility</li> </ul>  |
| Space-to-ground Interface Control Document (SGICD) | To define the interfaces between the satellite and the ground segment, including all ground stations  | The main interfaces to be addressed are at the level of command and control, Mission data and telecommunications aspects for which format, content and RF transmission need to be described. Satellite to Ground Segment I/F definition, including: <ul style="list-style-type: none"> <li>• system overview</li> <li>• satellite and orbit, range definition</li> <li>• data formats and rates, coding scheme and modulation</li> <li>• encryption, authentication</li> <li>• reference profile assumptions</li> <li>• telecommunications:</li> </ul>                           |

|                                     |  |  |
|-------------------------------------|--|--|
|                                     |  | <ul style="list-style-type: none"> <li>○ frequencies</li> <li>○ link budgets, indicating worst case link margins expressed in dB for meeting the bit error rate requirements expressed in the SRD</li> <li>● data formats</li> <li>● TM/TC formats</li> <li>● ground station front-end interfaces</li> <li>● ranging interfaces</li> <li>● database interface</li> <li>● satellite to Ground Segment verification (including RF suitcase)</li> </ul> |
| Satellite Operations Handbook (SOH) | To define in full detail, the on-orbit operation and control procedures of the satellite, for its subsystems, units. | <p>The document shall include:</p> <ul style="list-style-type: none"> <li>● all satellite operations procedures (including order of commands)</li> <li>● all ground test procedures</li> <li>● all default on board data table parameters settings</li> <li>● complete telecommand &amp; telemetry lists for the satellite operation</li> <li>● satellite database description</li> </ul>  |

## 2.2 Differences with small spacecraft ground systems

The ground systems architecture for small spacecraft missions often takes a different form compared to the classical architectures used for large spacecraft missions. Low-cost constraints and the accessibility to COTS technology for the space sector have not only changed how designers think about a spacecraft but also how a ground systems architecture can be conceived. An overview of such potential differences highlights the extent to which microsatellite ground systems can differ from their classical counterparts [5].

**Table 3. Fundamental differences between a small spacecraft ground system and classical ground systems for large spacecraft [5]**

| <b>Classical Ground System</b>  | <b>Microsatellite Ground System</b>  |
|---|--|
| Legacy systems  | New systems  |
| High-cost, high complexity  | Low-cost (COTS), low complexity  |
| Clear distinction between mission control and ground station network  | Standalone system: MCC, SOCC, POCC and principal ground station are often aggregated into a single entity  |
| Supports a small to moderate number of different missions in parallel. Different types of antennas and hardware enable capability of communicating with more than one spacecraft simultaneously | Capability to support a large number of missions sequentially. Only one antenna, therefore no capability to communicate with more than one spacecraft simultaneously |
| Supports missions with long lifetimes   | Supports missions with short lifetimes   |
| Provides high quality of service (security, reliability, etc.)  | Does not guarantee high quality of service   |
| Commercial or institutional operators   | Typically academic or amateur operators  |
| Hierarchical topology with a small number of nodes distributed strategically around the globe   | Peer-to-peer topology with typically a large number of ad-hoc nodes participating on a voluntary basis   |
| No flexibility in the use of the topology's individual nodes  | Many missions use nearly the same frequency bands, so individual nodes in the topology may be exchangeable   |
| S-band and higher frequencies   | Typically UHF and VHF  |
| CCSDS based long-haul communication protocols   | TCP/IP based communication protocols   |
| Big dishes  | Small dishes or no dish at all (Ham-type antennas)   |
| Support high power (> 40W) spacecraft   | Support low power (< 5W) spacecraft  |
| Large bandwidth, data rate and throughput   | Small bandwidth, data rate and throughput  |
| Large software requirements   | Small software requirements  |
| Large number of facilities and personnel with much expertise  | Small number of facilities and personnel with usually less expertise   |

### 3. The European Student Earth Orbiter Project

The European Student Earth Orbiter (ESEO) is a micro-satellite mission to Low Earth Orbit (LEO). It is being developed, integrated, and tested by European university students as an ESA Education Office project.

ESEO will orbit the Earth taking pictures, measuring radiation levels and testing technologies for future education satellite missions.

It is aimed at providing students with unparalleled hands-on experience to help preparing a well-qualified space-engineering workforce for Europe's future. For this purpose, the University of Bologna, coordinating a network of the European universities joining the ESEO project (Figure 4), organised university lecture courses and internship opportunities for 60 students out of about 200 students involved in the ESEO project. For the first time, academic credits (18 ECTS) are granted to students for their participation in hands-on projects of ESA's Education Office [6].



Figure 4. ESEO University Network and roles

In particular, ESEO has the following mission objectives:

- To take pictures of the Earth and/or other celestial bodies from Earth orbit for educational outreach purposes.
- To provide dosimetry and space plasma measurement in Earth orbit and its effects on satellite components.
- To test technologies for future education satellite missions.

The first one will be achieved by the use of a micro camera (uCAM) operating in the visible spectrum.

To fulfil the second objective two instruments will be operated on-board:

- Plasma diagnostic probe (LMP).
- Tri-dimensional dosimeter instrument (TRITEL).

In particular, the LMP shall measure:

- Electron density.
- Electron temperature.

While the TRITEL shall measure

- LET spectra;
- Absorbed dose.
- Dose equivalent.

In order to provide high-speed datalink for payload data transmission a dedicated S-band transmitter (HSTX) will be provided as payload complement.

The realization of third objective will consist in the flight test of GPS receiver for orbit determination and a de-orbit mechanisms (DOM) to be activated in order to comply with space debris mitigation policies.

Functional and performance tests will be performed during the satellite operative phase and the results examined on ground by the design team, in order to gain a full space qualification in view of their use on other educational missions.

The satellite will also carry on board a payload proposed by the AMSAT community; it will allow the satellite to be exploited by the radio-amateur community after the end of its operative phase. The satellite measures 33x33x63 cm and it will weight around 50 Kg.

The target orbit for ESEO mission is a circular Sun-Synchronous Orbit (SSO) 10:30 LTAN. The orbital parameters are reported in Table 4 [7].

**Table 4. ESEO orbital parameters**

| <b>Orbital Parameters</b> | <b>Mean System of Date</b> |
|---------------------------|----------------------------|
| Semi-major axis           | 6904.82699 km              |
| Eccentricity              | 0.00134790                 |
| Inclination               | 97.47884°                  |
| Ascending Node            | 137.34203°                 |

|                     |            |
|---------------------|------------|
| Argument of Perigee | 67.74183°  |
| True Anomaly        | 292.25995° |

The identified orbit produces a cycle of 106 orbits in a week, about 15 orbit per day, in order to complete the coverage of the selected areas of interest (Europe and South Atlantic Anomaly). The definition of the areas of interest was driven by the optical payload and the scientific instruments requirements [7].

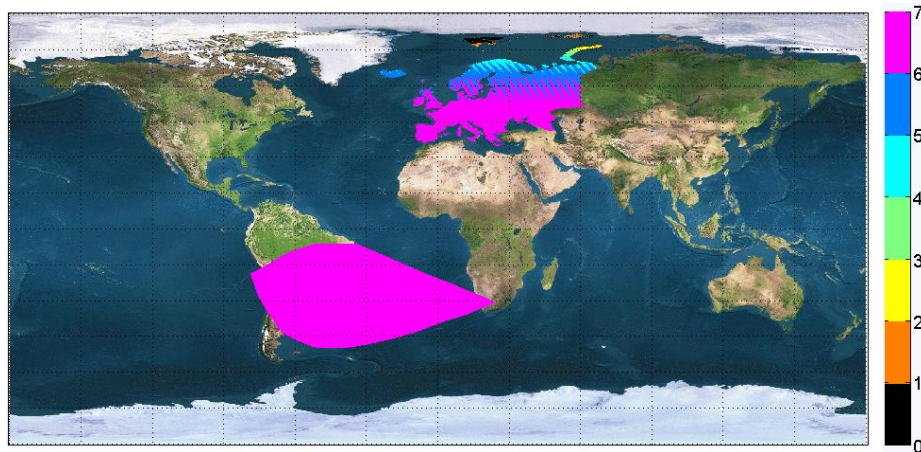


Figure 5. ESEO maximum revisit time (in days) for the observed points

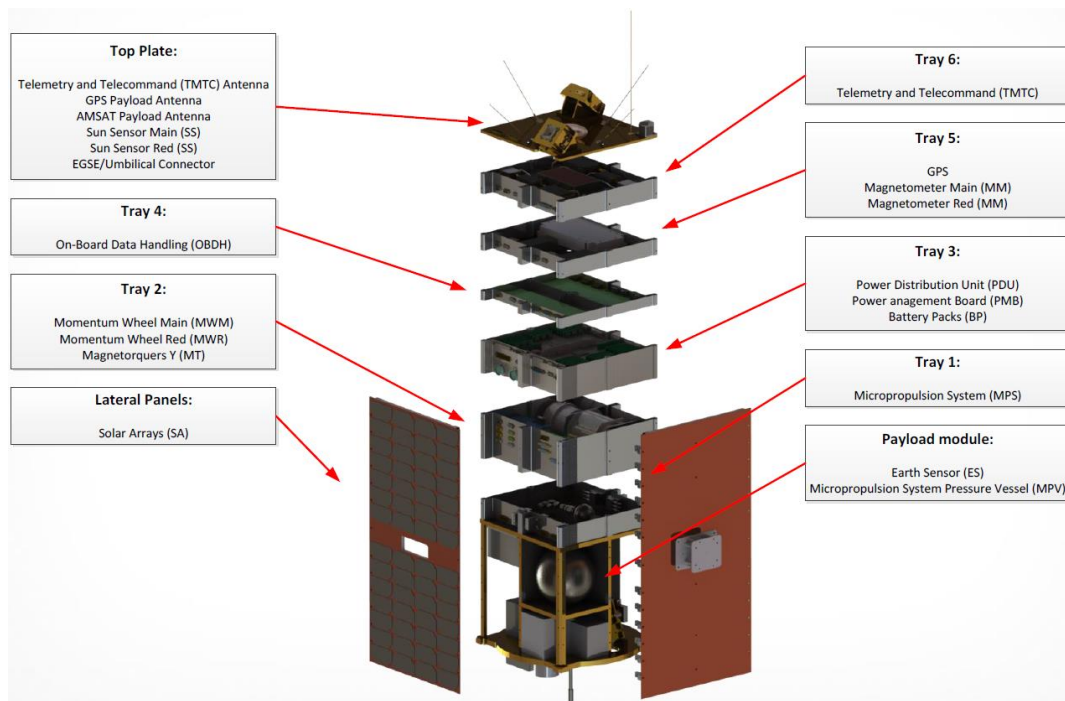


Figure 6. ESEO platform

The project started in January 2013, the Preliminary Design Review was successfully completed in November 2013 and the Critical Design Review in June 2015. Now the project is in phase D and the launch is foreseen in late 2016 or early 2017.

### **3.1 Telecommunication System**

The telecommunication system supports the functions of telemetry and telecommand (TMTC) for each phase of the mission. The spacecraft (S/C) telecommunication system consists of a redundant set of transceivers working at UHF-band for the uplink and the downlink. In addition, two payloads are included for telecommunication purposes, using L-band for uplink, and VHF and S-band for downlink. The VHF/L-band system being developed by AMSAT-UK is used for educational outreach as voice transponder and low data-rate telemetry (TM) downlink whilst the on-board S-band high-speed transmitter payload, being developed in Poland by a Wroclaw University of Technology team, will be used to download scientific payload data. The simultaneous downlink or uplink at different bands is currently not considered (but not excluded) for the mission. Similarly, full duplex communication is not foreseen at UHF band. Half-duplex communication is identified as the standard for TMTC communication. The platform communication subsystem is allocated for a space amateur-radio link with a downlink frequency of 437.000 MHz and an uplink frequency of 435.200 MHz. The selection of the modulation scheme at UHF-band is compliant with the space amateur regulation: the assumed modulation scheme is Pulse Code Modulation (PCM), Non-Return-to-Zero-Level (NRZ-L), Gaussian Frequency Shift Keying (GFSK) with a BT factor of the Gaussian filter equal to 0.5. The default data rate will be 9.6 kb/s, and can be changed to 4.8 kb/s, by a proper HPC. The S-band downlink can be performed at different modulations and data rates:

- Safe mode transmission
  - Data rate: up to 1 kbps
  - Modulation: BPSK
- Nominal transmission
  - Data rate: up to 4 Mbps
  - Modulation: OQPSK
- High data rate transmission (elevation angle  $> 35^\circ$ )
  - Data rate: up to 10 Mbps
  - Modulation: 4D-TCM-BPSK

### 3.1.1 Space-to-Ground communication protocol

The space-to-ground communication protocol for TMTC operations is based on the AX.25 radio amateur protocol [8], which has been preferred to the CCSDS protocol for its simplicity, diffusion among the university and radio amateur community and smaller overhead. This means that it requires less computational load to the on-board transceiver and a narrower bandwidth or shorter ground contact time to downlink the same amount of information. The large diffusion among the amateur and university community will be beneficial for receiving supports by other ground stations especially during the LEOP phase. For the sake of completeness, we report the main features of the communication protocol, you can refer to [9] for more details. Telecommands, telemetry data and acknowledgement/rejection messages are sent in small block of data, called frames. The AX.25 protocol identifies three general types:

- Information frame (I frame)
- Supervisory frame (S frame)
- Unnumbered frame (U frame)

Each frame is made up of several smaller groups, called fields. U and S frames consist of five fields, for a total amount of 19 and 20 bytes respectively (Table 5 and Table 6), while I frames have a variable length depending on the info field length which is limited to 128 bytes leading to a maximum length of 149 bytes for I frames (Table 7).

**Table 5. U frame structure**

| <b>First byte</b> |                |                |            |             |
|-------------------|----------------|----------------|------------|-------------|
| <b>Flag</b>       | <b>Address</b> | <b>Control</b> | <b>FCS</b> | <b>Flag</b> |
| 01111110          | 14 Bytes       | 1 Byte         | 2 Bytes    | 01111110    |

**Table 6. S frame structure**

| <b>First byte</b> |                |                |            |             |
|-------------------|----------------|----------------|------------|-------------|
| <b>Flag</b>       | <b>Address</b> | <b>Control</b> | <b>FCS</b> | <b>Flag</b> |
| 01111110          | 14 Bytes       | 2 Bytes        | 2 Bytes    | 01111110    |

The *Flag* field is one byte long. Since the flag delimits frames, it occurs at both the beginning and end of each frame. A flag consists of a zero followed by six ones followed by another zero: 01111110 (0x7E). As result of bit stuffing, this sequence is not allowed to occur anywhere else inside a complete frame.

The *Address* field contains the source and destination address, both composed by 7 bytes for a total of 14 bytes.

The *Control* field identifies the type of frame being sent and includes sequence number to maintain flow control. Since two bytes are used in S and I frames, seven bits are dedicated to the sequence number (modulo 128).

The *Frame Check Sequence* (FCS) field is a sixteen-bit number calculated by both the sender and receiver of a frame. It is used to ensure that the frame was not corrupted by the medium used to get the frame from the sender to the receiver. It is calculated using the whole packet content excluding the flag bytes.

**Table 7. I frame structure**

| <b>First byte</b> |                |                |            |             |            |             |
|-------------------|----------------|----------------|------------|-------------|------------|-------------|
| <b>Flag</b>       | <b>Address</b> | <b>Control</b> | <b>PID</b> | <b>Info</b> | <b>FCS</b> | <b>Flag</b> |
| 01111110          | 14 Bytes       | 2 Bytes        | 11110000   | N Bytes     | 2 Bytes    | 01111110    |

The external header of the I frame consists of 21 bytes. The same fields included in S frames are used, plus the protocol identifier and the info field.

The *Protocol Identifier* (PID) field identifies what kind of layer 3 protocol is in use. In ESEO mission, no layer 3 protocol is implemented then it is set to 0xF0 (11110000).

The *Info* field includes the internal header and the data bytes. The internal header is identified by the communication protocol between the on-board transceiver and the OBDH [10]. The interface is provided by means of an RS-422 serial link with a baud rate of 57600 bps. The flowchart of Figure 7 shows the bit operations and the frame detection during downlink operations. The bit stream coming from the demodulator undergoes a series of bit operations. The bit stuffing ensures that the flag bit sequence does not appear anywhere else in a frame, the scrambling increases the density of bit transitions easing time recovery and the NRZ to NRZI provides differential encoding of the bit stream easing clock recovery. Finally, the CRC-16-CCITT-1021 algorithm detects if the frame was corrupted during transmission. As shown by Figure 7, a frame is invalid if:

- it is not bounded by opening and closing flags
- it consists of less than 152 bits (including flags)
- it is not byte aligned (i.e. it has not an integral number of bytes)
- the CRC check is invalid

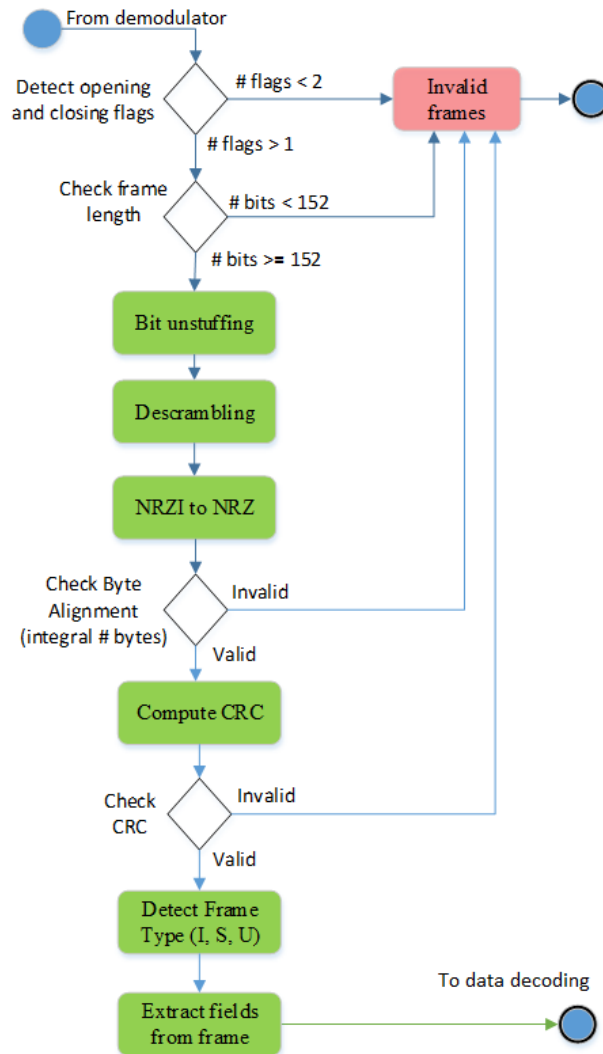


**Figure 7. Bit operations and frame detection (downlink)**

In the last two years, a significant interference has been experienced by different university satellite mission during uplink operations over the Europe in the UHF radio amateur frequency range 430-440 MHz as reported in [11], [12], and shown in Figure 8 [13].

For this reason, we decided to add channel coding. In particular, we added a Reed Solomon RS correction algorithm in the uplink chain, which is extremely powerful at burst error correction. The implemented RS algorithm is a shortened version with an error correcting capability of 8 bytes. Another useful expedient to alleviate the interference issue during uplink operations is to keep the length of TCs as short as possible due to the pulsing nature of the interference source.

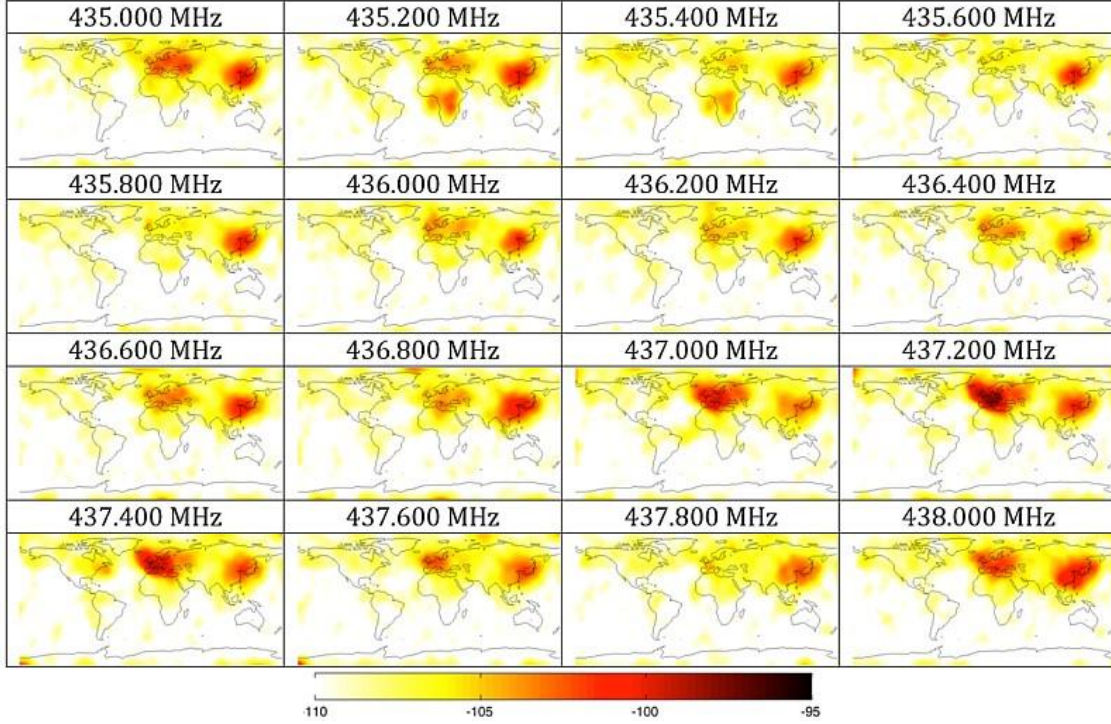


**Figure 8. RSSI (dBm) average interference world plot between 6/8/2014 and 11/8/2014**

The S-band downlink communication protocol is fully compliant to the ECSS standards [14], [15].

### 3.1.2 Link budget

The main purpose of the link budget is to verify that the communication system will operate according to plan, that is, the message quality (error performance) will meet the specifications. The link budget takes into account the gains and losses of the transmitted signal through the media to the receiver. The budget tells how much  $E_bN_0$  is received and how much safety margin exists beyond what is required [16]. The link budget computation is based on the range equation (3), which gives the carrier power at the receiver,  $C$  as the product between the power flux density at the receiver,  $M$  and the antenna effective area at the receiver,  $A_R$ :

$$M = \frac{P_T G_T}{4\pi d^2} = \frac{EIRP}{4\pi d^2} \quad (1)$$

$$A_R = \lambda^2 G_R / 4\pi \quad (2)$$

$$C = M \cdot A_R = EIRP \left( \frac{\lambda}{4\pi d} \right)^2 G_R = EIRP \cdot L_S \cdot G_R \quad (3)$$

Where  $d$  is the distance between the transmitter and the receiver,  $\lambda$  is the wavelength of the signal,  $EIRP$  is the effective isotropic radiated power,  $G_R$  is the gain of the receiver and  $L_S$  is the path loss, which is wavelength (frequency) dependent. From (3), we can compute the signal-to-noise ratio  $SNR$  and then the  $E_b N_0$  at the receiver, defining the thermal noise power,  $N$  as:

$$N = kT_S W \quad (4)$$

Where  $k$  is the Boltzmann's constant,  $T_S$  is the system temperature in Kelvin and  $W$  is the bandwidth in Hz. Knowing the definition of the bit energy  $E_b$  (5) and the single-sided noise power spectral density  $N_0$  (6), we can obtain the  $E_b N_0$  (7) and (8).

$$E_b = C \cdot T_b = C / R_b \quad (5)$$

Where  $T_b$  is the bit time and  $R_b$  is the bit rate

$$N_0 = N / W \quad (6)$$

$$\frac{E_b}{N_0} = \frac{C}{N} \cdot \frac{W}{R_b} = \frac{EIRP L_S L_a G_R}{K T_S R_b} \quad (7)$$

Where  $L_a$  are the additional losses (i.e. polarization, pointing, atmospheric attenuation and precipitation losses).

$$\left( \frac{E_b}{N_0} \right)_{dB} = EIRP (dBW) + L_S (dB) + L_a (dB) + \frac{G_R}{T_S} \left( \frac{dB}{K} \right) + 228.6 - 10 \log_{10} R_b (bps) \quad (8)$$

Where the ratio between  $G_R$  and  $T_S$  is named figure of merit. The system link margin is then given by the difference between the  $E_b N_0$  computed in (8) and the required  $E_b N_0$ , which can be read from Figure 9 for the desired value of BER. Figure 9 shows the theoretical BER curve for the non-coherent BFSK modulation described by (9).

$$BER = \frac{1}{2} e^{-0.5 \cdot E_b N_0} \quad (9)$$

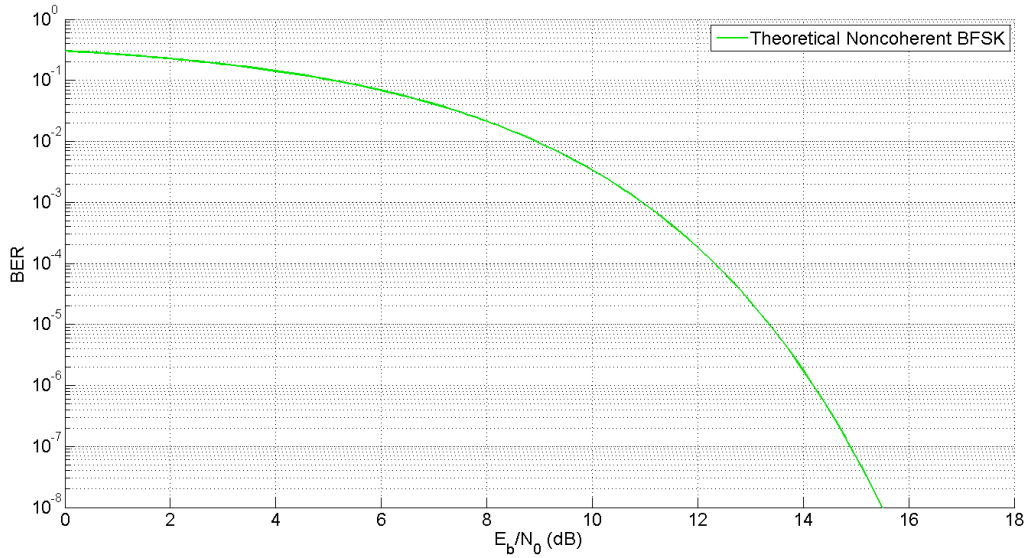


**Figure 9. Theoretical Noncoherent BFSK BER curve**

Table 8 and Table 9 reports the UHF downlink and uplink budget at 9.6 kbps respectively. The UHF link budget at 4.8 kbps and the S-band downlink budget can be found in [17]. This document also contains more detail about the space to ground interface.

**Table 8. UHF downlink budget at 9.6 kbps**

| Parameter                          | Value        |              |              | Units      |
|------------------------------------|--------------|--------------|--------------|------------|
|                                    | Best case    | Average case | Worst case   |            |
| Downlink frequency                 | 437          | 437          | 437          | MHz        |
| Wavelength                         | 0,686        | 0,686        | 0,686        | m          |
| Slant range                        | 2100         | 2100         | 2100         | Km         |
| Boltzmann's Constant               | -228,6       | -228,6       | -228,6       | dBW/K/Hz   |
| <b>Spacecraft S/C</b>              |              |              |              |            |
| S/C Transmitter Power Output       | 1,25         | 1,00         | 0,85         | W          |
|                                    | 0,97         | 0,00         | -0,71        | dBW        |
|                                    | 30,97        | 30,00        | 29,29        | dBm        |
| S/C total transmission line losses | -2,00        | -2,30        | -2,70        | dB         |
| S/C Antenna Gain                   | 4,50         | 4,30         | 3,00         | dBiC       |
| <b>S/C EIRP</b>                    | <b>3,47</b>  | <b>2,00</b>  | <b>-0,41</b> | <b>dBW</b> |
| <b>S/C EIRP</b>                    | <b>33,47</b> | <b>32,00</b> | <b>29,59</b> | <b>dBm</b> |
| <b>Downlink Path</b>               |              |              |              |            |
| S/C Antenna Pointing Loss          | -0,12        | -0,24        | -0,48        | dB         |

|   |                |                |                |             |
|---|----------------|----------------|----------------|-------------|
| Antenna Polarization Loss               | -0,80          | -1,90          | -3,00          | dB          |
| Path Loss                               | -151,71        | -151,71        | -151,71        | dB          |
| Tropospheric Loss                       | -1,00          | -1,00          | -1,00          | dB          |
| Ionospheric Loss                        | -0,20          | -0,20          | -0,20          | dB          |
| Rain Loss                               | 0,00           | 0,00           | 0,00           | dB          |
| <b>Isotropic Signal Level at GS</b>     | <b>-150,36</b> | <b>-153,05</b> | <b>-156,79</b> | <b>dBW</b>  |
| <b>Isotropic Signal Level at GS</b>     | <b>-120,36</b> | <b>-123,05</b> | <b>-126,79</b> | <b>dBm</b>  |
| <b>Ground Station GS</b>                |                |                |                |             |
| GS Antenna Pointing Loss                | -0,02          | -0,06          | -0,10          | dB          |
| GS Antenna Gain                         | 17,00          | 16,00          | 15,00          | dBic        |
| GS total transmission line losses       | -0,80          | -1,00          | -1,20          | dB          |
| GS Effective Noise Temperature          | 540,00         | 560,00         | 580,00         | K           |
| <b>GS Figure of Merit (G/T)</b>         | <b>-11,12</b>  | <b>-12,48</b>  | <b>-13,83</b>  | <b>dB/K</b> |
| GS Signal-to-Noise Power Density (S/No) | 67,10          | 63,01          | 57,87          | dBHz        |
| System Data Rate                        | 9600           | 9600           | 9600           | bps         |
|   | 39,82          | 39,82          | 39,82          | dBHz        |
| <b>Telemetry System Eb/No</b>           | <b>27,27</b>   | <b>23,19</b>   | <b>18,05</b>   | <b>dB</b>   |
| Telemetry System Required BER           | 1,00E-05       | 1,00E-05       | 1,00E-05       |             |
| Demodulator implementation loss         | 1              | 1              | 1              | dB          |
| Telemetry System Required Eb/No         | 13,80          | 13,80          | 13,80          | dB          |
| Eb/No threshold                         | 14,80          | 14,80          | 14,80          | dB          |
| <b>System Link Margin</b>               | <b>12,47</b>   | <b>8,39</b>    | <b>3,25</b>    | <b>dB</b>   |

Table 9. UHF uplink budget at 9.6 kbps

| Parameter                         | Value        |              |              | Units      |
|-----------------------------------|--------------|--------------|--------------|------------|
|                                   | Best case    | Average case | Worst case   |            |
| Uplink frequency                  | 435,2        | 435,2        | 435,2        | MHz        |
| Wavelength                        | 0,688        | 0,688        | 0,688        | m          |
| Slant range                       | 2100         | 2100         | 2100         | Km         |
| Boltzmann's Constant              | -228,6       | -228,6       | -228,6       | dBW/K/Hz   |
| <b>Ground Station GS</b>          |              |              |              |            |
| GS Transmitter Power Output       | 20,00        | 20,00        | 20,00        | W          |
|                                   | 13,01        | 13,01        | 13,01        | dBW        |
|                                   | 43,01        | 43,01        | 43,01        | dBm        |
| GS total transmission line losses | -3,00        | -3,70        | -5,00        | dB         |
| Antenna Gain                      | 17,00        | 16,00        | 15,00        | dBic       |
| <b>GS EIRP</b>                    | <b>27,01</b> | <b>25,31</b> | <b>23,01</b> | <b>dBW</b> |
| <b>GS EIRP</b>                    | <b>57,01</b> | <b>55,31</b> | <b>53,01</b> | <b>dBm</b> |
| <b>Uplink Path</b>                |              |              |              |            |
| Antenna Pointing Loss             | -0,20        | -0,30        | -0,50        | dB         |

|  |                |                |                |             |
|--|----------------|----------------|----------------|-------------|
| Antenna Polarization Loss                | -0,80          | -1,90          | -3,20          | dB          |
| Path Loss                                | -151,67        | -151,67        | -151,67        | dB          |
| Tropospheric Loss                        | -1,00          | -1,00          | -1,00          | dB          |
| Ionospheric Loss                         | -0,20          | -0,20          | -0,20          | dB          |
| Rain Loss                                | 0,00           | 0,00           | 0,00           | dB          |
| <b>Isotropic Signal Level at S/C</b>     | <b>-126,86</b> | <b>-129,76</b> | <b>-133,56</b> | <b>dBW</b>  |
| <b>Isotropic Signal Level at S/C</b>     | <b>-96,86</b>  | <b>-99,76</b>  | <b>-103,56</b> | <b>dBm</b>  |
| <b>Spacecraft S/C</b>                    |                |                |                |             |
| S/C Antenna Pointing Loss                | -1,00          | -2,00          | -3,00          | dB          |
| S/C Antenna Gain                         | 4,50           | 4,30           | 3,00           | dBic        |
| S/C total transmission line losses       | -1,70          | -2,00          | -3,00          | dB          |
| S/C Effective Noise Temperature          | 519,00         | 583,00         | 753,50         | K           |
| <b>S/C Figure of Merit (G/T)</b>         | <b>-24,35</b>  | <b>-25,36</b>  | <b>-28,77</b>  | <b>dB/K</b> |
| S/C Signal-to-Noise Power Density (S/No) | 76,39          | 71,48          | 63,27          | dBHz        |
| System Desired Data Rate                 | 9600           | 9600           | 9600           | bps         |
|  | 39,82          | 39,82          | 39,82          | dBHz        |
| <b>Telemetry System Eb/No</b>            | <b>36,56</b>   | <b>31,66</b>   | <b>23,44</b>   | <b>dB</b>   |
| Telemetry System Required BER            | 1,00E-05       | 1,00E-05       | 1,00E-05       |             |
| Demodulator implementation loss          | 1              | 1              | 1              | dB          |
| Telemetry System Required Eb/No          | 13,80          | 13,80          | 13,80          | dB          |
| Eb/No threshold                          | 14,80          | 14,80          | 14,80          | dB          |
| <b>System Link Margin</b>                | <b>21,76</b>   | <b>16,86</b>   | <b>8,64</b>    | <b>dB</b>   |

### 3.2 Ground Segment

For ESEO project, the University of Bologna is responsible for the overall GS and is collaborating with other universities to build an essential network of ground stations (Figure 10). The ESEO GSN consists of three stations located at:

- University of Bologna, in Forlì (Italy), used to transmit telecommands (TC) and receive the whole amount of TM data at UHF-band and as a secondary ground station to download the whole amount of data generated by the different payloads at S-band.
- University of Vigo (Spain), used as backup for TMTC operations at UHF-band.
- Technical University of Munich (Germany), used as primary ground station for the downlink of payload science data.

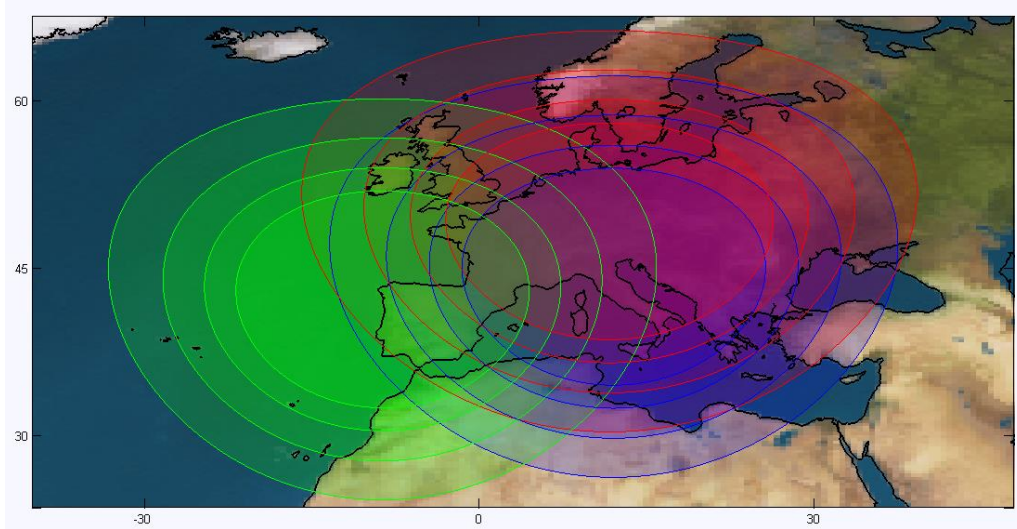


**Figure 10. Detail of the visibility circles of Forlì, Munich and Vigo stations (5°, 10°, 15° and 20° minimum elevations)**

Visibility analysis for the ground stations of the ESEO network has been performed and reported in [7]. Table 10 reports the statistics of ESEO contact durations with the stations of the network considering a minimum elevation of 5°. These results have been obtained considering the orbital parameters in Table 4.

**Table 10. Statistics of contact durations with the stations (5° minimum elevation)**

| <b>Station</b>               | Forlì | Munich | Vigo |
|------------------------------|-------|--------|------|
| <b>Minimum (min)</b>         | 1.60  | 1.90   | 2.77 |
| <b>Mean (min)</b>            | 7.20  | 7.34   | 7.56 |
| <b>Maximum (min)</b>         | 9.43  | 9.43   | 9.43 |
| <b>Blind orbits (of 106)</b> | 74    | 72     | 77   |

The network is coordinated from the MCC located in Forlì through a system named SATNet developed by CalPoly University. It mainly consists of two different types of clients and one central node [18]:

- Central node is the core of the network and it is named Network System (N-System). This node implements the services that enable the connection to the ground station network through a set of remotely invocable software interfaces.
- Software clients will be utilized for accessing the services provided by the N-System. Two different clients are expected to operate within this network:

- Ground Station Clients (G-Clients) will be used by Ground Station Operators (G-Operators) for accessing to the services of the network.
- Mission Operation Clients (M-Clients) will enable the access of Mission Operators (M-Operators) to the services of the network.

The services provided by the N-System are listed below:

- Management Service: it includes the Registration Service, which permits the registration of users and clients in the N-System, the Configuration Service, which allows configuring the capabilities of the Ground Station and the communications requirements of the S/C and the Information Service, which enables the remote access to additional information (e.g. statistics report).
- Scheduling Services: it is used by G and M clients for arranging a remote operation of an S/C.
- Communications Services: it is required for exchanging data message between the G and M clients of the network.

The block diagram depicted in Figure 11 shows the ESEO ground segment highlighting the information exchanged among the satellite, ground stations, mission control center and the user segment.

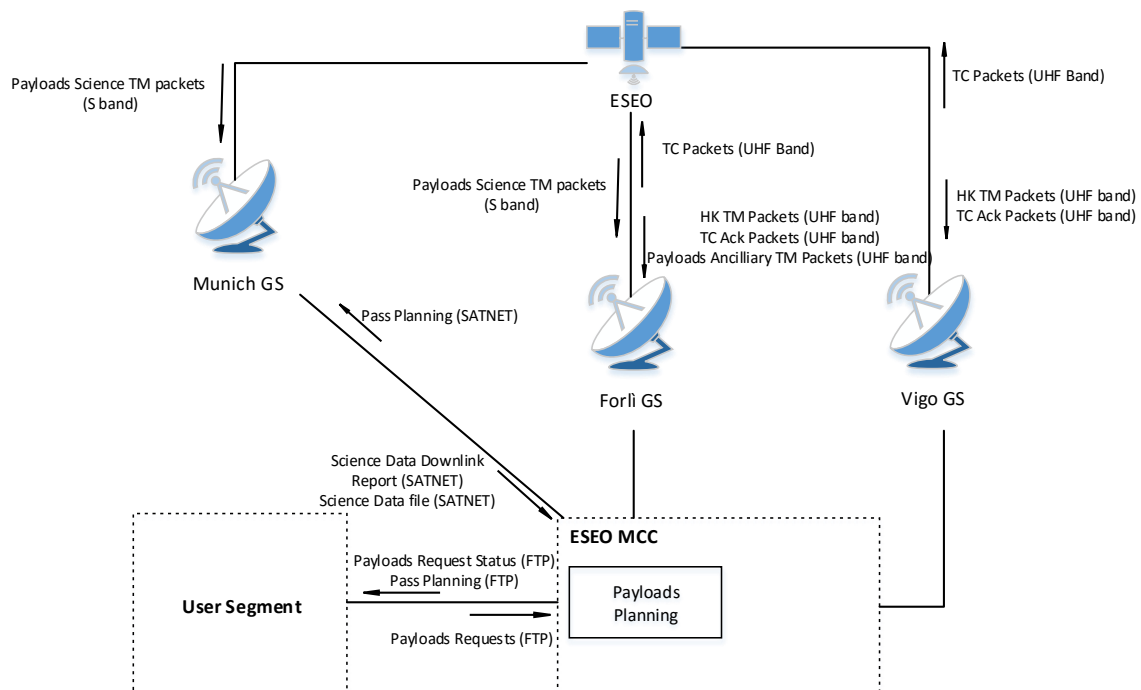


Figure 11. ESEO Ground Segment

A more detailed block diagram of ESEO ground segment is shown in Figure 12. It defines the connections between the software and hardware components and it highlights in different colours the contribution to the development of the ground segment by the different ESEO teams. In the left side, there is the ESEO SS with the S-band transmitter (HSTX), the TMTC transceiver and the AMSAT payload. The connections between the ESEO SS and the ground stations, illustrated in the next column, give information about the RF signal (frequency, modulation, bitrate). The components inside each ground station block represent the hardware and software used to move the antenna and receive/transmit messages from/to the SS. The messages are forward to the MCS through SATNet by using two different clients: the G-client at the ground station connected to demodulator software through a UDP connection and the M-client at the MCS connected to the TMTC data handling application through a UDP connection. The TM and the TC data are routed on two different ports. These messages are also stored for a limited time period in the SATNet DB implemented using PostgreSQL. The MCS is mainly based on a LabVIEW application connected to a MySQL DB for TMTC handling and it is widely described in 3.2.2. For a quick check of a selection of the most significant TM parameters from a smart phone, the TMTC software is connected to the LabVIEW Data Dashboard application. Engineering and payload science data are stored in two different DB scheme, which are available to the user community through a dedicated DB server.

The functional, interface, operation, design and performance requirements of the ground segment have been defined in [19].

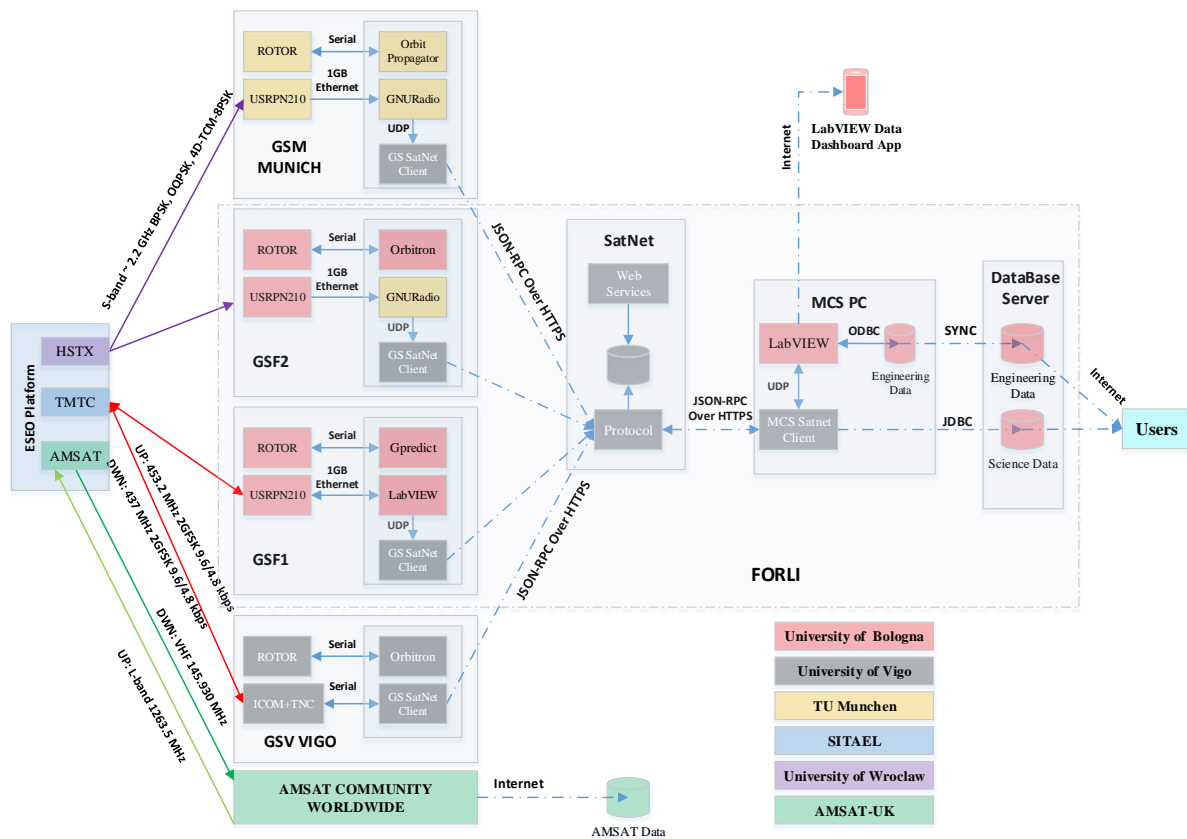
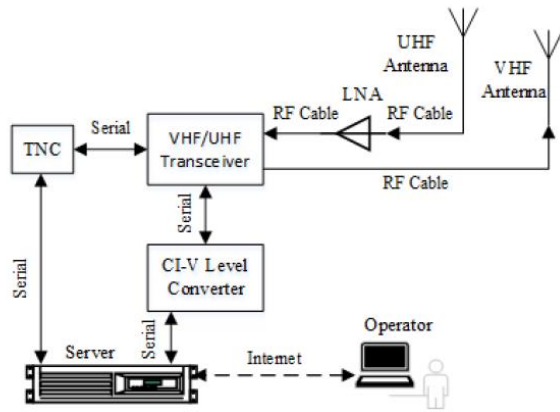


Figure 12. ESEO Ground Segment detailed block diagram

### 3.2.1 Forli Ground Station

To support ALMASat-1 operations, a ground station has been developed in Forlì through the years since 2003. The RF communications of the mission were established on VHF uplink and UHF downlink and the RF system was based on commercial analogic radio (ICOM IC-910H), low noise amplifier (LNA) and terminal node controller (Kantronics KPC-9612+), compliant with the International Amateur Radio Union (IARU) guidelines and with the AX.25 standard protocol (Figure 13).



**Figure 13. Forlì Ground Station configuration for ALMASat-1 mission**



**Figure 14. ALMASat-1 Ground Station**

The 2x9 elements VHF Yagi antenna, operating in the frequency range 144 – 146 MHz and the 2x19 elements UHF Yagi antenna, operating in the range 430 – 440 MHz (see Appendix A), are moved by an azimuth and elevation rotor by AlfaSpid (see Appendix B). We recently added a 3m parabolic dish equipped with a septum dish feed (Figure 15) tuned in the CCSDS S-band frequency ranges: 2025-2120 for uplink and 2200-2300 MHz for downlink (Figure 16). The datasheet for the parabolic dish from RF Hamdesign can be found in Appendix C.



**Figure 15. Septum dish feed mounted on a 3m parabolic dish by RF Hamdesign**

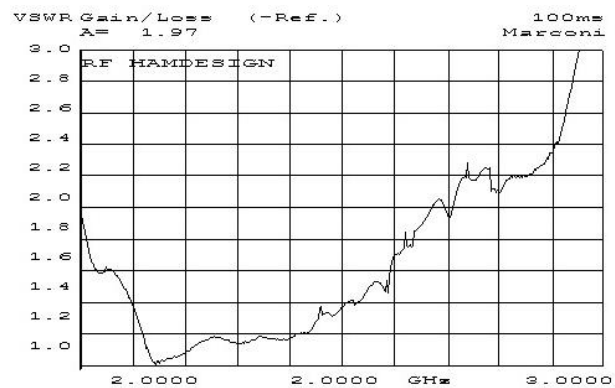


**Figure 16. VSWR plot for the RX port of the septum dish feed by RF Hamdesign**

The AMGS will be soon moved on the top of a new building hosting the UNIBO engineering labs and the mission control room (Figure 18).

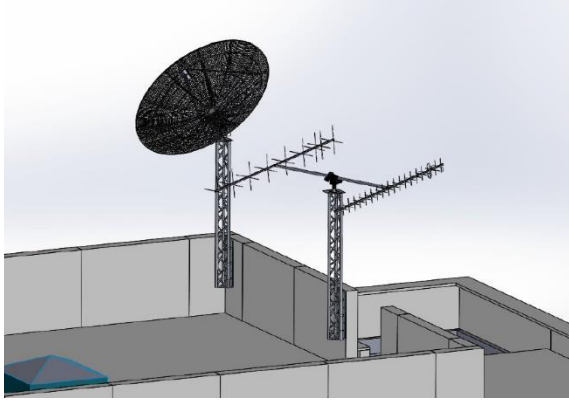


**Figure 17. S-band parabolic dish antenna and VHF/UHF Yagi antenna**



**Figure 18. Mission control room**

In the framework of the ESEO mission, we enhanced the Forlì ground station (AMGS) capabilities by introducing a software-defined radio (SDR). These radios are becoming every day more popular in amateur and university ground stations for satellite communications. They allow fast and cheap reconfiguration of the ground station for satellite missions using a different modulation scheme, communication protocol and frequency. This is possible thanks to the wide frequency band of RF front-end and because the signal is digitally processed at software level. In fact, unlike the ICOM IC-910H radio which is only capable of communicating in the 2 m and 70 cm bands and optionally the 23 cm band (see Table 11), the USRP uses modular daughterboards, which allow to communicate over a wide range of frequencies [20].

**Table 11. ICOM IC-910H frequency coverage in Italy**

| <b>Band</b> | <b>Range</b>                   |
|-------------|--------------------------------|
| 2 m         | 144.0-146.0                    |
| 70 cm       | 430.0-434.0<br>435.0-438.0     |
| 23 cm       | 1240.0-1245.0<br>1270.0-1298.0 |

Moreover, SDR is very beneficial for education purposes: engineering students can simply develop digital communications algorithms on a computer applying their knowledge in communication theory to practical applications. Furthermore, thanks to its versatility, an SDR-based ground station will allow easily participating to many university satellites GSN

opening beneficial collaborations among universities. A ground station using a hardware radio and a TNC is only capable of communicating with satellites, which communicate using the AX.25 protocol. The SDR system for the AMGS comprises the USRP platform by Ettus Research, model N210, hosting the FPGA and the ADC/DAC (Figure 19), the wide bandwidth transceiver named SBX daughterboard (Figure 20) and the host PC running a dedicated software.



**Figure 19. USRP N210 by Ettus Research**



**Figure 20. SBX daughterboard by Ettus Research**

Figure 21 shows the block diagram of the USRP: the incoming signal attached to the standard SMA connector of the USRP are mixed down using a direct-conversion (homodyne) receiver to baseband I/Q components, which are sampled by a two-channel, 100 MS/s, 14-bit analog-to-digital converter (ADC). The digitised I/Q data follows parallel paths through a digital down conversion (DDC) process that mixes, filters and decimates the input 100 MS/s signal to a user-specified rate. The down converted samples, when represented as 32-bit numbers (16 bits each for I and Q), are passed to the host computer at up to 25 MS/s over a standard Gigabit Ethernet connection.

For transmission, baseband I/Q signal samples are synthesised by the host computer and fed to the USRP at up to 25 MS/s over Gigabit Ethernet when represented with 32-bits (16-bits each for the I and Q components). The USRP hardware interpolates the incoming signal to 400 MS/s using a digital up conversion (DUC) process and then converts the signal to analog with a dual-channel, 16-bit digital-to-analog converter (DAC). The resulting analog signal is then mixed up to the specified carrier frequency.

An available 8-bit mode, in which 16-bits total are used to represent the I and Q values of a down converted sample or sample to be up converted, can enable a transfer rate of up to 50 MS/s over the Gigabit Ethernet connection between the host PC and the USRP.

The SBX daughterboard provides up to 100mW (20 dBm) of output power, a typical noise figure of 5 dB and 40 MHz of bandwidth. The local oscillators for the receive and transmit chains operate independently, which allows dual-band operation in the 400-4400 MHz

range. The low power signal transmitted by the SDR is then amplified using a high power amplifier (HPA) whose datasheet can be found in Appendix D.

The block diagram in Figure 22 shows the connection between the components of the VHF/UHF ground station listed in Table 12. The UHF chain, which will be used for the ESEO mission, is based on the SDR technology whilst the VHF chain has not been changed from ALMSat-1 version. Another example of an SDR-based ground station for university satellite missions can be found in [21]. For the S-band ground station, the components are listed in Table 13 whilst their connections are highlighted in the block diagram of Figure 23.

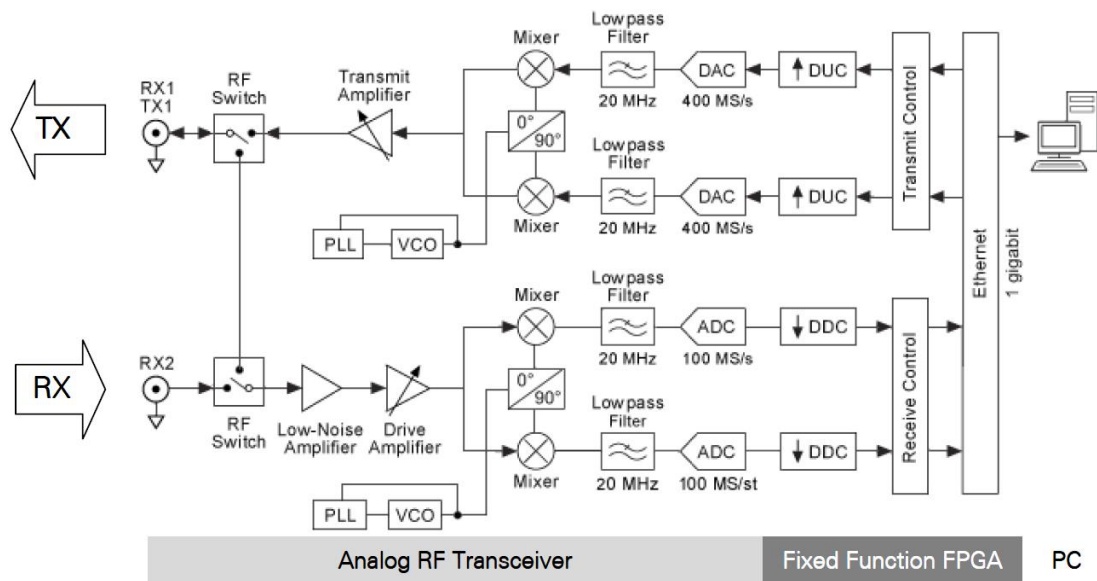


Figure 21. USRP block diagram

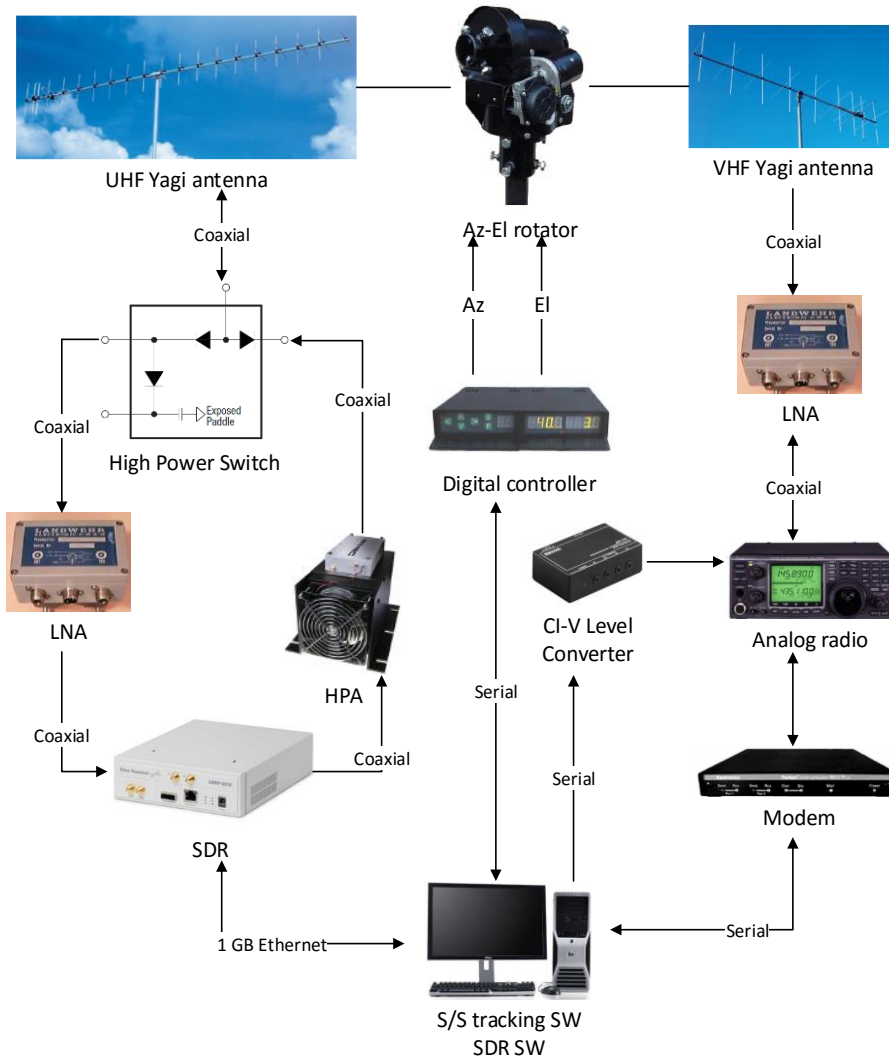


Figure 22. VHF/UHF ground station

Table 12. VHF/UHF ground station components

| Component                | Vendor         | Model                        |
|--------------------------|----------------|------------------------------|
| UHF antenna              | AFT            | 2x19 Yagi (430-440 MHz)      |
| VHF antenna              | AFT            | 2x9 Yagi (144-146 MHz)       |
| Az-El rotor              | RF Hamdesign   | SPID RAS Az-El rotator       |
| Rotor digital controller | RF Hamdesign   | SPID RAS Az-El controller    |
| High Power Switch        | SKYWOKS        | SKY12208-478LF               |
| VHF LNA                  | Landwehr       | N GaAs 145 MAS               |
| UHF LNA                  | Landwehr       | N GaAs 435 MAS               |
| HPA                      | MiniCircuits   | ZHL-50W-52                   |
| SDR                      | Ettus Research | USRPN210 + SBX daughterboard |
| Analog radio             | ICOM           | IC-910H                      |
| Modem                    | Kantronics     | KPC 9612+                    |
| CI-V Level Converter     | ICOM           | CT-17                        |

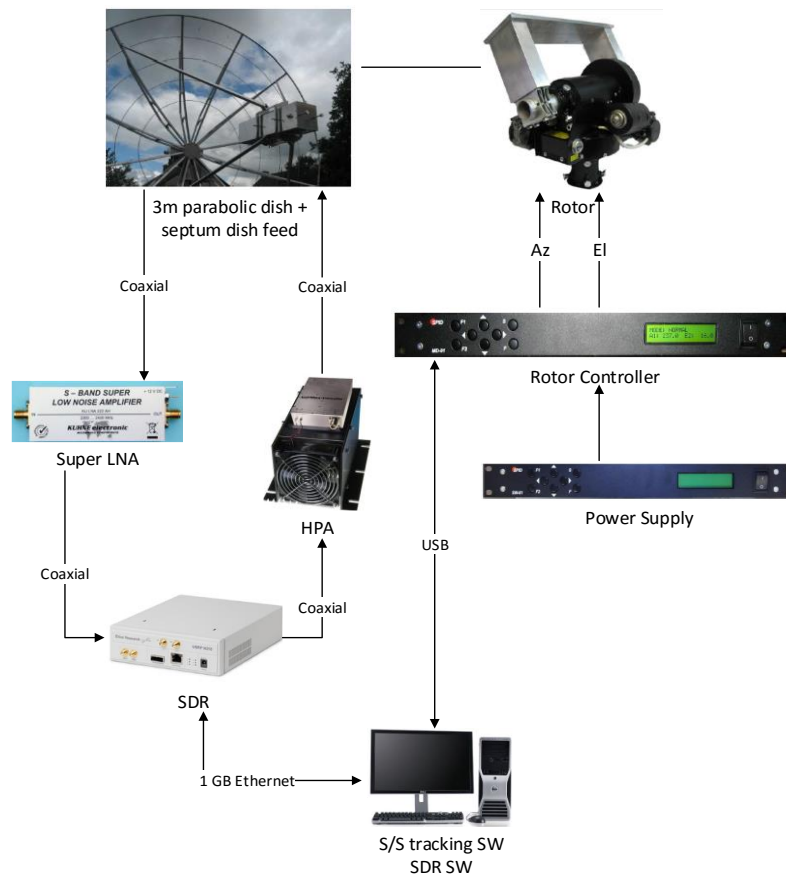


Figure 23. S-band ground station

Table 13. S-band ground station components

| Component        | Vendor           | Model                        |
|------------------|------------------|------------------------------|
| Parabolic dish   | RF Hamdesign     | 3m up to 11 GHz              |
| Septum dish feed | RF Hamdesign     | dual mode, LHCP/RHCP         |
| Az-EI rotor      | RF Hamdesign     | SPID BIG-RAS/HR Az-EI rotor  |
| Rotor controller | RF Hamdesign     | SPID BIG-RAS/HR MD-01        |
| Power Supply     | RF Hamdesign     | SPID PS-01                   |
| Super LNA        | KUHNE electronic | KU LNA 222 AH <sup>1</sup>   |
| HPA              | MiniCircuits     | ZHL-100W-242+                |
| SDR              | Ettus Research   | USRPN210 + SBX daughterboard |

### 3.2.1.1 Satellite Tracking Software

Pointing the ground station antennas to the satellite is the first step for uplink and downlink operations. The antennas are moved by a rotor around the azimuth and elevation angles

<sup>1</sup> Datasheet can be found in Appendix E.

through a digital controller connected to a computer running a satellite tracking software. There are several real-time satellite tracking and orbit prediction programs and the most popular are: Gpredict, Orbitron and Nova for Windows. They implement the NORAD SGP4/SDP4 algorithms to solve Kepler's equation of orbital motion. The Keplerian elements are extracted from the TLE (as shown in Table 24) retrieved from the internet or local files. For our ground station, we selected Gpredict, an open source program which offers several views as depicted in Figure 25. It allows automated ground station operation providing both Doppler tuning for radios and antenna rotator control through Hamlib.

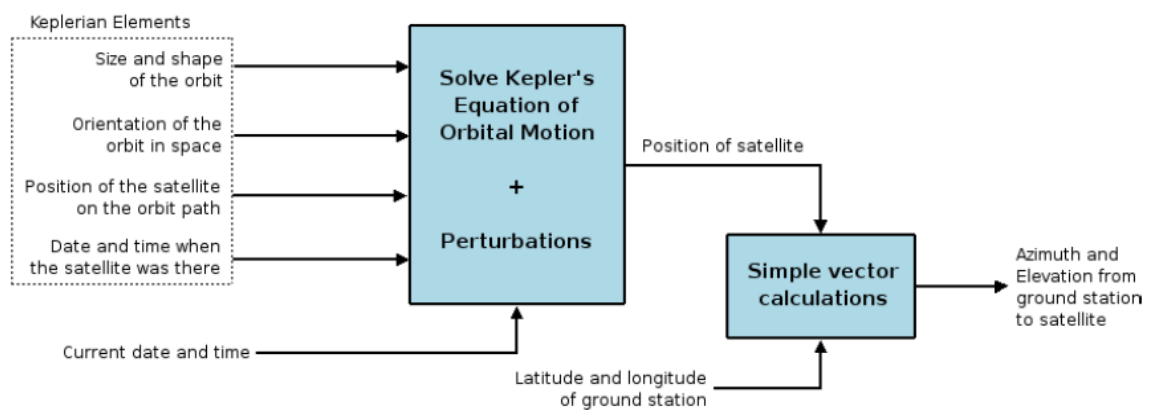


Figure 24. Computation of azimuth and elevation from ground station to satellite

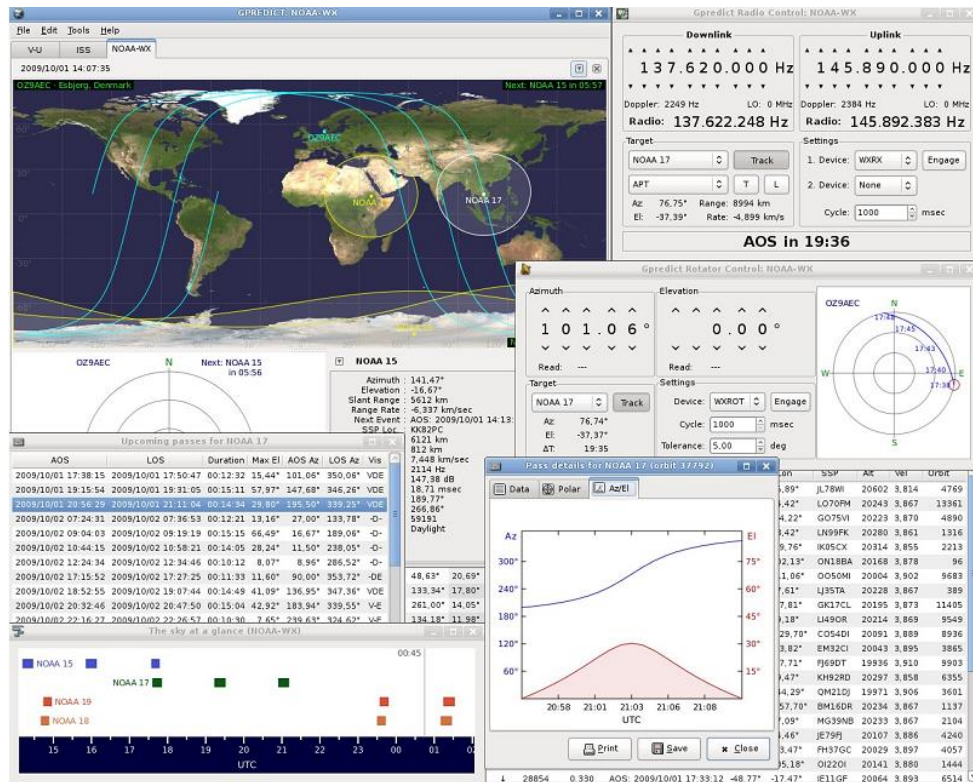


Figure 25. Gpredict satellite tracking software

### 3.2.1.2 Software Defined Radio implementation

Three main programming languages can be used to develop a customised software for SDR: LabVIEW, MATLAB/Simulink and GNURadio (GR) [22]. GR uses a two-tier structure: the computationally intensive processing functions are implemented in C++ while application-defined control and coordination of blocks are developed in Python. A description of GR working mechanism can be found in [23]. A first software model for AMGS was implemented in GNURadio and presented in [24] but the final model was developed in LabVIEW since it offers more functionalities for our purposes compared to the other possible solutions. The software takes advantage of the NI USRP and Modulation toolkit to interface with the USRP hardware and perform modulation [25] and it has been implemented using five parallel loops:

- Signal acquisition and display
- Signal IQ data recording
- Signal demodulation and UDP connection
- UDP connection and signal modulation and transmission.
- Orbitron DDE connection

The signal acquisition loop forwards the IQ data to the signal recording and modulation loops using queue operations functions.

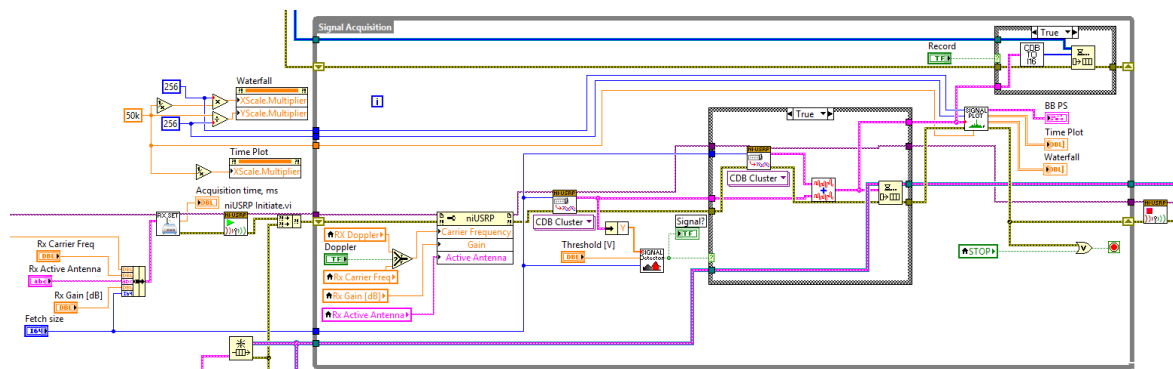


Figure 26. LabVIEW block diagram of the signal acquisition loop of the SDR software

The signal acquisition loop shown in Figure 26, comprises several functionalities. In the left top of the block diagram, some values used to define the signal displays are set as constant. For the STFT-based spectrogram (Figure 29), the time-frequency sampling info, which specifies the density to use to sample the signal in the time-frequency domain and defines the size of the resulting 2D time-frequency array, is specified in terms of time steps

and frequency bins. The former specifies the sampling period, in samples, along the time axis and it is set equal to 256 whilst the latter is the FFT block size of the STFT and it must be a power of two, here equal to 256. For the double-sided power spectrum density (Figure 27), we set the frequency range to 50 kHz. In the left bottom of the diagram, the five USRP parameters are set from controls in the GUI (Figure 27) and the USRP is initiated. Inside the loop, first of all the USRP RX carrier frequency, gain and active antenna values are refreshed. This is particularly useful to correct automatically the frequency for the Doppler shift. Then, received baseband samples are fetched from the USRP as complex (in-phase and quadrature-phase), double-precision floating-point data in a cluster, which also includes sampling information. These data are passed to a signal detector to check if the signal level is above or below to a defined threshold (e.g. 250  $\mu$ V). If above, the signal display turns on, the next samples are fetched from the USRP and the two bunches of samples are concatenated. Finally, samples are displayed in different graphs through the signal plot block, enqueued to a buffer, which will be processed by the demodulation and decoding parallel loop, and if the record option is checked, converted to the 16-bit signed integer data representation and enqueued to a buffer, which will be read by the signal recording parallel loop. This loop stores the IQ data as an interleaved array of signed 16-bit integers ( $I_0, Q_0, I_1, Q_1, \dots, I_n, Q_n$ ), the same format in which the data are transferred over the Ethernet bus and stored in the PC memory, so that the only processing is simply copying the data from PC memory to disk. In fact, it is important to minimize the amount of processing applied to the data during recording to stream data to disk at high rates.

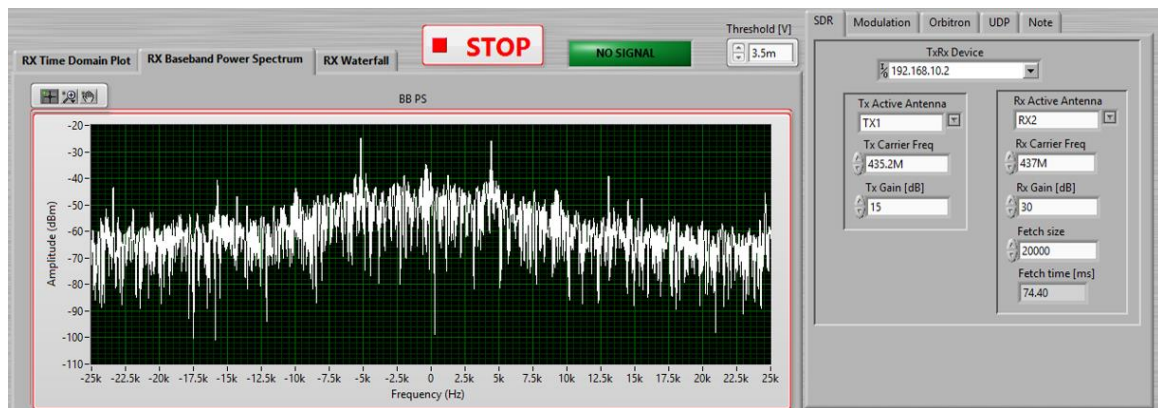


Figure 27. SDR software GUI

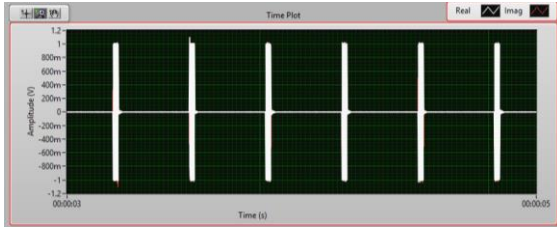


Figure 28. GFSK signal time plot

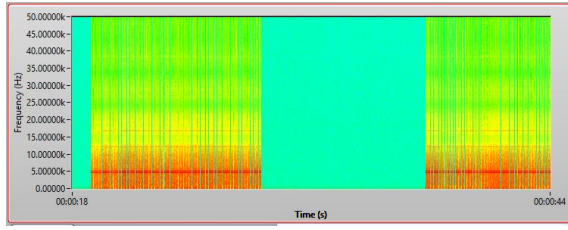


Figure 29. GFSK signal waterfall plot

The SDR can be configured through five basic parameters:

- Device name: is the IP address of the USRP device. This is used to identify the HW connected to the PC (e.g. 192.168.10.2).
- Antenna: is the selected antenna port to transmit from (TX1 is the only option) and receive from (RX1 for half-duplex and RX2 for full-duplex)
- Carrier frequency: is the TX/RX carrier frequency of interest in the range 400-4400 MHz.
- Gain: is the amplification of signal before digitising the signal (0-25 dB for TX and 0-32 dB for RX with a step of 0.5 dB).
- Fetch size: specifies how many samples  $N$  are acquired at each iteration. It is correlated to the fetch time  $T_f$  and the IQ rate  $F_s$  by the following expression:

$$T_f = N/F_s \quad (10)$$

The number of samples should be large enough to acquire all the samples inside a single frame but at the same time, the fetch time should be small enough to allow real time operations, meaning that the fetch rate should be larger than the number of separated frames sent in one second. Table 14 shows different possible values of fetch size, time and rate. The loop rate is half of the fetch rate, since the acquisition loop (Figure 26) performs two fetch operations at each iteration. Loop rate values have an upper limit due to the software computational speed. Tests have shown that the loop rate is limited to 9 frames per seconds, which means that the software cannot execute more than 9 iterations of the signal acquisition loop per second.

**Table 14. Different values of the SDR fetch size, time and rate**

| Fetch size (kS) | Fetch time (ms) | Fetch rate (N/s) | Loop rate (N/s) |
|-----------------|-----------------|------------------|-----------------|
| 80              | 297.6           | 3.360            | 1.680           |
| 70              | 260.4           | 3.840            | 1.920           |
| 60              | 223.2           | 4.480            | 2.240           |
| 50              | 186.0           | 5.376            | 2.688           |
| 40              | 148.8           | 6.720            | 3.360           |
| 30              | 111.6           | 8.961            | 4.480           |
| 20              | 74.4            | 13.441           | 6.720           |
| 10              | 37.2            | 26.882           | 13.441          |

The modulation scheme selected for the ESEO TMTC operations is a non-coherent BFSK preceded by a Gaussian filter. In this scheme, a change from one frequency to the other does not adhere to the current phase of the signal as shown in Figure 30.

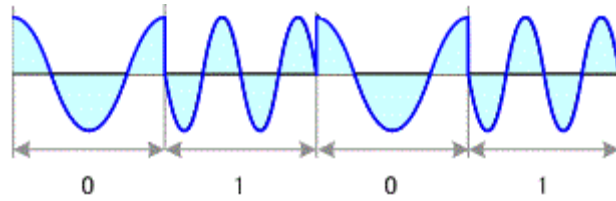


**Figure 30. Non-coherent BFSK signal**

The Gaussian pulse-shaping filter reduces the levels of side-lobes of the FSK spectrum. In the GUI it is possible to select this filter class (other options are raised cosine filter, root raised cosine filter and no filter), the filter length and either alpha or BT. The filter length specifies the length of the transmit pulse shaping filter in symbol whilst BT is the product between the -3 dB bandwidth and the symbol period for a Gaussian filter.

A characteristic parameter for the FSK modulation scheme is the frequency deviation  $f_d$ :

$$f_d = \frac{R_s k}{2} \quad (11)$$

where  $k$  is the modulation index and  $R_s$  is the symbol rate, the number of transmitted symbols per second. This is related to  $R_b$ , the bit rate by the following equation:

$$R_s = R_b/m \quad (12)$$

where  $m$  is the number of bits transmitted with each symbol. For the BFSK,  $m$  is equal to 1 meaning that  $R_s = R_b$ . For the ESEO TMTC, the bit rate and hence the symbol rate can be 9.6 or 4.8 kbps. The user can change between these two values in the GUI, and the software automatically sets the number of samples per bit  $Spb$  and the IQ rate using the following relation:

$$R_b = Spb/F_s \quad (13)$$

The IQ rate aka sample rate can be adjusted to values ranging from 195.312 kS/s to 25 MS/s. However not all values in this range are supported by the USRP, hence coerced values are used by the SDR. In order to set the bit rate to 9.6 kbps and 4.8 kbps, the number of samples per bit can be properly adjusted as shown in Table 15 and Table 16.

**Table 15. SDR settings for bit rate equal to 9.6 kbps**

| <b>Spb</b> | <b>Desired IQ rate (kSps)</b> | <b>Coerced IQ rate (kSps)</b> | <b>Coerced bit rate (bps)</b> | <b>Error (Hz)</b> |
|------------|-------------------------------|-------------------------------|-------------------------------|-------------------|
| 20         | 192.000                       | 195.312                       | 9765.60                       | 165.60            |
| 22         | 211.200                       | 211.864                       | 9630.18                       | 30.18             |
| 24         | 230.400                       | 229.358                       | 9556.58                       | 43.42             |
| 26         | 249.600                       | 250.000                       | 9615.38                       | 15.38             |
| <b>28</b>  | <b>268.800</b>                | <b>268.817</b>                | <b>9600.61</b>                | <b>0.61</b>       |
| 30         | 288.000                       | 287.356                       | 9578.53                       | 21.47             |

**Table 16. SDR settings for bit rate equal to 4.8 kbps.**

| <b>Spb</b> | <b>Desired IQ rate (kSps)</b> | <b>Coerced IQ rate (kSps)</b> | <b>Coerced bit rate (bps)</b> | <b>Error (Hz)</b> |
|------------|-------------------------------|-------------------------------|-------------------------------|-------------------|
| 40         | 192.000                       | 195.312                       | 4882.8                        | 82.8              |
| <b>42</b>  | <b>201.600</b>                | <b>201.613</b>                | <b>4800.31</b>                | <b>0.31</b>       |
| 44         | 211.200                       | 211.864                       | 4815.09                       | 15.09             |
| 46         | 220.800                       | 221.239                       | 4809.54                       | 9.54              |
| 48         | 230.400                       | 229.358                       | 4778.29                       | 21.71             |
| 50         | 240.000                       | 240.385                       | 4807.70                       | 7.70              |

The occupied bandwidth  $BW$  is then given by:

$$BW = (1 + BT)R_s + 2f_d \quad (14)$$

The SDR software is connected to a satellite tracking software, named Orbitron, through a dynamic data exchange (DDE). This is needed for automatic Doppler shift frequency correction. This application can be then connected to SATNet or directly to the S/C M&C system through an UDP connection.

### 3.2.1.3 Compatibility Tests

This section describes the set-up and results for compatibility tests between the SDR used as the UHF transceiver of the AMGS and the ESEO on-board transceiver. The latter is the CC1020 UHF transceiver, designed by Texas Instruments. This integrated circuit is a low power device well suited for critical application as microsatellite platform where the power consumption and the overall dimension are strict parameters. The CC1020 transceiver has flight heritage in space communication application, as it has successfully used in small satellite platform such as the CAPE-1 and PICPOT. More details can be found in its datasheet [26]. Figure 31 shows the RF output signal of the engineering model of the TMTC board. It is obtained setting the CC1020 in transmit mode with the maximum output power available on-board (10 dBm) and selecting a final data rate of 4.8 kbps. The occupied channel bandwidth is 12.5 KHz, respecting the specification of the IARU recommendation for channel spacing. For a data rate of 9.6 kbps a channel of at least 25 KHz is necessary, requiring the assignment of at least two adjacent channel of the spectral resources managed by IARU [27].

The objectives of these tests are:

- Check the radio frequency compatibility between the SDR and the CC1020.
- Check modulation/demodulation scheme compatibility between the SDR and the CC1020.
- Check coding/decoding operations compatibility between the SDR and the CC1020.
- Check the packet error rate PER at different values of SNR.

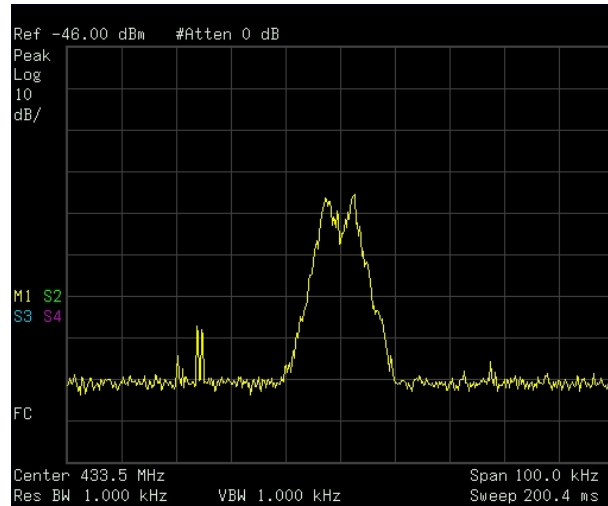


**Figure 31. GFSK signal spectrum**

Figure 32 shows the test setup: the SDR is composed of the USRP N210 device connected through a 1 GB Ethernet cable to a laptop running a LabVIEW VI. The on-board transceiver (TMTC) comprises the CC1020 device programmed from a laptop running the IAR Embedded Workbench software through the AVR JTAGICE device. They are both connected through coaxial cables to a manual step attenuator, ranging from 0 to 110 dB with 10 dB steps which allows to perform tests at different values of SNR.

The running VI implements the SDR software described in 3.2.1.1 with a modified interface for testing purposes and a functionality that allows saving the instantaneous power in band value in a binary file using the spectral measurement toolkit. These values are then processed to compute the SNR value at the receiver.

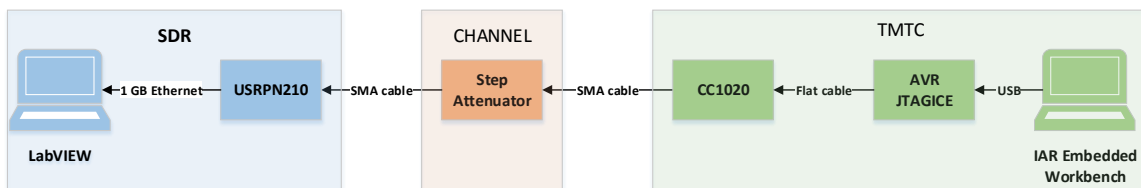


**Figure 32. SDR Test setup**

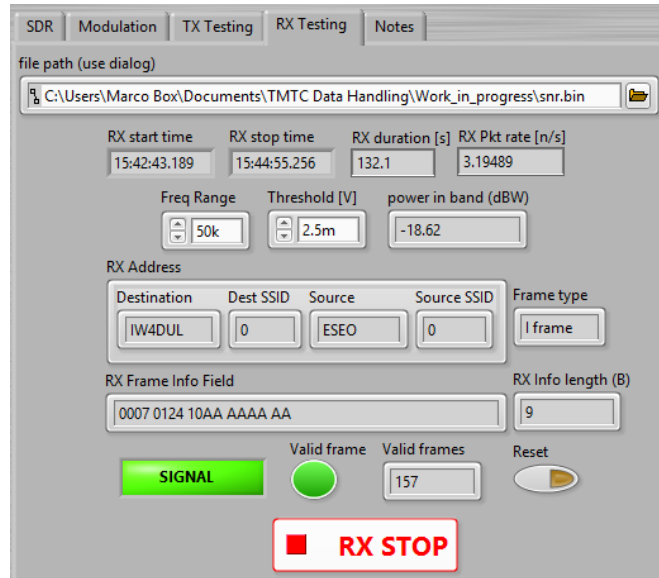


Figure 33. SDR software for testing purposes

Table 17 reports the results in terms of PER at the SDR side for different values of SNR measured by the SDR software. Each frame consists of 152 bytes (1216 bits).

Table 17. Packet Error Rate for different Signal-to-Noise Ratio values in downlink testing

| Frames | Bits (k) | Duration (M:S) | Frame rate (n/s) | RX frames | SNR (dB) | PER    |
|--------|----------|----------------|------------------|-----------|----------|--------|
| 1000   | 1216     | 5:13           | 3.19             | 1000      | 60.3     | 0      |
| 1000   | 1216     | 5:13           | 3.19             | 1000      | 40.4     | 0      |
| 1000   | 1216     | 5:13           | 3.19             | 1000      | 20.4     | 0      |
| 1000   | 1216     | 5:13           | 3.19             | 1000      | 16.9     | 0      |
| 5000   | 6080     | 26:03          | 3.20             | 5000      | 12.6     | 0      |
| 1000   | 1216     | 5:13           | 3.19             | 1000      | 12.5     | 0      |
| 5000   | 6080     | 26:03          | 3.20             | 4998      | 11.8     | 4e-4   |
| 5000   | 6080     | 26:03          | 3.20             | 4993      | 11.5     | 1.4e-3 |
| 1000   | 1216     | 5:13           | 3.19             | 998       | 11.4     | 2e-3   |
| 5000   | 6080     | 26:03          | 3.20             | 4985      | 10.7     | 3e-3   |
| 1000   | 1216     | 5:13           | 3.19             | 997       | 10.5     | 3e-3   |

### 3.2.2 Spacecraft Monitoring and Control

To operate efficiently a satellite, a complete and easy-to-use S/C M&C system is essential. The system has been implemented in LabVIEW because the GUI is a very important aspect of this system and students can easily learn this programming language allowing them to

modify the software for future satellite missions. This application is connected to a MySQL DB for TMTC storing and retrieving operations using the Database Connectivity Toolkit. For further information about DB schema definition, see 3.2.2.1. It can be also connected to SATNet or directly to the SDR software through an UDP connection receiving and transmitting TM and TC packets. The application consists of three views: the main display (Figure 34), the TM data display (Figure 35) and the TC set display (Figure 36).

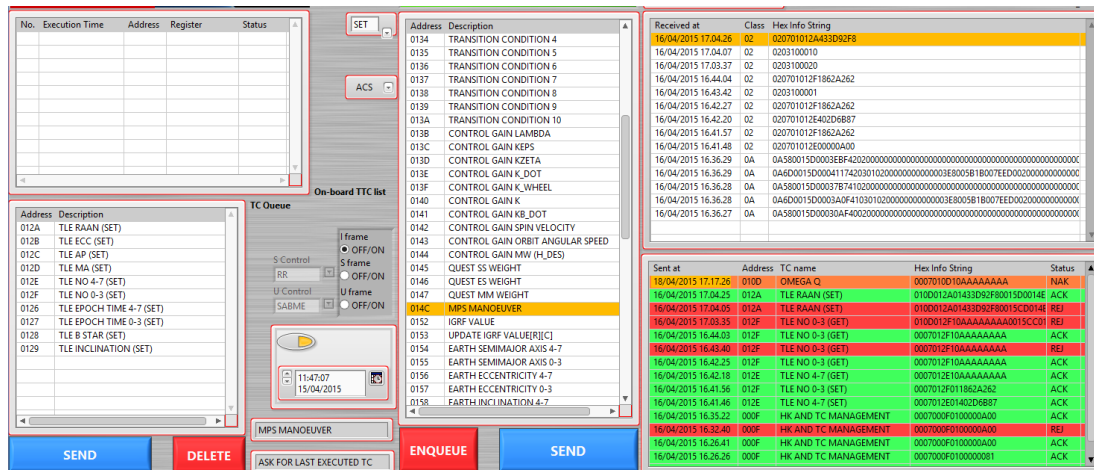


Figure 34. Spacecraft Monitoring and Control GUI

The main display allows the operator to select the commands filtering by equipment/payload and type (SET/GET) and enable the time tag option specifying the execution time through a calendar widget. The command can be directly sent to the S/C or queued into the TC stack. From the TC stack, the command can be sequentially sent to the S/C or deleted. The two list boxes in the right side of the interface shows in real time, the received TM packets (top) in hexadecimal representation and the sent TC (bottom). TM packets can also be filtered by class. The class is the type of the packet:

- TC acknowledgment message
- Beacon of type 1 (general): contains information from various subsystems
- Beacon of type 2 (power system)
- Beacon of type 3 (OBDH)
- Beacon of type 4 (AOCS and sensor/actuator)
- Beacon of type 5 (FDIR and TMTC)
- Beacon of type 6 (payload)
- HK data page

- HK history
- PS high rate history
- Death report
- ES IR image

The rows of the sent TCs list box are highlighted in different colours according to the acknowledgment status: green for acknowledged (ACK), red for rejected (REJ) and orange for not acknowledged (NAK). An acknowledgment message sent from the S/C in response to a TC, indicates that the TC has been correctly executed on-board if immediate or that the command has been successfully inserted into the TTC on-board schedule if time-tagged. A rejection message sent from the S/C in response to a TC highlights one of the following error:

- CRC error due to frame corruption.
- Invalid address (out of range): the command identifier (address) does not exist.
- Invalid address (equipment/payload is OFF): the receiver of the TC (equipment/payload) is off.
- Invalid address (type combination): the sent TC type (SET/GET) is not available for the specified address.
- Invalid time: the time tag of the sent TC is in the past.
- Time tagged of type GET is invalid: TTC can be only of SET type.
- Destination equipment timeout/not answering.
- Sequence number error: the expected sequence number is different.
- Unable to process TC request: the content of the TC is invalid.

If after a defined timeout (5 sec) from the sent TC, an acknowledgement message is not received, the TC is considered as NAK.

Another list-box will show the current content of the TTC on-board schedule based on the successfully sent TTCs, the TCs to handle the schedule (disable a scheduled TTC, clear all the schedule) and the TCs to get information on the scheduled TTCs. The list box contains information about the TC identifier, execution time and status. The latter can be one of the following:

- Pending: the row contains a TTC that will execute at execution time and then deleted.

- Disabled: the row contains a TTC that will not execute at execution time and then deleted.
- Cleared: the row is free, it does not contain a TTC.

The on-board schedule has a maximum capability of 120 TTCs.

The operator can display the value of each TM parameter in a dedicated view (Figure 35). Values are expressed in engineering units and with the textual calibration. Each parameter value is visualised by an indicator (numeric displays, slides, lights) that the operator can easily find by selecting the desired equipment/payload tab. A LED indicator above the name of each subsystem highlights if there is an error (e.g. OOL value) in that subsystem and an automatic warning e-mail informs the engineers about possible issues. Warnings are triggered by a change in the equipment/payload error array.

In the view shown in Figure 36, the operator can change the values of all settable parameters before sending the corresponding SET TC from the main view. TC parameters are grouped by equipment/payload (one for each tab) and values are textual calibrated or limited between acceptable minimum and maximum values if applicable.

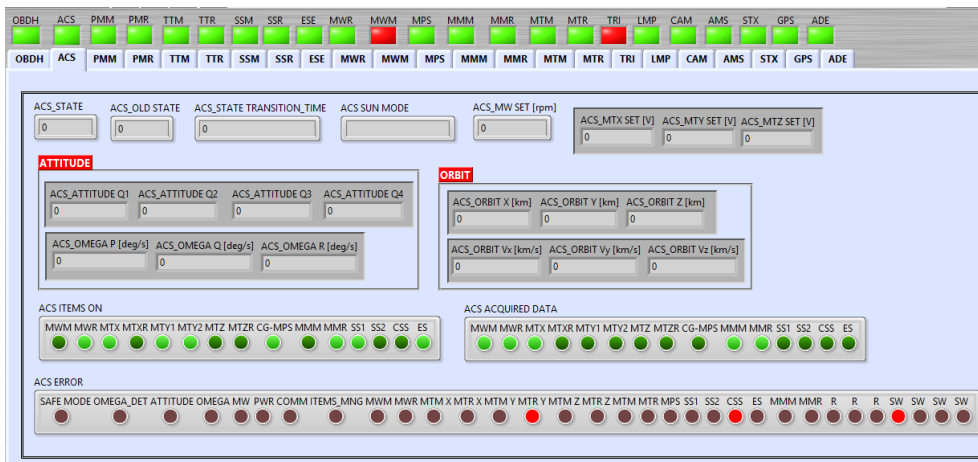


Figure 35. AOCs Telemetry display

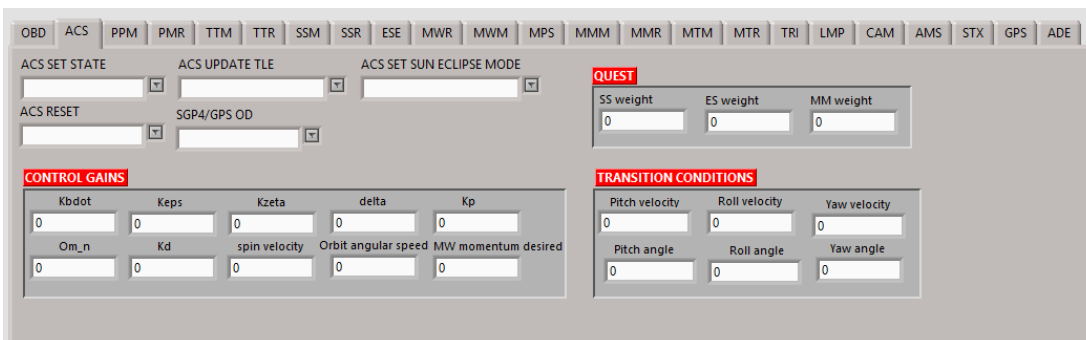
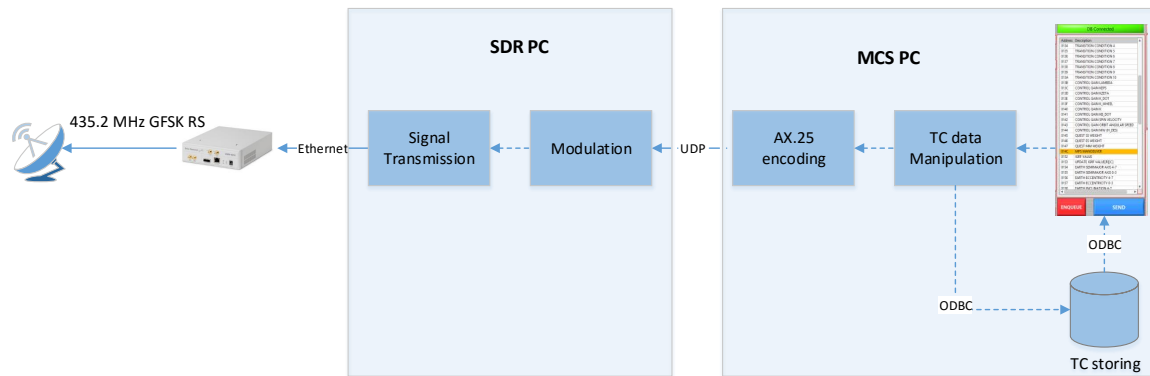
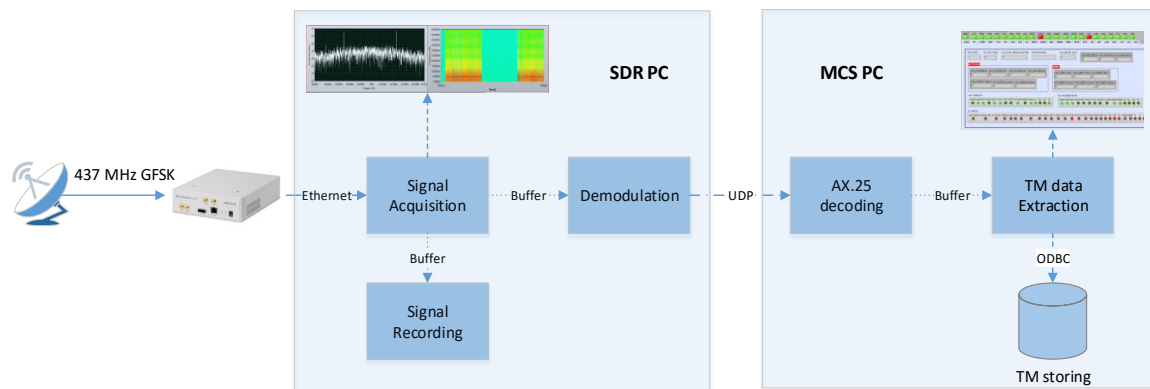


Figure 36. AOCs Telecommands display

Figure 37 and Figure 38 highlights all the functionalities implemented in LabVIEW for the uplink and downlink chain respectively.



**Figure 37. Uplink chain flowchart**



**Figure 38. Downlink chain flowchart**

### 3.2.2.1 Database definition

ESEO has around 500 TM parameters and 500 TCs needed to know the health status and command the on-board equipment and payloads. The full list of TM and TC can be found in [28]. Therefore, to store all the S/C parameters, the history of sent TCs and received HK data in an orderly manner, a proper database schema definition is required. The selected relational database management system (RDMS) is MySQL for its popularity, simple and intuitive syntax and it can be connected to a large variety of software. The DB is populated with flat (spreadsheet-like) tables containing:

- TM parameters list: label, equipment/payload (Table 18), description, default and limit values, units and data types.
- TC list: label, equipment/payload, address and type (GET/SET)

- TM packets history: class, hex raw string, timestamp (date and time)
- TC packets history: equipment/payload, address, timestamp, status (ACK, REJ, NAK), hex raw string.
- TM data: one table for each equipment/payload (parameters, timestamp)

**Table 18. ESEO equipment/payloads**

| <b>Equipment/Payload</b>                   | <b>Prefix</b> |
|--|---------------|
| OBDH equipment                             | OBD           |
| TMTC main                                  | TTM           |
| TMTC redundant                             | TTR           |
| Power Management Unit main                 | PMM           |
| Power Management Unit redundant            | PMR           |
| AOCS algorithms                            | ACS           |
| Sun sensor main                            | SSM           |
| Sun sensor redundant                       | SSR           |
| Earth sensor                               | ESE           |
| Magnetometer main                          | MMM           |
| Magnetometer redundant                     | MMR           |
| Magnetic Torquer main                      | MTM           |
| Magnetic Torquer redundant                 | MTR           |
| Momentum Wheel main                        | MWM           |
| Momentum Wheel redundant                   | MWR           |
| TRITEL                                     | TRI           |
| Langmuir Probe                             | LMP           |
| uCAM                                       | CAM           |
| De-orbit mechanism                         | DOM           |
| AMSAT-UK                                   | AMS           |
| S-Band transmitter                         | STX           |
| GPS receiver                               | GPS           |
| TU-Delft attitude determination experiment | ADE           |

Different levels of privileges are granted to the different users. The customer (ESA), the system prime contractor (SITAEL) and the ground segment responsible (UniBO) are granted with read privileges on all mission data. Payload teams are granted with read privileges only for data on their payload whilst the MCS administrator (from UniBO) is

granted with full privileges. DB backup is performed automatically using the free version of MySQL Backup FTP. This tool creates remote MySQL DB backups, zips, encrypts and sends backups to a local or online folder. It runs on a flexible schedule and sends email confirmations on job success or failure. This allows automatic and planned data backups. For more detailed information about the DB schema definition and examples, please refer to [29].

### 3.2.2.2 Automatic procedures

Some procedures have been identified and reported in the ESEO satellite operations handbook [30]. These procedures contains a set of telecommanding and TM checks and have been implemented as MATLAB scripts, which can be started from a dedicated interface. The operations procedures style guide is compliant to [31] and each procedure is written in a dedicated Excel file. This file comprises three sheets:

- Change log: records the change made to the procedure.
- Procedure header: contains information about duration, criticality, title, objective, related procedures, authorisation, etc.
- Procedure body: within the procedures, the basic structure consists of steps and sub-steps. All actions (e.g. send, verify, select, etc.) must take place in the sub-steps of the procedure body. The first two steps in a procedure must always be preparation and initial verifications. Afterwards, each sub-step can refer to telecommanding, telemetry monitoring, control structures (i.e. if, goto, case, wait for/until) or ground segment interaction (e.g. select display).

The procedure body contains the following items:

- Step: is the number of the step and sub-step.
- Operations: gives information about the action performed in the corresponding step and contains the keyword of the action (e.g. send, verify, etc.).
- TC: identifies the TC to be sent.
- Data: is the value assigned to the TC.
- Description: gives a short description of the sent TC or the monitored TM parameter.
- TM: identifies the TM parameter.
- TM Data: is the expected value of the TM parameter.
- Display: identifies the display containing the specified TC or TM value.

### 3.2.2.3 Telemetry Visualisation and Analysis Tool

Spacecraft telemetry gives a complete description of the health status of the satellite and a careful analysis of these data can spot future possible issues. For this reason, we developed a software tool for TM data analysis. The user can select the TM parameters to analyse from a list and specify the datetime interval (Figure 39). Data are then presented in graphical (Figure 41) and scrollable (Figure 40) displays. They can be displayed as engineering units values and raw values (binary, hexadecimal or decimal representation). A quick statistical analysis of these values (mean, standard deviation, maximum and minimum values) is also possible and data can be compared with default, minimum and maximum values where applicable. This application is connected to the DB to retrieve the TM parameter definition and the TM data.

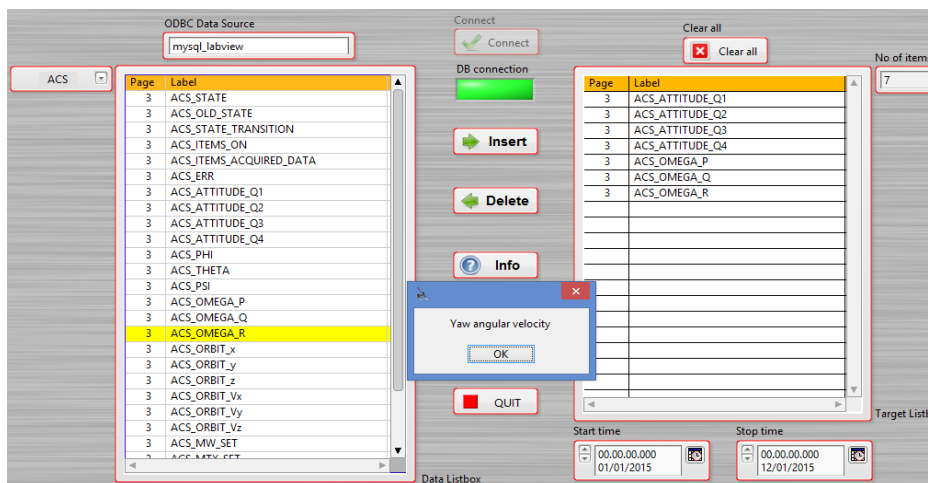


Figure 39. Telemetry Visualisation and Analysis Tool

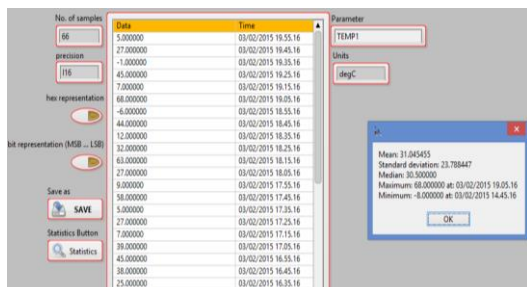


Figure 40. TM Scrollable display and statistical analysis

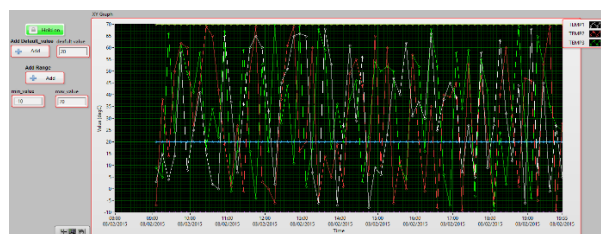


Figure 41. TM Graphical display

#### 3.2.2.4 Users' Requests

Considering the unusually large number of payloads, which will fly on-board ESEO, it is essential to plan an efficient mechanism to handle the numerous payload requests that will arise from the user segment during the mission. Figure 42 shows the lifecycle for each individual user segment payload request at MCC, highlighting the interaction between the MCC and the user segment. The operator and the automatic follow-up system will be in charge of changing the requests' status. The status can be one of the following:

- **ACCEPTED:** on reception of a new payload request, it is first syntactically verified (the operator checks that all required information are provided). In case of no error, it is stored in the DB with the 'accepted' status
- **READY:** simulations have shown that the request can be uploaded to the satellite.
- **REJECTED:** if the request has been uploaded but the satellite has rejected the TC.
- **ACKNOWLEDGED:** the satellite has been successfully executed the request (immediate TC) or inserted into the on-board schedule (TTC).
- **DELETED:** If for any reason, the request is invalid by itself, or cannot be scheduled without violating a predefined constraint. The reason of this rejection is written in the comment text field attached to the request.

In case of contingencies, the operator can manually cancel the upload of a previously "accepted" or "ready" payload request.

If the user segment wishes to re-plan a request, their actions will depend on whether or not the request has already been uploaded or not.

If the user segment wishes to change a TTC that has already been uploaded on-board then the US will notify the S/C operator to delete the request. If the operator cannot delete the request, (e.g. the request will be executed before the next AOS) then the request will be executed.

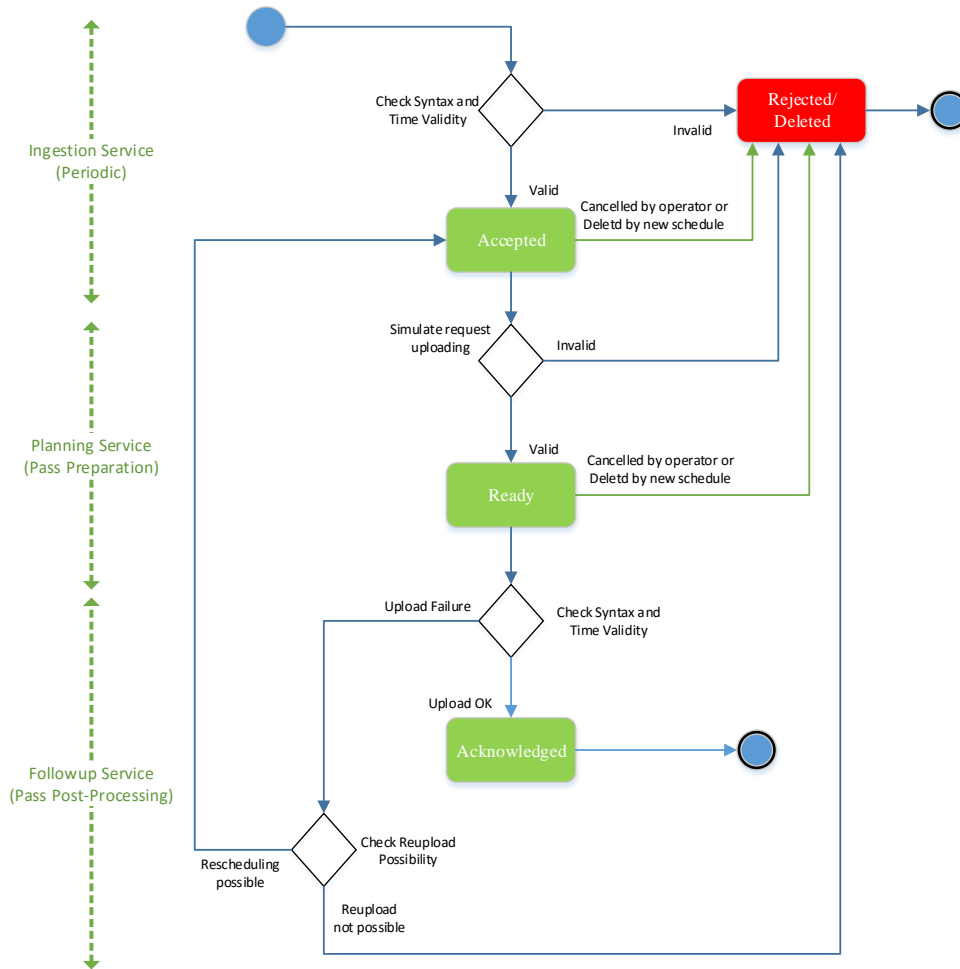


**Figure 42. Lifecycle for each individual payload request at MCC**

### 3.2.3 Spacecraft Simulator

In order to test the automatic procedures and train future S/C operators, an existing satellite mission simulator has been improved adding TM and TC functionalities. The original simulator is based on MATLAB/Simulink and it propagates the attitude and orbit of the satellite considering orbital perturbations, internal and external torques. Recently, we also added the thermal model and the power simulator of the satellite to increase the number of simulated S/C variables [32]. Figure 43 shows the interaction between the ground segment software and the S/C simulator as well as the internal connections. The S/C simulator is composed of three main components:

- AOCS and EPS simulator: it simulates the orbital and attitude dynamics of the S/C, the thermal subsystem and the electrical power subsystem. It is implemented in MATLAB/Simulink/Simscape.

- TMTC interface: it allows to command the simulator through telecommands sent by the ground segment and to collect TM data to be sent to the ground segment [33]. It is implemented in MATLAB/Simulink.
- TXRX, OBDH simulator: this is the counterpart of the software developed for the ground station SDR. Simulating the on-board transceiver, it implements signal acquisition, demodulation and AX.25 decoding and then it forwards the data content to the OBDH. This subsystem is simulated checking if the received command is valid (see 3.2.2) and storing the TTC in a schedule. Immediate and valid commands are directly forward to the TMTC interface whilst TTC are forwarded to the TMTC interface when the execution time expires. Similarly, in uplink operations the same functionalities are performed.

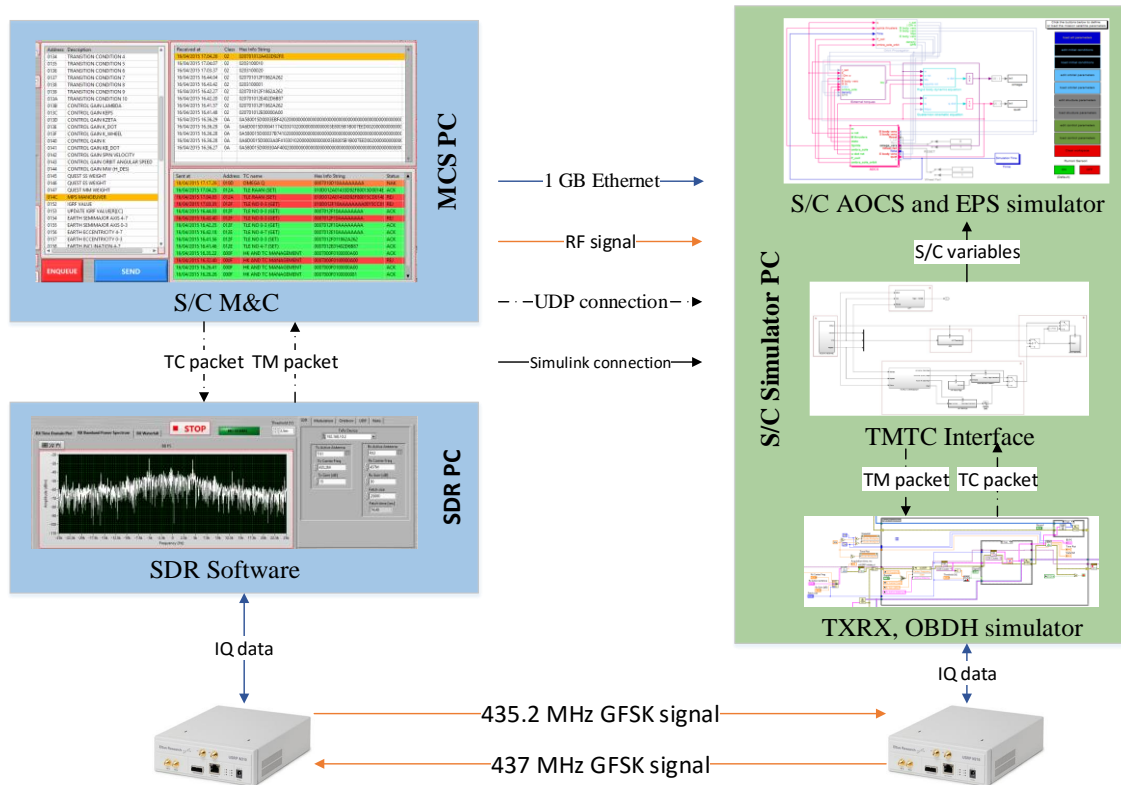


Figure 43. S/C simulator block diagram

### 3.2.4 Code review

The solutions designed for the ESEO ground segment required an extensive code implementation in LabVIEW. Therefore, a systematic examination of source code with the

intent of finding and fixing mistakes that were overlooked during development was needed.

The items to examine during a code review include the following:

- Correctness of implementation
- Interaction with other components
- Robustness and error handling
- Conformance to coding standards/practices
- Readability
- Maintainability
- Reusability
- Completeness

For Testing and Validation (Figure 44), we used an incremental approach, which means: for every delta implementation, we performed a delta testing and validation. LabVIEW offers two tools for this task:

- LabVIEW VI Analyzer: a tool that inspects VIs and recommends modifications to the front panel, block diagram, VI properties and documentation that improves code performance, usability and maintainability. The toolkit includes over 60 different tests that can be run on any VI such as cyclomatic complexity, modularity index and many others.
- LabVIEW Unit Test Framework: a tool for LabVIEW that can be used to automate unit testing, requirements-based validation and regression testing of VIs.



**Figure 44. Software Engineering Process**

## 4. EUMETSAT Ground Station Software Solutions

During an internship at EUMETSAT within the Ground Station and External Interfaces GSEI team lead by Dr. Thomas Sheasby, some innovative software solutions have been implemented to improve ground stations operations. EUMETSAT operates both GEO and LEO satellites to acquire and disseminate Earth observation data for climate change studies weather forecasts.

The currently operative LEO satellites are Metop-A and Metop-B whilst the launch of Metop-C is foreseen for 2018. There are two separate Command and Data Acquisition (CDA) stations located on Spitsbergen, Svalbard, (78°N), providing the capacity to receive the data from all Metop orbits (Figure 45). The stations can also acquire data from the NOAA satellites, in particular for those orbits that are not visible (NOAA blind orbit support) from the NOAA ground stations in Fairbanks and Wallops Island in the USA.



**Figure 45. The Metop satellites are operated via two CDAs collocated in Svalbard, Norway and linked to the operational ground segment in Darmstadt via fibre-optic and satellite communications links**

There are two generations of active GEO satellites: Meteosat First Generation (MFG) and Meteosat Second Generation (MSG), providing images of the full Earth disc and data for weather forecasts. The Primary Ground Station (PGS) supporting the MSG satellites is in Usingen, Germany, about 30 km north of Frankfurt. This ground station is unmanned and can be remotely monitored and controlled from the MCC in Darmstadt. A separate Back-up and Ranging Ground Station (BRGS) is located in Maspalomas, Spain.

The following sections will describe the software solutions implemented for the M&C of these ground stations.

## 4.1 Ground Station Analysis and Reporting Tool

GSAR, the Ground Station Analysis and Reporting tool is a project built on top of the CHART-core framework. CHART (Component Health Assessment and Reporting Tool) is a framework for developing telemetry monitoring tools. It has been used to create CHART-EPS, SAPHIRE, CHART-MSG and other projects. These tools can ingest data from multiple sources, produce automated reports, and offer interactive websites for ad-hoc analysis [34].

The GSAR project receives and ingests telemetry data from Svalbard CDA1 and CDA2. Once ingested, data can be used to build reports or visualised with web-based tools. Each ground station maintains a telnet link to the MCS, which it uses to report a stream of telemetry messages in ASCII form. Each message includes a timestamp, parameter name, a raw and a calibrated value. The incoming messages can be divided into 3 categories:

- Normal background telemetry, sent continually at a low data rate.
- High frequency data bursts during satellite data acquisition periods.
- Parameter refresh, where every 15 minutes the value of all parameters is sent regardless of changes.

In the first two cases, messages are generally only sent when a value changes. All categories have the same data format. The database is Oracle 11g and it is sized to store the data of both ground stations for 3 years ( $\approx 3$  TB) [35].

### 4.1.1 Motivations and Background

Ground station operations and maintenance engineers need to monitor and control the two CDAs in Svalbard in a timely and effective manner to ensure that satellite data are not lost. For this purpose, they can read TM data generated by all devices inside the CDA using a software named *TMPropagator* [36]. This software supports several types of real time display: Alphanumeric Displays (ANDs) show data in text fields, Graphical Displays (GRDs) show the history of one or more parameters graphically as a function of time and mimics (Figure 46) shows the connection between the equipment and highlights warnings and alarms. Data can be retrieved in both real time and playback mode.

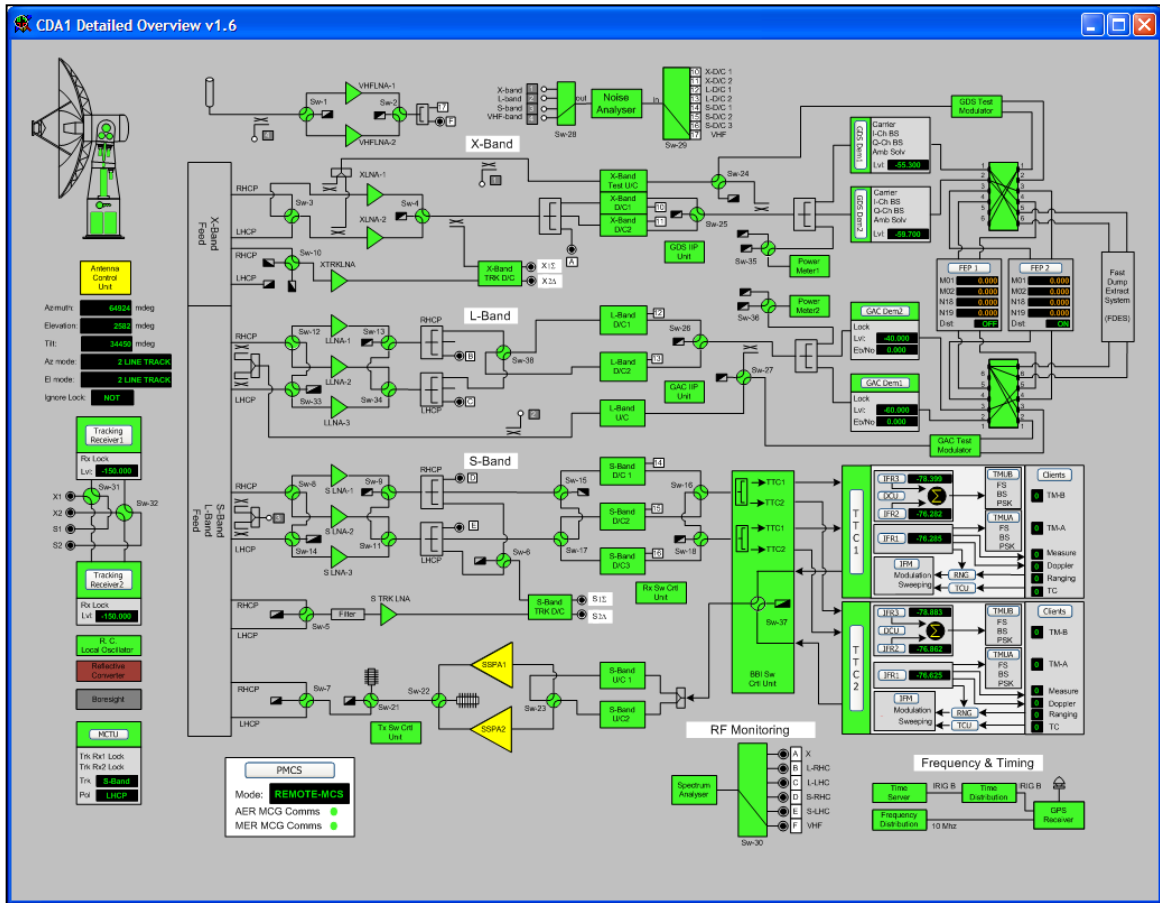


Figure 46. TmPropagator client, CDA1 mimic display

In addition to this tool, ground station engineers would have reports containing a set of CDAs' TM data displayed in tables and plots for both a quick overview and a more detailed investigation. These reports should be generated automatically and periodically and they should be available on a web page through a calendar interface (Figure 47).

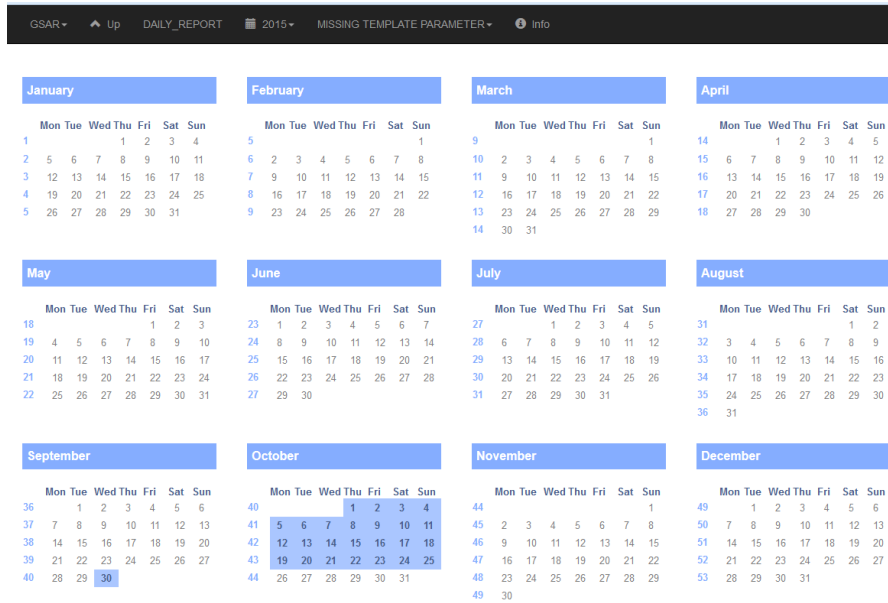


Figure 47. GSAR reports web calendar interface

### 4.1.2 Reports generation

Each report is generated from a template, which is specified by an XML file containing a list of selected widgets. CHART core widgets can be used but they are not always suitable for the requirements of ground station engineers. Therefore, we implemented some GSAR custom widgets, which are described in 4.1.4. The widgets are coded as python classes, which retrieve TM and FD data from the database, build tables and generate plots using the *matplotlib* package. The automatic generation is handled by an XML schedule file, which contains the generation period (i.e. daily, weekly, monthly), time, the name of the activity to perform and the identification of the CDA (cda1 or cda2). The activity is another XML file, which contains the file name of the template. For the content of these files and for a complete development guide, refer to [37].

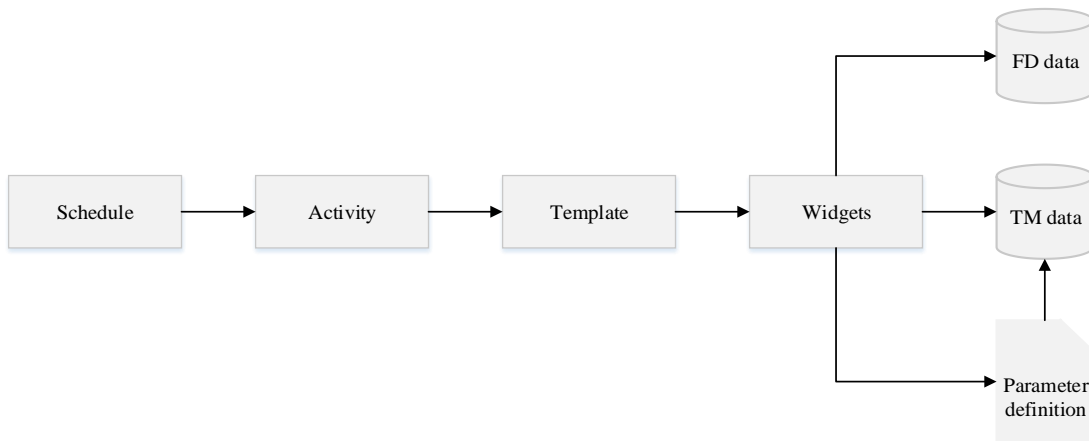


Figure 48. Reports generation flowchart

### 4.1.3 Database definition

Raw TM data injected from the PMCS are stored in a time series key-value store table. In a key-value table, there is a timestamp column, a key (or name) column, and a value column. This is different to a flat (or spreadsheet-like) table where there would be a timestamp column followed by one column for each parameter. In a flat table a complete packet of data, where every field has the same timestamp, can be written as a single row. For GSAR a key-value store is the safest storage mechanism because it allows the possibility of storing highly irregular data efficiently, if every parameter has a unique timestamp, this can be stored easily. A flat table is more efficient for packet-based data, where parameters tend to arrive in groups with the same timestamp. There are around 2000 parameters defined for each CDA and they are enumerated types, counters and physical variables (e.g. temperatures,  $E_bN_0$ , SNR, etc.). The full list of parameters, their descriptions, units, data types and keys is defined in a CSV file constantly updated by ground stations engineers. Another DB table containing FD data is used to retrieve the orbit number of the passes tracked by each CDA.

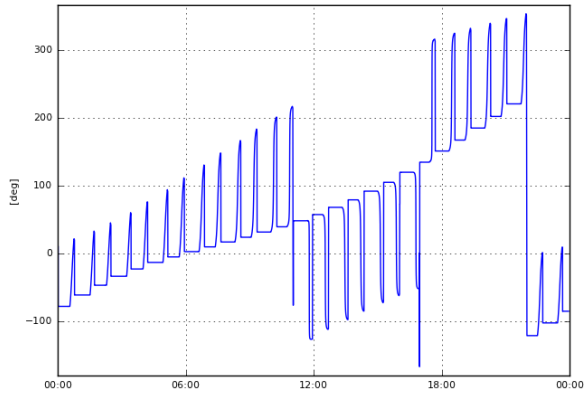
### 4.1.4 Reports content

This section shows how CDAs' TM data are displayed in the reports. These reports completely satisfies the requirements collected from the ground stations engineers. The first widget inserted in the report displays a table containing the number of passes tracked by the selected CDA for each satellite (i.e. M01, M02, N18 and N19) as shown in Figure 49.

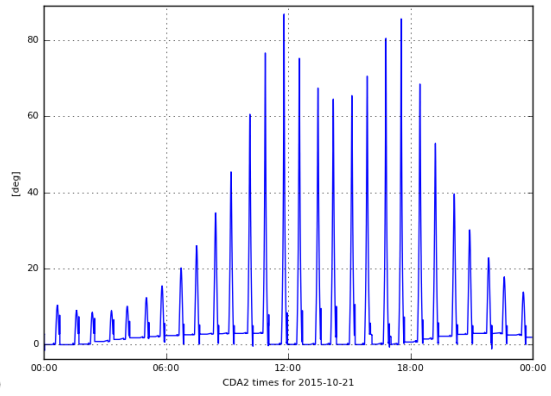
| M01 | M02 | N18 | N19 | Total |
|-----|-----|-----|-----|-------|
| 14  | 14  | 0   | 0   | 28    |

Figure 49. CDA tracked passes counter

Engineers are also interested in monitoring the antenna movement in azimuth (Figure 50), elevation (Figure 51) and tilt (Figure 52 and Figure 53) along a whole day to check that there were not issues in the ACU.



**Figure 50. CDA2 Antenna Azimuth, 21/10/2015**



**Figure 51. CDA2 Antenna Elevation, 21/10/2015**

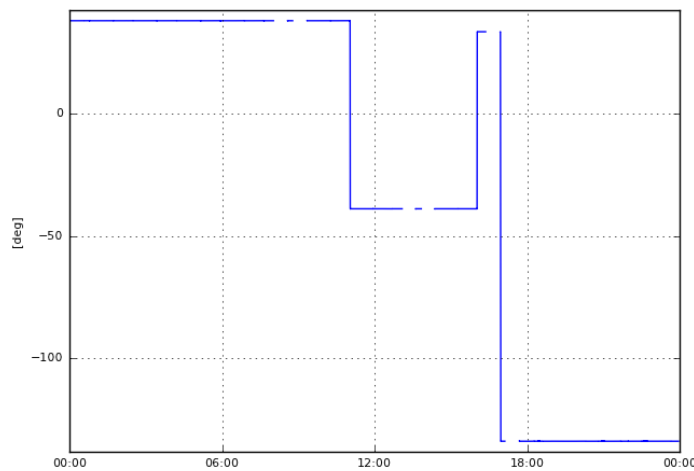


**Figure 52. CDA2 Antenna Tilt, 21/10/2015**

| from [datetime]            | to [datetime]              | delta [datetime] | from [deg] | to [deg] | delta [deg] |
|----------------------------|----------------------------|------------------|------------|----------|-------------|
| 2015-10-21 11:02:10.149000 | 2015-10-21 11:02:52.825000 | 0:00:42.676000   | 38.09      | -38.87   | -76.96      |
| 2015-10-21 16:01:53.418000 | 2015-10-21 16:02:34.173000 | 0:00:40.755000   | -38.87     | 33.57    | 72.44       |
| 2015-10-21 16:57:05.905000 | 2015-10-21 16:58:11.744000 | 0:01:05.839000   | 33.55      | -133.98  | -167.53     |

**Figure 53. CDA2 Antenna Tilt movements, 21/10/2015**

The tilt movements are computed using information on the azimuth and elevation axis since tilt movements occur only when the azimuth and elevation axis are blocked. The state of some CDAs' devices is indicated by dedicated enumerated parameters, which can assume the values reported in Table 19.

**Table 19. CDA's devices status**

| Raw value | Text value         | Mimic colour |
|-----------|--------------------|--------------|
| 0         | Active             | Green        |
| 1         | Connection lost    | Brown        |
| 2         | Alarm              | Red          |
| 3         | Acknowledged alarm | Orange       |
| 4         | Maintenance        | Blue         |
| 5         | Absent             | Cyan         |

| Parameter                              | Active | Cnx Lost | Alarm | Ack Alarm | Maint | Absent |
|--|--------|----------|-------|-----------|-------|--------|
| VANT100: ACU Status                    | 24     | 0        | 76    | 0         | 0     | 0      |
| VTMC600: SSPA 1 Status                 | 28     | 0        | 75    | 0         | 0     | 0      |
| VTMC700: SSPA 2 Status                 | 28     | 0        | 75    | 0         | 0     | 0      |
| VTMC300: TTC 1 Status                  | 59     | 0        | 0     | 0         | 0     | 0      |
| VTMC800: TTC 2 status                  | 58     | 0        | 0     | 0         | 0     | 0      |
| VHDR001: HRDFEP1: HRD1 Status          | 58     | 0        | 0     | 0         | 0     | 0      |
| VHDR350: HRDFEP2: HRD1 Status          | 58     | 0        | 0     | 0         | 0     | 0      |
| VTMC200: RX Switch Control Unit Status | 59     | 0        | 0     | 0         | 0     | 0      |
| VTMC510: TX Switch Control Unit Status | 59     | 0        | 0     | 0         | 0     | 0      |

**Figure 54. CDA2 devices status, 21/10/2015**

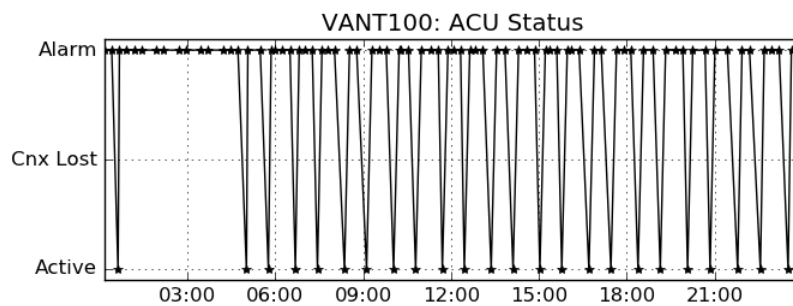


**Figure 55. CDA2 ACU status, 21/10/2015**

More information about the performance of a ground station can be obtained by displaying data for each pass correlating TM data with FD data. Ground station engineers can detect issues during a pass by reading the values listed in Figure 56 and have more information on each pass by looking at the plots generated for each pass (Figure 57).

| SC  | Orbit | AOS time                   | HRDFEP1: FEP1: BTS | HRDFEP2: FEP1: BTS | HRDFEP1: FEP1: Corrected frames | HRDFEP1: FEP1: Uncorrected frames | HRDFEP2: FEP1: Corrected frames | HRDFEP2: FEP1: Uncorrected frames | HRDFEP1: FEP1: Outputs | HRDFEP2: FEP1: Outputs |
|-----|-------|----------------------------|--------------------|--------------------|---------------------------------|-----------------------------------|---------------------------------|-----------------------------------|------------------------|------------------------|
| M02 | 46717 | 2015-10-21 00:34:22.647000 | 4                  | 4                  | 275                             | 1                                 | 269                             | 1                                 | 3674111                | 3674108                |
| M01 | 16031 | 2015-10-21 01:31:07.617000 | 1                  | 1                  | 313                             | 0                                 | 324                             | 0                                 | 3674142                | 3674130                |
| M02 | 46718 | 2015-10-21 02:17:38.067000 | 2                  | 2                  | 168                             | 1                                 | 172                             | 1                                 | 3674154                | 3674164                |
| M01 | 16032 | 2015-10-21 03:14:05.817000 | 1                  | 1                  | 123                             | 1                                 | 122                             | 1                                 | 3674098                | 3674088                |
| M02 | 46719 | 2015-10-21 04:00:13.891000 | 2                  | 2                  | 264                             | 0                                 | 262                             | 0                                 | 3674109                | 3674106                |
| M01 | 16033 | 2015-10-21 04:56:17.060000 | 0                  | 1                  | 331                             | 0                                 | 335                             | 1                                 | 3662200                | 3674129                |
| M02 | 46720 | 2015-10-21 05:42:04.187000 | 1                  | 2                  | 122                             | 1                                 | 119                             | 3                                 | 3674104                | 3674120                |
| M01 | 16034 | 2015-10-21 06:37:49.221000 | 1                  | 1                  | 1                               | 0                                 | 1                               | 0                                 | 3674107                | 3674123                |
| M02 | 46721 | 2015-10-21 07:23:22.190000 | 0                  | 1                  | 0                               | 0                                 | 0                               | 1                                 | 3670026                | 3674101                |
| M01 | 16035 | 2015-10-21 08:18:54.934000 | 1                  | 1                  | 0                               | 1                                 | 0                               | 1                                 | 3674106                | 3674121                |
| M02 | 46722 | 2015-10-21 09:04:17.505000 | 0                  | 1                  | 0                               | 0                                 | 0                               | 1                                 | 3662200                | 3674555                |
| M01 | 16036 | 2015-10-21 09:59:40.269000 | 1                  | 1                  | 0                               | 1                                 | 0                               | 1                                 | 3674111                | 3674110                |
| M02 | 46723 | 2015-10-21 10:44:53.524000 | 1                  | 1                  | 0                               | 1                                 | 0                               | 1                                 | 3674471                | 3674469                |

**Figure 56. CDA2 tracked passes with FD information (S/C, orbit, AOS time) and TM data (BTSE, corrected, uncorrected and received frames), 21/10/2015**

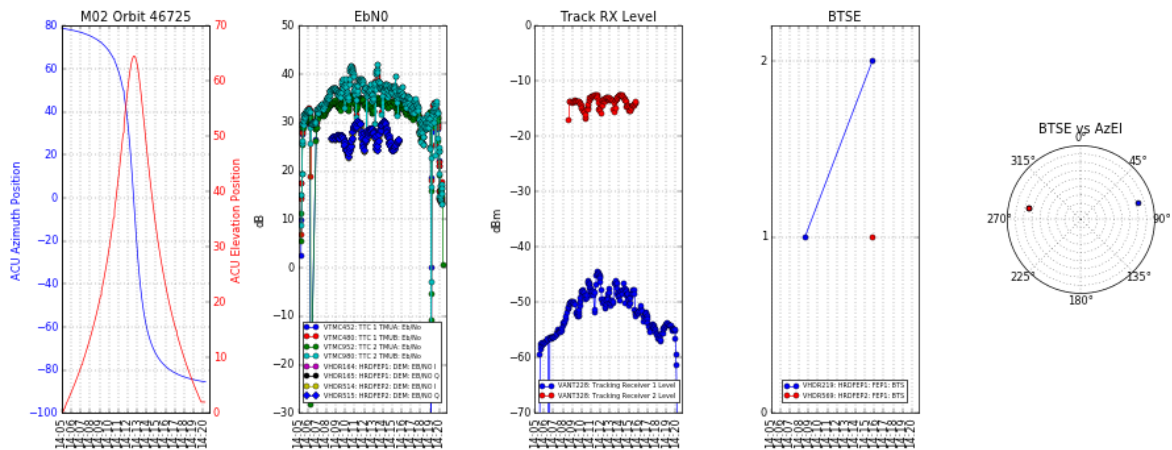


**Figure 57. CDA2 TM data during M02 pass, orbit 46725**

Figure 57 shows five subplots displaying a selection of significant TM data during Metop-A pass. The first subplot shows the antenna azimuth and elevation on twin axes, the second subplot displays the  $E_b/N_0$  values for different frequency bands; the third subplot illustrates the tracking receiver levels (S-band in blue and X-band in red); the last two subplots show the number of the BTSE counted by the HRDFEP in hot redundancy (HRDFEP1 and HRDFEP2) in a time scale and in a polar plot. To generate the polar plot we needed to interpolate the azimuth and elevation timestamp with the BTSE timestamps since each parameter is sampled at a different time.

When analysing the plots like the one shown in Figure 57, we should take into consideration that NOAA satellites payload downlink is at L-band while Metop satellites payload

downlink is at X-band and telemetry data are downloaded at S-band for both satellites (see Table 20 and Figure 58).

**Table 20. Metop and NOAA satellites frequencies**

| Satellite    | TT&C Uplink [MHz]     | TT&C Downlink [MHz]   | Data Downlink [MHz]          |
|--------------|-----------------------|-----------------------|------------------------------|
| <b>Metop</b> | 2026 (S-band) @ 2kbps | 2230 (S-band) @ 4kbps | 7750-7900 (X-band) @ 70 Mbps |
| <b>NOAA</b>  | 2053 (S-band)         | 2247.5 (S-band)       | 1698, 1702.5, 1707 (L-band)  |

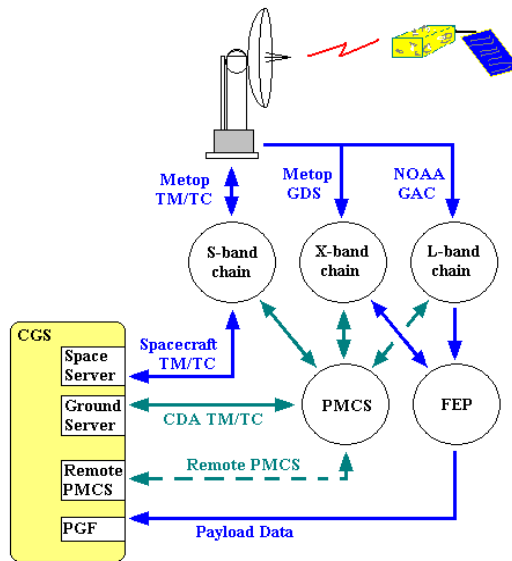


**Figure 58. CDA high level block diagram**

Another aspect to take into consideration is that the X-band downlink occurs around the maximum elevation point as highlighted in Figure 67.

#### 4.1.5 Repeat cycle analysis

If Earth makes an integral number of rotations in the time taken for the LEO satellite to complete an integral number of orbits, the sub-satellite track repeats exactly. This time span is called repeat cycle. The existence of a repeat cycle means that a whole number of revolutions can be completed in exactly a whole number of days. The orbital period determines the number of orbits  $N$  that the satellite runs in 24 hours, which is normally not an integer. In order to obtain a repeat cycle of  $m$  days, the orbital period is adjusted to ensure that  $N \cdot m$  is an integer.  $N$  can then be expressed in the following form where  $n$  and  $l$  are respectively the quotient and remainder of the integer division of  $N \cdot m$  by  $m$ :

$$N = n + l/m, \text{ with } n, l \text{ and } m \text{ integers } (l < m)$$

Metop satellites orbit has been designed to have a repeat cycle as reported in Table 21. The repeat cycle is of particular interest because TM data, like  $E_bN_0$  and tracking receiver levels can be compared during a pass under the same conditions in terms of azimuth and elevation.

**Table 21. Metop repeat cycle values**

| <b>Period</b> | <b>No. of orbits per day</b> | <b>Cycle</b> | <b>Revs/cycle</b> | <b>Main sub-cycles</b> |
|---------------|------------------------------|--------------|-------------------|------------------------|
| 101.36 min    | 14 + 6/29                    | 29 days      | 412               | 5 days                 |

Nominally, ground stations operations engineers schedule Metop passes to one CDA and NOAA passes to the other CDA. However, due to CDAs maintenance and upgrades, the assignement is changed from time to time: this is named mission swap. Therefore, due to the mission swap, the CDA used to track the same satellite can be different when we analyse several cycles. The script can detect the right CDA by counting the number of items returned by the DB selection query. In fact, as stated in 4.1, data are acquired at a higher frequency during a pass, resulting in a higher number of items from the DB if the query is submitted for the time period corresponding to a pass. This script also needs FD data, since it retrieves the AOS and LOS values for the initial given orbit number and for the previous orbits every cycle (412 orbits). Figure 59 shows the result generated from this script for the S-band  $E_bN_0$  of Metop-A. Each subplot contains the value for this parameter during a pass where the orbit number is given by:

$$n_i = n_0 - i \cdot 412, i = 0, \dots, N$$

where  $n_0$  is the initial orbit number given as input and  $N$  is the number of cycles to be investigated. In order to ease the comparison, the y-axis is shared and x-axis is given in terms of the antenna elevation instead of time.

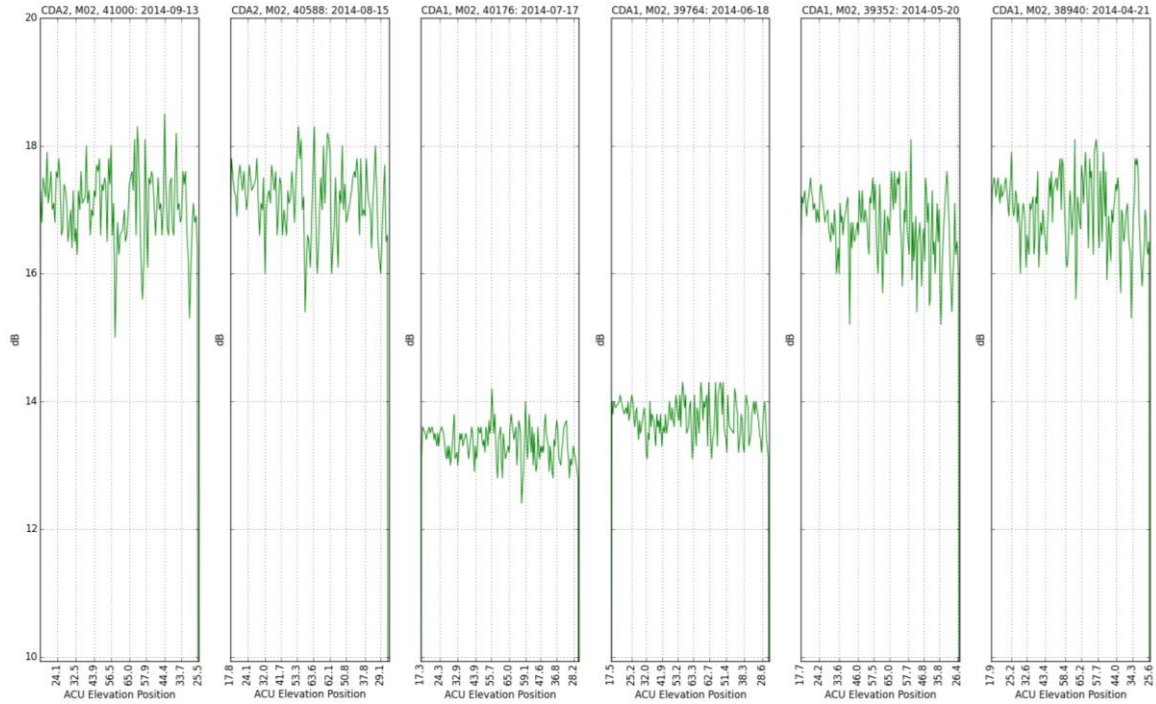


**Figure 59. Metop-A S-band  $E_bN_0$  repeat cycle comparison**

#### 4.1.6 Code verification and results validation

Before installing the implemented code in the operational environment, it has been checked using *pylint* for coding standard and error detection. Some of the coding standards checks are line-code's length, trailing whitespaces, missing spaces around operators, if imported modules are used, missing docstrings, etc. It is important to be compliant to this standard to enhance code readability and ease its maintainability.

The results generated by this tool have been validated by comparing the plots and values with *TMPPropagator* displays as shown in Figure 60 and Figure 61.

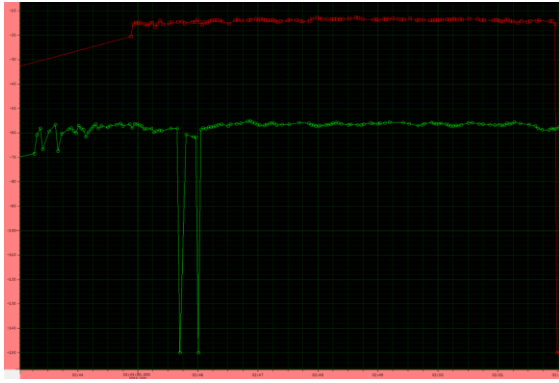


**Figure 60.** *TMPropagator* GRD, CDA tracking receiver levels

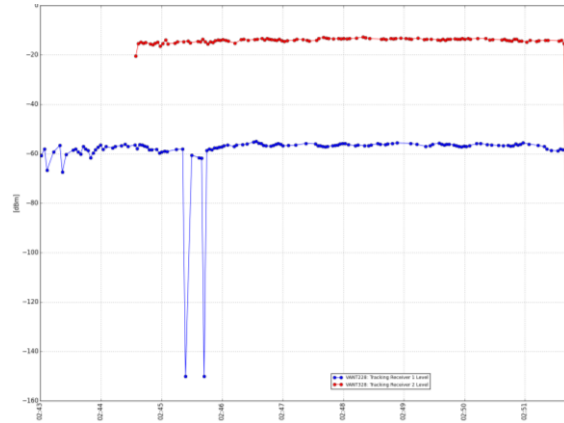


**Figure 61.** GSAR, CDA tracking receiver levels

## 4.2 Satellite Passes And Conflicts Engine

SPACE, the satellite passes and conflicts engine is an application developed in *python* which offers an easy way to compute visibility passes of a satellite group over a GSN, detect and resolve pass conflicts based on a satellite priority list defined for each ground station.

The application is based on a TLE propagator, which implements the simplified perturbation model SGP4. The user can select between the *pyephem* [38] and *pyorbital* [39] *python* packages. *Pyephem* is built on top of *XEphem*, a C library for basic astronomical computations and is used by other projects, like SATNet [40] and SatNOGS [41]. *Pyorbital* is part of a project named *pytroll*, which provides different free and open source *python* modules for the reading, interpretation and writing of weather satellite data. SPACE can be used through a simple and intuitive interface and results are presented as pictures and tables in HTML pages.

### 4.2.1 Applications

SPACE have been implemented and validated at EUMETSAT for the Initial Joint Polar System IJPS. The SS of the IJPS comprises the satellites listed in Table 22.

The considered GSN comprises EUMETSAT and NOAA ground stations and the ESTRACK core network (see Table 23). Svalbard CDAs track Metop satellites and offer support to NOAA satellites, mainly during blind orbits. These CDAs are far enough north to track all 14 orbits a day. Fairbanks and Wallops track NOAA satellites but they cannot offer a coverage for all 14 orbits a day.

**Table 22. IJPS satellites**

| Satellite | Launch Date     | Inclination (deg) | Altitude (km) | LTAN     | Period (min) | Operational Status |
|-----------|-----------------|-------------------|---------------|----------|--------------|--------------------|
| METOP-A   | 19/10/2006      | 98.70             | 817           | 21:29:05 | 101.36       | AM Backup          |
| METOP-B   | 17/09/2012      | 98.70             | 817           | 21:31:45 | 101.36       | AM Primary         |
| METOP-C   | 2018 (foreseen) | N/A               | N/A           | N/A      | N/A          | N/A                |
| NOAA-18   | 20/05/2005      | 98.74             | 854           | 16:58:11 | 102.12       | PM Secondary       |
| NOAA-19   | 06/02/2009      | 98.70             | 870           | 14:09:47 | 102.14       | PM Primary         |

**Table 23. Ground Stations location**

| Antenna       | Longitude (deg) | Latitude (deg) | Altitude (km) |
|---------------|-----------------|----------------|---------------|
| Svalbard CDA1 | 15.388229269    | 78.228981740   | 0.490818934   |
| Svalbard CDA2 | 15.401320535    | 78.228562464   | 0.495385340   |
| Fairbanks     | -147.505823340  | 64.973760002   | 0.397033060   |
| Wallops       | -75.462919721   | 37.947340276   | -0.021250002  |
| McMurdo       | 166.650000022   | -77.849999998  | 0.157000215   |
| Kourou        | -52.804663716   | 5.251439108    | -0.014670939  |
| Villafranca   | -3.952597571    | 40.445595405   | 0.664791780   |
| Perth         | 115.885163931   | -31.802518955  | 0.022160714   |
| Maspalomas    | -15.633800861   | 27.762889290   | 0.205117772   |

McMurdo ground station tracks Metop passes within the Antarctic Data Acquisition (ADA) service halving the data transfer from satellite to ground station as illustrated in Figure 62.

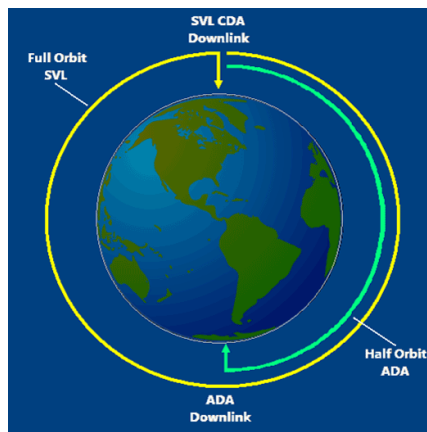


**Figure 62. Antarctic Data Acquisition service. © EUMETSAT**

The ground stations horizon mask are given as CSV files where the first column is a sequence of azimuth values from 0° to 359° with a step of 1° and the second column is the corresponding elevation value of the mask with an accuracy ranging from 0.1° to 1° depending on the ground station.

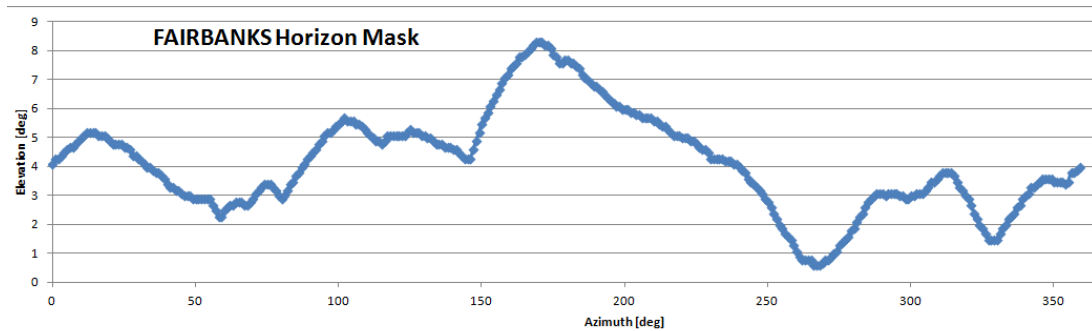


Figure 63. Fairbanks horizon mask

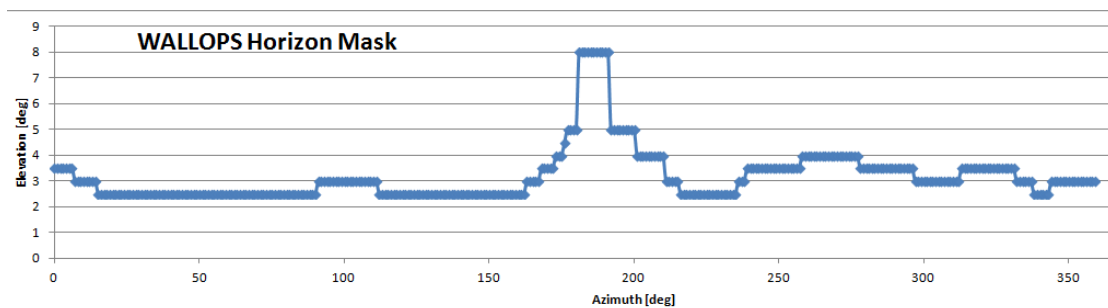


Figure 64. Wallops horizon mask

The usage of SPACE can be easily extended to other LEO satellites and ground stations. An XML configuration file allows the user to specify the list of satellites and ground stations. SPACE has also been tailored to meet the requirements of EUMETSAT ground stations operations engineers adding a section, which allows computing NOAA blind orbits according to the definition given in the ICD:

*“Pass where visibility is less than 7 minutes between FRT and LRT at both the Fairbanks and Wallops CDAs”.*

Where FRT stands for first receive time and it is defined as:

*“A NOAA term for the time (rounded up to the nearest 10 seconds) when the elevation of a rising satellite is equal to the elevation of the CDA’s horizon mask. The delta time between AOS(0) and FRT is constrained by SOMS to be no less than 30 seconds”.*

Similarly, LRT stands for last receive time and it is defined as:

“A NOAA term for the time (rounded down to the nearest 10 seconds) when the elevation of a setting satellite is equal to the elevation of the CDA’s horizon mask. The delta time between LRT and LOS(0) is constrained by SOMS to be no less than 30 seconds”.

In a nominal scenario, NOAA passes are scheduled to one Svalbard CDA and Metop passes to the other CDA as depicted in Figure 65 but when one of the two CDAs undergoes maintenance or upgrades, it is needed to prepare a conflict-free pass planning over the available CDA.

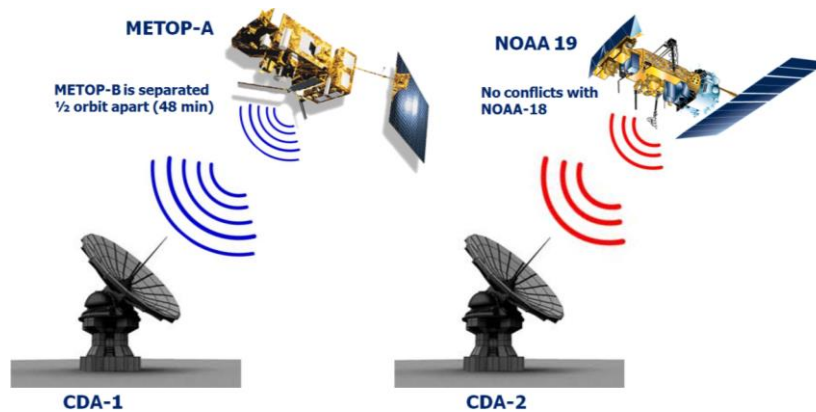


Figure 65. Svalbard CDAs nominal pass planning

#### 4.2.2 Graphical User Interface

The GUI for the SPACE application (Figure 66) has been implemented using *Tkinter*, the most commonly used GUI programming toolkit for *python*. In the menu bar, there are three available options: *File*, *Edit* and *Help*. The *File* option contains the *Data* command, which opens an HTML page containing tables listing ground stations location and satellites TT&C frequencies and the *Quit* command to exit the application. Data are presented directly from the configuration file using an XSL transformation. The *Edit* option contains the *Configuration* command to open the configuration file in edit mode. The *Help* option contains the *About* command to open an EUMETSAT web page about the EPS and the *Help Contents* to open a user guide.

The three tabs allows to separate the different functionalities provided by the application: the first tab allows computing passes and resolve conflicts for any satellites group and GSN; the second tab is tailored for NOAA blind orbits support from Svalbard CDA and the third tab allows computing detailed information for the next pass of a selected satellite over a selected ground station.

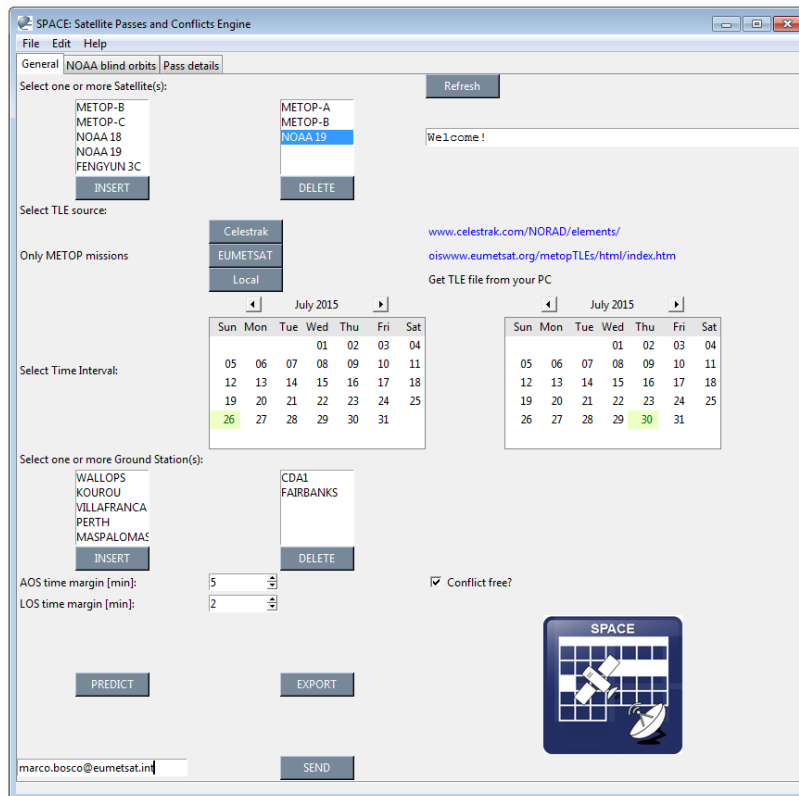


Figure 66. SPACE graphical user interface

The TLEs can be retrieved from *CelesTrack* [42], EUMETSAT website [43] or from a local folder. The TLE should follow the NORAD format:

```

AAAAAAAAAAAAAAAAAAAAAAAAAAAA
1 NNNNNU NNNNNAAA NNNNN.NNNNNNNNN +.NNNNNNNN +NNNNN-N +NNNNN-N N NNNNN
2 NNNNN NNN.NNNN NNN.NNNN NNNNNNNN NNN.NNNN NNN.NNNN NN.NNNNNNNNNNNNNNN

```

Where columns with a space or period can have no other character. Columns with an 'N' can have any number 0-9 or, in some cases, a space. Columns with an 'A' can have any character A-Z or a space. The column with a 'C' can only have a character representing the classification of the element set, normally either a 'U' for unclassified data or an 'S' for secret data (of course, only unclassified data are publicly available). Columns with a '+' can have either a plus sign, a minus sign, or a space and columns with a '-' can have either a plus or minus sign (if the rest of the field is not blank) [42].

Here an example of METOP-B TLEs:

```

METOP-B
1 38771U 12049A 15316.45144032 .00000093 00000-0 62456-4 0 9990
2 38771 98.6795 14.0746 0001866 111.1497 340.7088 14.21505995163482

```

**Table 24. TLE set format definition**

| <b>Line 1</b> |   |                |
|---------------|---|----------------|
| <b>Column</b> | <b>Description</b>  | <b>Example</b> |
| <b>01</b>     | Line Number of Element Data   | [1]            |
| <b>03-07</b>  | Satellite Number  | [38771]        |
| <b>08</b>     | Classification (U = Unclassified)   | [U]            |
| <b>10-11</b>  | International Designator (Last of two digits of launch year)  | [12]           |
| <b>12-14</b>  | International Designator (Launch number of the year)  | [049]          |
| <b>15-17</b>  | International Designator (Piece of the launch)  | [A]            |
| <b>19-20</b>  | Epoch Year (Last two digits of year)  | [15]           |
| <b>21-32</b>  | Epoch (Day of the year and fractional portion of the day)   | [316.45144032] |
| <b>34-43</b>  | First Time Derivative of the Mean Motion, revolutions per day   | [ .00000093]   |
| <b>45-52</b>  | Second Time Derivative of Mean Motion (decimal point assumed)   | [ 00000-0]     |
| <b>54-61</b>  | BSTAR drag term (decimal point assumed) for SGP4 perturbations (otherwise radiation pressure coefficient) | [ 62456-4]     |
| <b>63</b>     | Ephemeris type  | [0]            |
| <b>65-68</b>  | Element number  | [ 999]         |
| <b>69</b>     | Checksum (Modulo 10)<br>(Letters, blanks, periods, plus signs = 0; minus signs = 1)                       | [0]            |
| <b>Line 2</b> |   |                |
| <b>Column</b> | <b>Description</b>  | <b>Example</b> |
| <b>01</b>     | Line Number of Element Data   | [2]            |
| <b>03-07</b>  | Satellite Number  | [38771]        |
| <b>09-16</b>  | Inclination (degrees)   | [ 98.6795]     |
| <b>18-25</b>  | Right Ascension of the Ascending Node (degrees)   | [ 14.0746]     |
| <b>27-33</b>  | Eccentricity (decimal point assumed at beginning)   | [0001866]      |
| <b>35-42</b>  | Argument of Perigee (degrees)   | [111.1497]     |
| <b>44-51</b>  | Mean Anomaly (degrees)  | [340.7088]     |
| <b>53-63</b>  | Mean Motion (revs per day)  | [14.21505995]  |
| <b>64-68</b>  | Revolution number at epoch (revs)   | [16348]        |
| <b>69</b>     | Checksum (modulo 10)  | [2]            |

The spin-boxes labelled by AOS and LOS time margin can be used to set the time in minutes to allow for time margin between two passes to compute conflicts. This means that for each pass:

$$AOS_{time} = AOS_{time} - AOS_{margin}$$

$$LOS_{time} = LOS_{time} + LOS_{margin}$$

These margins named *conf* and *stby* are highlighted in Figure 67. It also shows some other events during a pass like the time when the satellite is first above and below the horizon mask during rising and setting (*AOS\_M* and *LOS\_M*), the AOS(0) time plus 5 minutes (*AOS\_5*) and LOS(0) time minus 5 minutes (*LOS\_5*) and the start and stop of the X-band dump (XBS). Currently, there is an ongoing investigation to reduce these time margins to allow scheduling more passes which means providing greater support to NOAA, greater maintenance options and in the future also accommodating METOP-C passes (to be launched in 2018) and supporting EPS-SG (to be launched in 2020). This tool helps to investigate for these potential benefits by changing the AOS and LOS time margin and compare the results for different values.

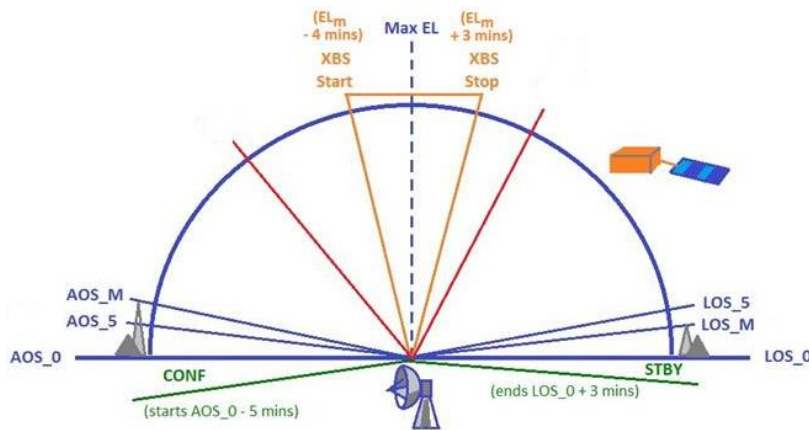


Figure 67. Satellite pass events

#### 4.2.2.1 Error handling

To avoid an application to crash ungracefully it is important to handle errors properly. *Python*, like some other languages (e.g. *LabVIEW*, *Java* ...) offers some built-in functions that can be used for this purpose. A message or warning error pops up when the user inserts unexpected values to the application through the interface. Below some possible cases:

- “Cannot connect to URL” is displayed when the user tries to download TLEs from the website but this is not available.
- “Please select at least one satellite” is displayed when the user tries to get TLEs before selecting at least one satellite.
- “Please insert an e-mail address” is displayed if the user tries to send the report before inserting an e-mail address.
- “Invalid datetime range” is displayed when the stop date is equal or less than the start date.

- “Please select at least one ground station” is displayed if the user tries to predict passes before selecting at least one ground station.
- “No tables to save” is displayed when the user tries to export data before predicting passes.
- “Failed to send e-mail to address” is displayed if the e-mail cannot be sent due to connectivity issues (e.g. connection to SMTP server)
- “Syntax error in the configuration file” is displayed at the application start or later after the file has been edited if the XML syntax has not been respected.

### 4.2.3 Results

This section reports some of the outputs generated by this application. Pictures are generated using *matplotlib* whilst tables are created using *pandas*. An extract of the list of passes ordered by ground station and AOS time is shown in Figure 68 and a small table summarises the number of passes of each satellite over each ground station (Figure 69). The duration is computed as the difference between the rise time, AOS(0) and the set time, LOS(0) whilst the real duration is computed as the difference between FRT and LRT.

| GS   | Spacecraft | Rise Time (UTC)     | Rise Az (deg) | Max El Time (UTC)   | Max El (deg) | Set Time (UTC)      | Set Az (deg) | Duration | Real Duration | Orbit |
|------|------------|---------------------|---------------|---------------------|--------------|---------------------|--------------|----------|---------------|-------|
| CDA1 | NOAA19     | 2015-07-18 23:58:13 | 7.7           | 2015-07-19 00:05:37 | 24.5         | 2015-07-19 00:13:02 | 144.8        | 14:48    | 12:40         | 33198 |
| CDA1 | METOP-B    | 2015-07-19 00:34:12 | 279.2         | 2015-07-19 00:40:16 | 10.6         | 2015-07-19 00:46:20 | 22.3         | 12:8     | 10:50         | 14695 |
| CDA1 | METOP-A    | 2015-07-19 01:21:15 | 294.9         | 2015-07-19 01:27:05 | 9.2          | 2015-07-19 01:32:56 | 32.8         | 11:40    | 10:30         | 45382 |
| CDA1 | NOAA19     | 2015-07-19 01:39:52 | 22.4          | 2015-07-19 01:47:43 | 42.3         | 2015-07-19 01:55:34 | 180.2        | 15:41    | 13:0          | 33199 |
| CDA1 | METOP-B    | 2015-07-19 02:17:24 | 310.2         | 2015-07-19 02:23:13 | 8.6          | 2015-07-19 02:29:03 | 46.7         | 11:39    | 9:30          | 14696 |
| CDA1 | METOP-A    | 2015-07-19 03:04:15 | 323.0         | 2015-07-19 03:10:05 | 8.9          | 2015-07-19 03:15:55 | 60.1         | 11:39    | 9:50          | 45383 |
| CDA1 | NOAA19     | 2015-07-19 03:21:09 | 37.9          | 2015-07-19 03:29:14 | 71.4         | 2015-07-19 03:37:18 | 213.7        | 16:9     | 14:30         | 33200 |
| CDA1 | METOP-B    | 2015-07-19 04:00:04 | 334.8         | 2015-07-19 04:06:05 | 10.1         | 2015-07-19 04:12:06 | 76.3         | 12:1     | 9:20          | 14697 |
| CDA1 | METOP-A    | 2015-07-19 04:46:32 | 344.2         | 2015-07-19 04:52:50 | 12.1         | 2015-07-19 04:59:08 | 92.7         | 12:36    | 10:40         | 45384 |
| CDA1 | NOAA19     | 2015-07-19 05:02:18 | 56.0          | 2015-07-19 05:10:19 | 78.0         | 2015-07-19 05:18:20 | 244.4        | 16:2     | 14:40         | 33201 |
| CDA1 | METOP-B    | 2015-07-19 05:42:03 | 353.5         | 2015-07-19 05:48:41 | 15.3         | 2015-07-19 05:55:20 | 111.2        | 13:16    | 11:40         | 14698 |
| CDA1 | METOP-A    | 2015-07-19 06:28:10 | 0.8           | 2015-07-19 06:35:16 | 19.4         | 2015-07-19 06:42:22 | 129.4        | 14:11    | 12:40         | 45385 |

Figure 68. Visibility passes list

|         | CDA1 | FAIRBANKS | TOTAL |
|---------|------|-----------|-------|
| METOP-A | 57   | 46        | 103   |
| NOAA19  | 57   | 47        | 104   |
| METOP-B | 56   | 45        | 101   |
| TOTAL   | 170  | 138       | 308   |

Figure 69. Visibility passes summary

The maximum elevation and pass duration are plotted for each ground station as shown in Figure 70 and Figure 71.

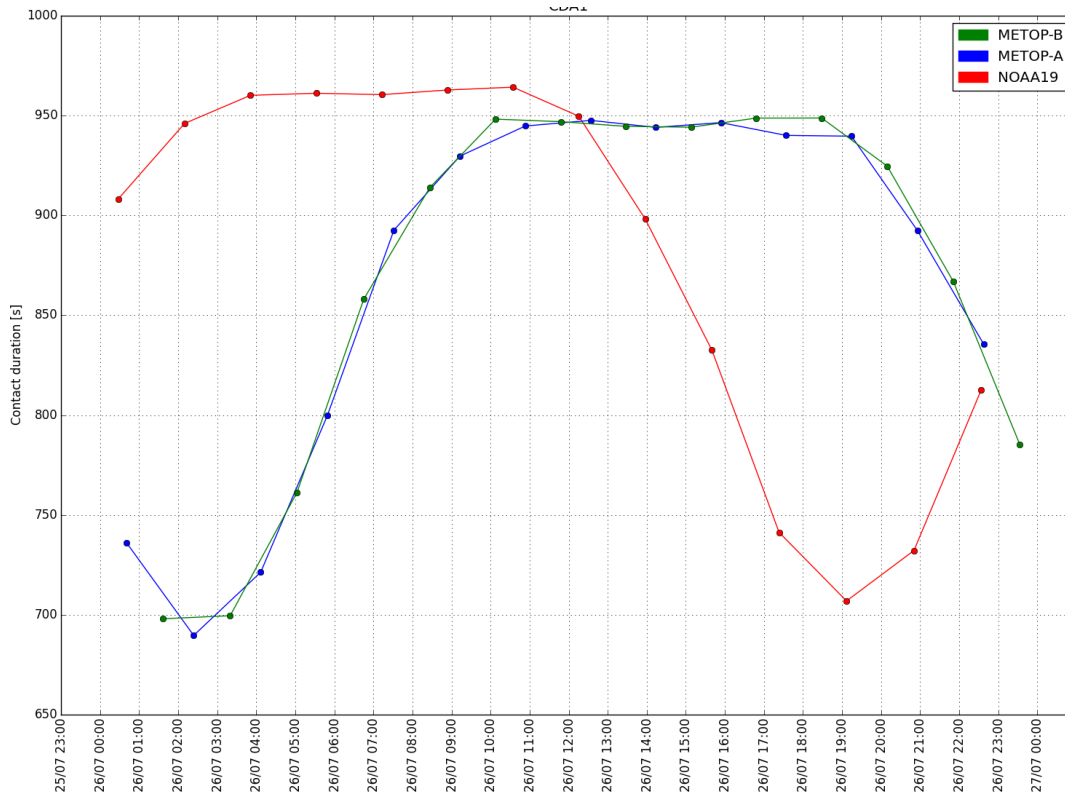


Figure 70. Satellites passes duration over CDA1 during one day

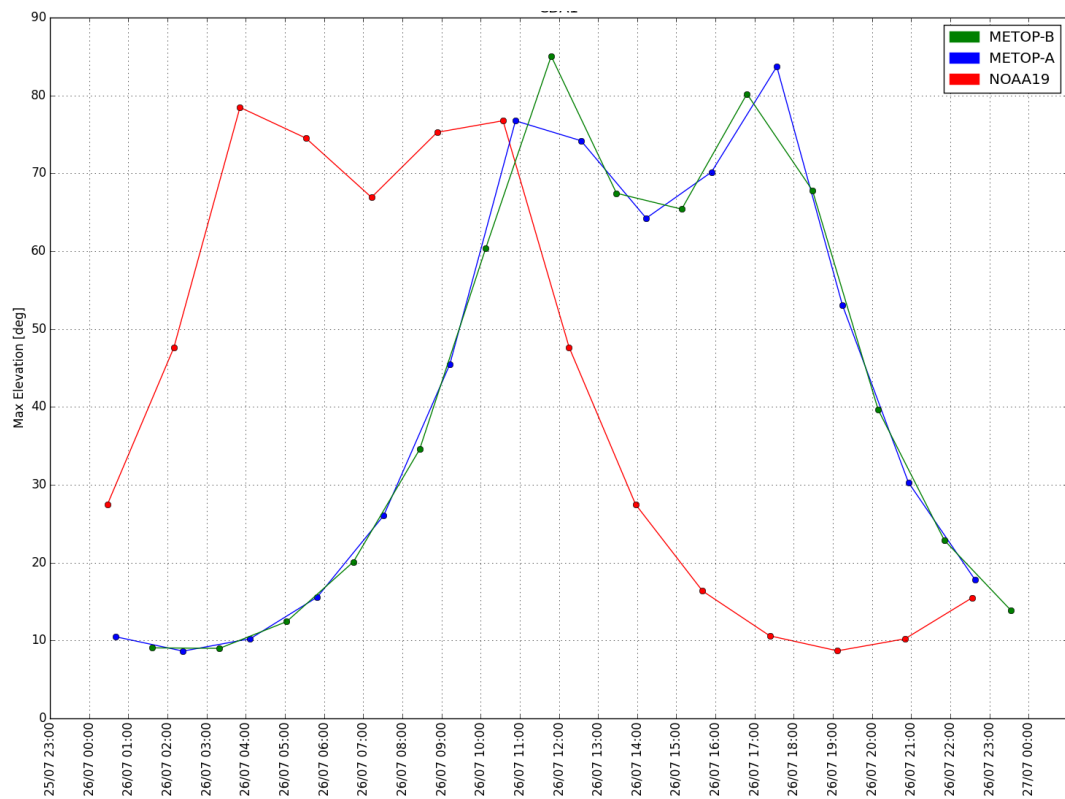


Figure 71. Satellites passes maximum elevation over CDA1 during one day

Another table (Figure 72) shows the conflicts between pairs of satellites passes over the same ground station. The conflict duration also takes into account the AOS and LOS margins.

|    | GS   | S/C pair          | start time (UTC)    | stop time (UTC)     | duration |
|----|------|-------------------|---------------------|---------------------|----------|
| 0  | CDA1 | (METOP-A, NOAA19) | 2015-07-26 00:29:44 | 2015-07-26 00:37:35 | 0:7:51   |
| 1  | CDA1 | (METOP-A, NOAA19) | 2015-07-26 02:12:57 | 2015-07-26 02:19:49 | 0:6:52   |
| 2  | CDA1 | (METOP-A, NOAA19) | 2015-07-26 03:55:37 | 2015-07-26 04:01:12 | 0:5:35   |
| 3  | CDA1 | (METOP-A, NOAA19) | 2015-07-26 05:37:34 | 2015-07-26 05:42:14 | 0:4:40   |
| 4  | CDA1 | (METOP-A, NOAA19) | 2015-07-26 07:18:49 | 2015-07-26 07:22:47 | 0:3:58   |
| 5  | CDA1 | (METOP-A, NOAA19) | 2015-07-26 08:59:50 | 2015-07-26 09:03:25 | 0:3:35   |
| 6  | CDA1 | (METOP-A, NOAA19) | 2015-07-26 10:40:23 | 2015-07-26 10:44:27 | 0:4:4    |
| 7  | CDA1 | (METOP-A, NOAA19) | 2015-07-26 12:20:47 | 2015-07-26 12:25:33 | 0:4:46   |
| 8  | CDA1 | (METOP-A, NOAA19) | 2015-07-26 14:00:43 | 2015-07-26 14:07:01 | 0:6:18   |
| 9  | CDA1 | (METOP-A, NOAA19) | 2015-07-26 15:40:38 | 2015-07-26 15:49:05 | 0:8:27   |
| 10 | CDA1 | (METOP-A, NOAA19) | 2015-07-26 17:20:54 | 2015-07-26 17:31:26 | 0:10:32  |
| 11 | CDA1 | (METOP-A, NOAA19) | 2015-07-26 19:01:26 | 2015-07-26 19:14:49 | 0:13:23  |
| 12 | CDA1 | (METOP-A, NOAA19) | 2015-07-26 20:42:59 | 2015-07-26 20:58:36 | 0:15:37  |
| 13 | CDA1 | (METOP-A, NOAA19) | 2015-07-26 22:25:17 | 2015-07-26 22:42:35 | 0:17:18  |

Figure 72. Satellites passes conflicts table

If the conflict resolution checkbox is checked, SPACE generates a conflict-free schedule displayed as a table, Gantt chart (Figure 73) and pie chart for each ground station (Figure 74).

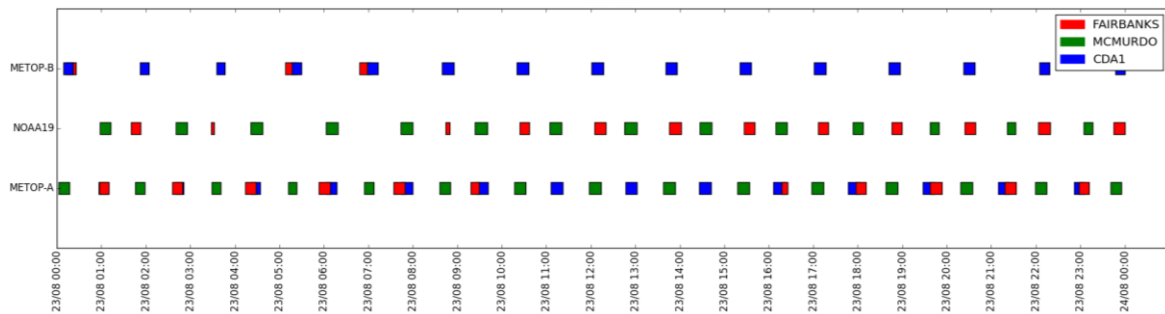


Figure 73. One-day conflict-free schedule for Metop-A, Metop-B, NOAA19 over Fairbanks, McMurdo and Svalbard

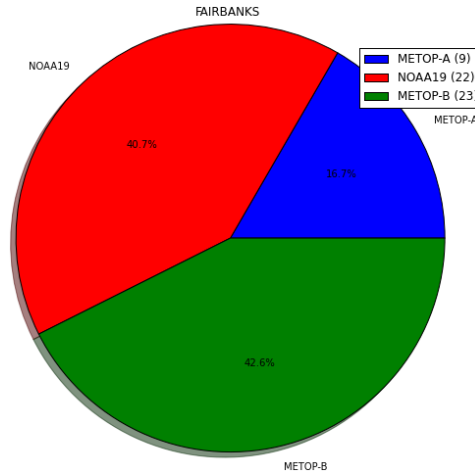


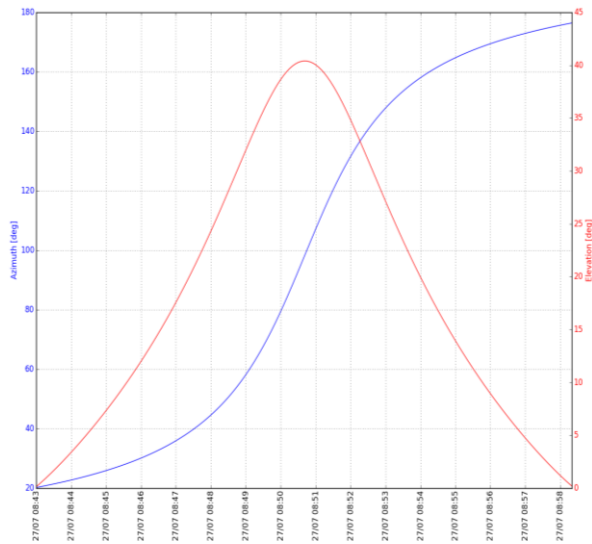
Figure 74. Conflict-free passes percentage over Fairbanks for Metop-A, Metop-B and NOAA19

SPACE gives also details on a single pass in terms of azimuth, elevation, range, range rate and Doppler corrected frequencies with a given sampling time as shown in Figure 75.

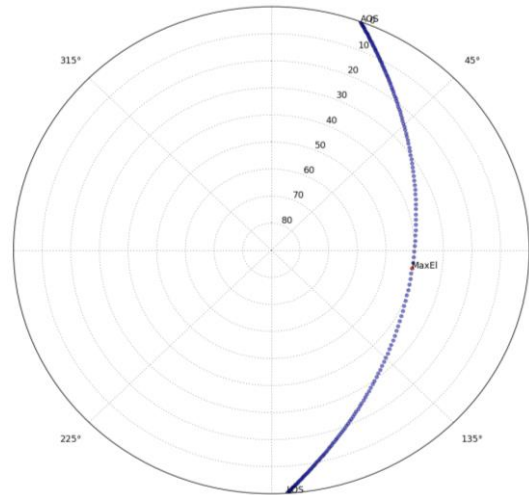
|    | Time (UTC)                 | Azimuth (deg) | Elevation (deg) | Mask (deg) | Range (Km) | Range Velocity (km/s) | Doppler Up Freq (MHz) | Doppler Dwn Freq (MHz) | Eclipse |
|----|----------------------------|---------------|-----------------|------------|------------|-----------------------|-----------------------|------------------------|---------|
| 0  | 2015-07-27 08:43:53.167891 | 20.2          | 0.1             | 1.4        | 3409.16    | -5.977                | 2230.044461           | 2053.499194            | False   |
| 1  | 2015-07-27 08:44:23.167890 | 21.4          | 1.7             | 1.4        | 3219.04    | -5.948                | 2230.044246           | 2053.498996            | False   |
| 2  | 2015-07-27 08:44:53.167889 | 22.7          | 3.4             | 1.4        | 3030.03    | -5.907                | 2230.043942           | 2053.498716            | False   |
| 3  | 2015-07-27 08:45:23.167889 | 24.2          | 5.3             | 1.4        | 2842.55    | -5.852                | 2230.043529           | 2053.498335            | False   |
| 4  | 2015-07-27 08:45:53.167889 | 25.9          | 7.3             | 1.4        | 2657.13    | -5.778                | 2230.042977           | 2053.497827            | False   |
| 5  | 2015-07-27 08:46:23.167889 | 27.9          | 9.6             | 1.4        | 2474.44    | -5.680                | 2230.042251           | 2053.497159            | False   |
| 6  | 2015-07-27 08:46:53.167889 | 30.1          | 12.0            | 1.4        | 2295.33    | -5.552                | 2230.041300           | 2053.496283            | False   |
| 7  | 2015-07-27 08:47:23.167888 | 32.8          | 14.7            | 1.4        | 2120.90    | -5.385                | 2230.040056           | 2053.495137            | False   |
| 8  | 2015-07-27 08:47:53.167887 | 36.0          | 17.6            | 1.4        | 1952.61    | -5.166                | 2230.038424           | 2053.493634            | False   |
| 9  | 2015-07-27 08:48:23.167887 | 39.8          | 20.8            | 2.6        | 1792.37    | -4.877                | 2230.036278           | 2053.491658            | False   |
| 10 | 2015-07-27 08:48:53.167887 | 44.6          | 24.3            | 3          | 1642.72    | -4.498                | 2230.033455           | 2053.489059            | False   |
| 11 | 2015-07-27 08:49:23.167887 | 50.6          | 28.1            | 2.8        | 1506.99    | -4.000                | 2230.029752           | 2053.485648            | False   |
| 12 | 2015-07-27 08:49:53.167887 | 58.2          | 32.0            | 3.6        | 1389.43    | -3.354                | 2230.024952           | 2053.481228            | False   |
| 13 | 2015-07-27 08:50:23.167886 | 67.7          | 35.7            | 3.7        | 1295.11    | -2.540                | 2230.018891           | 2053.475648            | False   |
| 14 | 2015-07-27 08:50:53.167885 | 79.5          | 38.7            | 3.2        | 1229.52    | -1.557                | 2230.011580           | 2053.468915            | False   |
| 15 | 2015-07-27 08:51:23.167884 | 93.0          | 40.3            | 3          | 1197.45    | -0.448                | 2230.003335           | 2053.461323            | False   |
| 16 | 2015-07-27 08:51:53.167884 | 107.2         | 40.0            | 2.4        | 1201.62    | 0.700                 | 2229.994793           | 2053.453458            | False   |
| 17 | 2015-07-27 08:52:23.167884 | 120.4         | 38.0            | 2.1        | 1241.69    | 1.787                 | 2229.986710           | 2053.446014            | False   |
| 18 | 2015-07-27 08:52:53.167884 | 131.6         | 34.8            | 2.5        | 1314.33    | 2.735                 | 2229.979659           | 2053.439521            | False   |
| 19 | 2015-07-27 08:53:23.167884 | 140.7         | 31.0            | 3.3        | 1414.49    | 3.511                 | 2229.973882           | 2053.434202            | False   |
| 20 | 2015-07-27 08:53:53.167884 | 147.8         | 27.1            | 3.8        | 1536.71    | 4.122                 | 2229.969338           | 2053.430018            | False   |
| 21 | 2015-07-27 08:54:23.167883 | 153.5         | 23.4            | 4.2        | 1676.07    | 4.592                 | 2229.965843           | 2053.426799            | False   |
| 22 | 2015-07-27 08:54:53.167882 | 158.0         | 20.0            | 5.3        | 1828.55    | 4.950                 | 2229.963180           | 2053.424347            | False   |
| 23 | 2015-07-27 08:55:23.167882 | 161.7         | 16.8            | 5.8        | 1991.01    | 5.222                 | 2229.961154           | 2053.422481            | False   |
| 24 | 2015-07-27 08:55:53.167882 | 164.8         | 13.9            | 6.5        | 2161.06    | 5.430                 | 2229.959610           | 2053.421059            | False   |
| 25 | 2015-07-27 08:56:23.167882 | 167.3         | 11.3            | 7          | 2336.91    | 5.589                 | 2229.958430           | 2053.419973            | False   |
| 26 | 2015-07-27 08:56:53.167882 | 169.5         | 8.9             | 7          | 2517.19    | 5.710                 | 2229.957526           | 2053.419141            | False   |
| 27 | 2015-07-27 08:57:23.167881 | 171.3         | 6.8             | 7          | 2700.86    | 5.803                 | 2229.956836           | 2053.418505            | False   |
| 28 | 2015-07-27 08:57:53.167880 | 173.0         | 4.7             | 7          | 2887.12    | 5.873                 | 2229.956311           | 2053.418021            | False   |
| 29 | 2015-07-27 08:58:23.167880 | 174.4         | 2.9             | 7          | 3075.34    | 5.926                 | 2229.955916           | 2053.417658            | False   |
| 30 | 2015-07-27 08:58:53.167880 | 175.7         | 1.2             | 6.9        | 3265.01    | 5.965                 | 2229.955627           | 2053.417392            | False   |

Figure 75. Pass details: Metop-A over CDA1, orbit 45500, sampling time 30 seconds

Azimuth and elevation are plotted on a time axis (Figure 76) and on a polar plot (Figure 77).



**Figure 76. Predicted azimuth and elevation on a time axis**



**Figure 77. Predicted azimuth and elevation on a polar plot**

The uplink and downlink frequency corrected for the Doppler shift together with the uplink and downlink centre frequencies are plotted versus time (Figure 78).

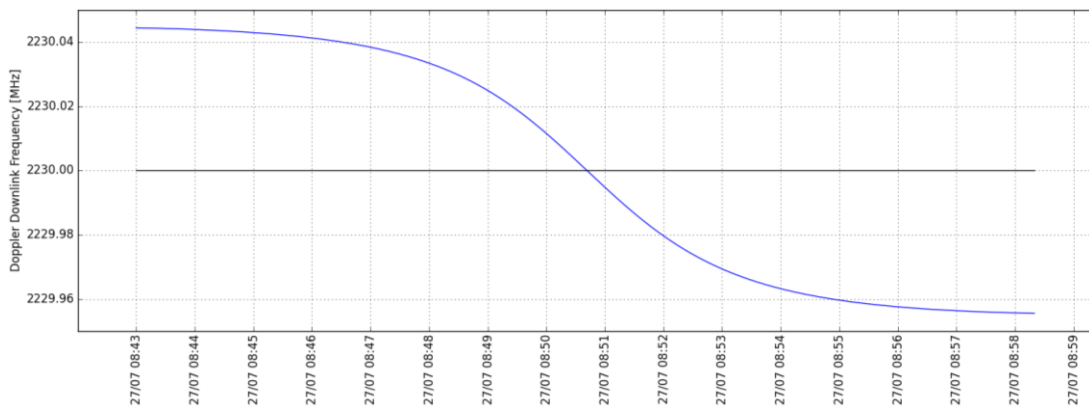


**Figure 78. Doppler corrected downlink frequency for Metop-A pass over CDA1, orbit 45500**

#### 4.2.4 Validation

At EUMETSAT, the FD team generates pass prediction files (called *wimpy*) for both short term (1 month) and long term (1 year). Passes for Metop satellites are computed over Svalbard, Fairbanks, Wallops and McMurdo. Passes for NOAA are computed over Svalbard CDA, Fairbanks and Wallops. These files, one for each satellite, contain the datetime, orbit number and pass events over the ground stations. We implemented a Python script to read these files, to perform a validation test campaign of the pass prediction results.

The values that have been analysed are the maximum elevation time and maximum elevation angle. These tests have been performed covering a prediction time of two weeks. Results have been generated for Metop-A, Metop-B and NOAA19 passes over Svalbard, Fairbanks and Wallops from 14/08/2015 12:00:00 UTC to 27/08/2015 12:00:00 UTC. The TLEs used for these tested are reported hereafter:

METOP-A

1 29499U 06044A 15224.56533007 .00000034 00000-0 35384-4 0 9994  
2 29499 98.6712 282.9342 0001269 61.3615 74.8830 14.21497318457295

NOAA 19

1 33591U 09005A 15224.43157467 .00000127 00000-0 94161-4 0 9991  
2 33591 98.9936 174.4573 0014459 16.0535 344.1092 14.11965220335422

METOP-B

1 38771U 12049A 15224.80641553 .00000032 00000-0 34482-4 0 9998  
2 38771 98.6929 283.8945 0001764 71.2312 22.3257 14.21489399150461

Results show that *pyorbital* has a higher accuracy compared to *pyephem*. However, the latter is around four times faster in performing computations.

**Table 25. Errors between results given by *pyephem* and EUMETSAT FD team**

| S/C     | G/S       | No. of orbits | TCA Error [s] |      | Max El Error [deg] |     |
|---------|-----------|---------------|---------------|------|--------------------|-----|
|         |           |               | Mean          | Max  | Mean               | Max |
| NOAA19  | Svalbard  | 197           | 5.2           | 12.9 | 0.3                | 3   |
|         | Fairbanks | 155           | 5.6           | 16.1 | 0.2                | 2   |
|         | Wallops   | 83            | 4.3           | 13.4 | 0.2                | 3   |
| METOP-A | Svalbard  | 171           | 7.6           | 11.8 | 0.2                | 3   |
|         | Fairbanks | 135           | 4.7           | 13.4 | 0.1                | 4   |
|         | Wallops   | 71            | 3.5           | 10.8 | 0.1                | 2   |
| METOP-B | Svalbard  | 199           | 4.5           | 11.5 | 0.2                | 3   |
|         | Fairbanks | 156           | 5.1           | 12.5 | 0.1                | 2   |
|         | Wallops   | 82            | 3.9           | 12.6 | 0.3                | 3   |

**Table 26. Errors between results given by *pyorbital* and EUMETSAT FD team.**

| S/C    | G/S       | No. of orbits | TCA Error [s] |     | Max El Error [deg] |     |
|--------|-----------|---------------|---------------|-----|--------------------|-----|
|        |           |               | Mean          | Max | Mean               | Max |
| NOAA19 | Svalbard  | 197           | 0.4           | 1.0 | 0.0                | 1   |
|        | Fairbanks | 155           | 0.3           | 1.0 | 0.0                | 0   |
|        | Wallops   | 83            | 0.3           | 1.0 | 0.0                | 0   |

|         |           |     |     |     |     |   |
|---------|-----------|-----|-----|-----|-----|---|
| METOP-A | Svalbard  | 171 | 0.3 | 1.0 | 0.0 | 1 |
|         | Fairbanks | 135 | 0.3 | 0.8 | 0.0 | 0 |
|         | Wallops   | 71  | 0.4 | 1.0 | 0.0 | 0 |
| METOP-B | Svalbard  | 199 | 0.4 | 1.1 | 0.0 | 1 |
|         | Fairbanks | 156 | 0.4 | 1.0 | 0.1 | 2 |
|         | Wallops   | 82  | 0.4 | 1.0 | 0.3 | 3 |

NOAA blind orbits are not highlighted by the FD team in the *wimpy* files, thus results generated from this application are checked against NOAA blind orbits support requests. Results generally match the requests from NOAA but we noticed that some 9ish orbits defined blind from NOAA are not highlighted by this application. This occurs for orbits when there is a low elevation pass (below 10°) over Fairbanks or Wallops. In this case, the real duration of the pass computed by this tool is a few tenths of seconds greater than 7 minutes, which makes this orbit not blind according to the definition. There are some reasons that may lead to this mismatch:

- The accuracy of the TLE propagator.
- TLE source is different: SPACE uses *CelesTrak* TLEs for NOAA satellites whilst NOAA uses four line elements (4LE) generated by its FD team.
- Rounding up and down to compute FRT and LRT, according to the definition, may amplify the error in the worst-case scenario. For instance, consider the following FRTs:

09:36:29 rounds up to 09:36:30

09:36:31 rounds up to 09:36:40

An initial error of 2 seconds leads to an error of 10 seconds. Then consider the following LRTs:

09:43:49 rounds down to 09:43:40

09:43:51 rounds down to 09:43:50

Again, an initial error of 2 seconds leads to an error of 10 seconds. However, since we are interested in the real duration (LRT - FRT), the error may cancel out, sum up giving 20 seconds of total error or remain equal to 10 seconds.

- Satellite elevation check against horizon mask elevation can be made every  $n$  seconds. Then as soon as the satellite elevation is equal to the mask elevation, that time is taken as FRT or LRT. Lower values of  $n$  gives a better resolution in terms of time increasing the accuracy.
- The horizon masks used at EUMETSAT may be slightly different from the masks used by NOAA.

However, this issue can be easily overcome by increasing the minimum pass duration by a few tenths of seconds or one minute to generate conservative results, which means predicting a slightly higher number of 9ish blind orbits.

### **4.3 Ground Station Centralised M&C Simulator**

The Ground Stations Centralised High Level Monitoring and Control (HL M&C) is a system responsible for the operational real-time monitoring and control of EUMETSAT ground stations from the MCC or MCC backup facilities. Within each ground station there is an M&C system, which is used to monitor and manage the activities within the ground station. This system is often referred to as the Ground Station Low Level M&C (LL M&C). The communications interface between the LL M&C computers and the HL M&C computers for control, monitoring, event and schedule information is well described in [44]. The implementation of this communication interface is the purpose of the simulator described in this chapter. The simulator is based on Device Simulator, DS tool, which is described in 4.3.2. The data flows between the HL M&C in the MCC and the LL M&C servers within the individual EUMETSAT Ground Station facilities are summarised in 4.3.1.

#### **4.3.1 Data Flows**

This section summarises the interface, which provides real time commanding, telemetry, events and schedule information from a ground station LL M&C system to the ground station centralised HL M&C at the EUMETSAT prime and backup control centre. For a complete description of the communication interface, please refer to [44].

The Interface comprises the following data towards the ground station LL M&C:

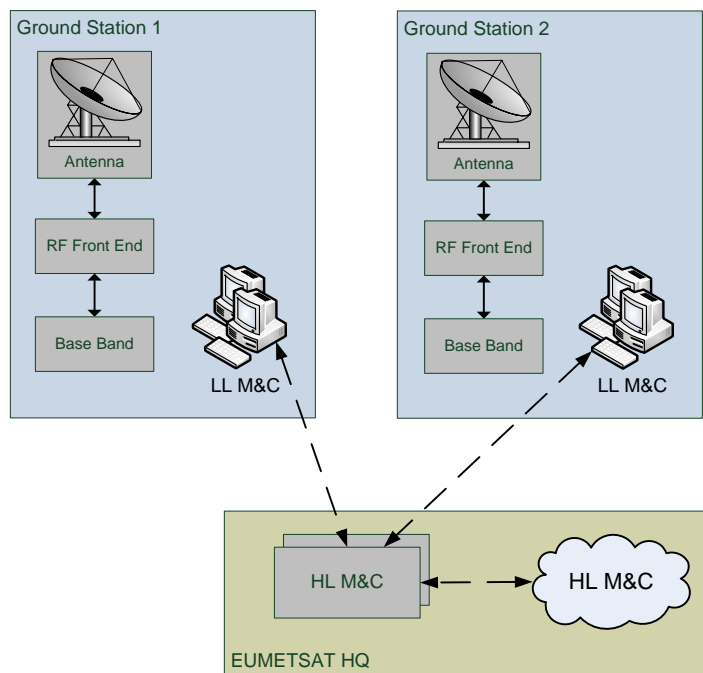
- Request for a set of telemetry values for a given set of telemetry points.

- Request for a set of Event Messages.
- Request for schedule information.
- Control Messages to set parameter values / trigger macros / schedule macros.

The Interface comprises the following data from the ground station LL M&C:

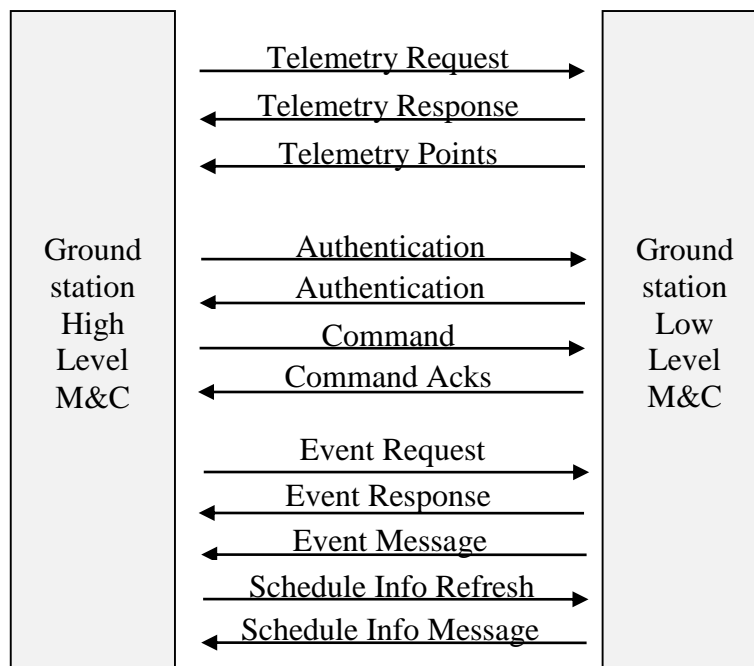
- Telemetry request acknowledgements.
- Telemetry point values in engineering units, raw values, status and timestamps.
- Control message acknowledgements.
- Event messages.
- Schedule information.

Figure 79 illustrates the communication interface between LL and HL M&C. The HL M&C will connect to multiple ground stations, which each contain a single LL M&C instance. Each LL M&C instance will provide the requested real time TM parameters, Events and Schedule information to the HL M&C. The HL M&C is also able to issue control messages to the LL M&C to trigger procedures or set individual parameters either immediately or added to the schedule for later execution.



**Figure 79. HL and LL M&C connection**

Figure 79 shows that two instances of the HL M&C servers (Prime and Backup) are deployed. The Backup HL M&C server is in hot standby. If there are problems with the prime server, the swap to the backup server is performed automatically. The HL M&C supports auto redundancy switching towards the LL M&C of each ground station, meaning that if the Prime LL M&C server is unavailable then it will try to connect to the Backup and vice versa. The HL M&C is designed to M&C an unbounded number of ground stations by utilising their LL M&C function. Figure 80 shows the data stream exchanged between a LL M&C instance and the HL M&C.



**Figure 80. Kinds of data streams exchanged over the interface**

### 4.3.2 Device Simulator

The functionality of the Device Simulator is intended to be a generic Lego set, which allows a user to easily create an interface of any of the supported types:

- TCP client/server
- Simple Network Management Protocol, SNMP
- Serial (RS-232, RS-422, RS-485)
- GPIB (IEEE-488)

In addition, it allows generating the packets and packet interactions that allow realistic simulation of the subject device / facility interface.

The Device Simulator was originally developed for the EUMETSAT ground station team to allow the simulation of ground station monitoring and control interfaces. After the initial development, the generic nature and flexibility of the software meant that the context quickly grew beyond the ground stations to be applicable GS wide.

The benefits of using DS are:

- Shorten the time to market:
  - Parallel development of the various SW
  - Rapid prototyping
- Reduce development and testing costs:
  - Find interface problems early
  - Easily create complex test scenarios
- Improve quality:
  - Automate test cases
  - Fast regression testing

The implementation of any type of device specific functionality (e.g. packet definition, command execution, etc.) is very flexible thanks to an extensive use of user definable macro Java code. This gives the user the ability to implement any kind of desired functionality.

For any user definable macro the user has the ability to:

- Read any of the monitoring packet parameters.
- Read any of the incoming command packet parameters.
- Read any of the monitoring request packet parameters.
- Read any of the command acknowledgement packet parameters.
- Write to any of the monitoring packet parameters.
- Write to any of the command acknowledgement packet parameters.
- Send any monitoring packet.
- Send any command acknowledgement packet.
- Execute high-level programming language functions like:
  - Logical operators
  - Arithmetic operators
  - Comparative operators
  - IF THEN ELSE operations
- Access the system time.

These macros are then executed at the sending or reception of a defined packet or with a specified time interval.

The definition and configuration of devices can be a labour intensive activity for the user, especially configuring all of the packet definitions. To significantly speed up this part of the simulator configuration a series of wizards are available to the user. There is a separate wizard for each of the following types of definition (Figure 81):

- Interface definition
- Monitoring Packet definition
- Monitoring Request Packet definition
- Command Packet definition
- Command Acknowledgement Packet definition

The wizards guides the user through the complex definition process providing extra information where necessary. Within the wizards, there is also a series of tools implemented to speed up the definition process [45].

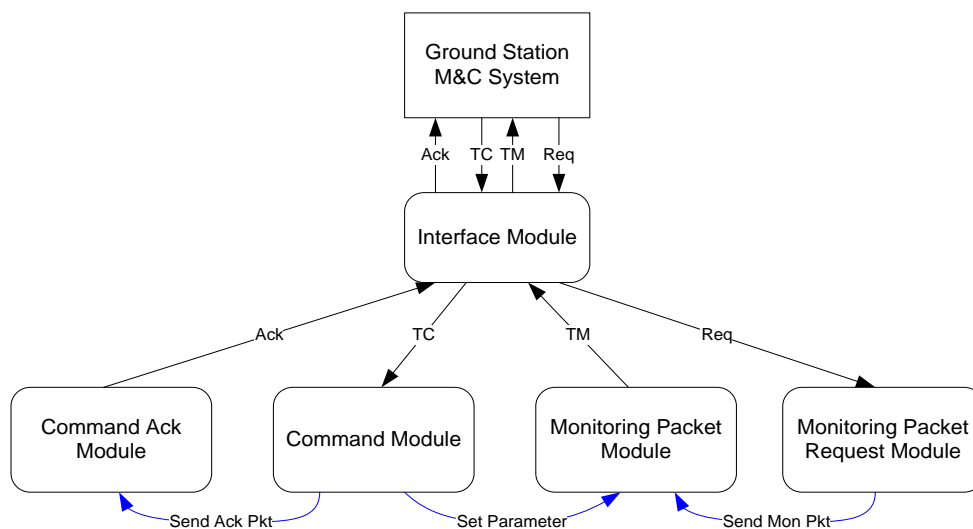


**Figure 81. Definition of a device mechanism**

### 4.3.3 Simulator

The communication interface described in [44] has been implemented in DS implementing a ground station centralised M&C simulator. The exchanged packets have been implemented using the DS Editor shown in Figure 82 and they are listed in Table 27.

**Table 27. Exchanged messages between HL and LL M&C**

| Message                          | ID      | Direction | Folder             |
|----------------------------------|---------|-----------|--------------------|
| Telemetry Request                | TLMREQ  | HL > LL   | Monitoring Request |
| Telemetry Response               | TLMRESP | LL > HL   | Monitoring         |
| Telemetry Points                 | TLM     | LL > HL   | Monitoring         |
| Event Request                    | EVTREQ  | HL > LL   | Monitoring Request |
| Event Response                   | EVTRESP | LL > HL   | Monitoring         |
| Event Message                    | EVTMSG  | LL > HL   | Monitoring         |
| Schedule Request                 | SCHREQ  | HL > LL   | Monitoring Request |
| Schedule Info Message            | SCHMSG  | LL > HL   | Monitoring         |
| Authentication Request           | AUTREQ  | HL > LL   | Command            |
| Authentication                   | AUT_LL  | LL > HL   | Command Ack        |
| Authentication                   | AUT_HL  | HL > LL   | Command            |
| Control Message/Schedule Control | CTLMSG  | HL > LL   | Command            |
| Acknowledgments                  | ACK     | LL > HL   | Command Ack        |

We also implemented some dummy packets containing setting parameters:

- *KeyConfig* (at LL M&C):
  - *HLKey* (default value: “S2jJ90Lkgh79F6GH7h8H”): HL M&C passkey (random sequence of numbers and upper and lower case characters concatenated together).
  - *LLKey* (default value: “FK6G37in7GW47m78hSDx”): LL M&C passkey (random sequence of numbers and upper and lower case characters concatenated together).
  - *AUT* (default value: 1): authentication mechanism override (0 authentication required, 1 authentication not required).
- *SchedConfig* (at LL M&C):
  - *SCH* (default value: 1): schedule usage (0 agreed to not be implemented, 1 agreed to be implemented).
- *KeyConfig* (at HL M&C):
  - *HLKey* (default value: “S2jJ90Lkgh79F6GH7h8H”): HL M&C passkey.

- *LLKey* (default value: “FK6G37in7GW47m78hSDx”): LL M&C passkey.
- *PackConfig* (at HL M&C):
  - *TLMREQ* (default value: 100): number of telemetry requests to be packed in a single TCP call.
  - *EVTREQ* (default value: 100): number of event requests to be packed in a single TCP call.

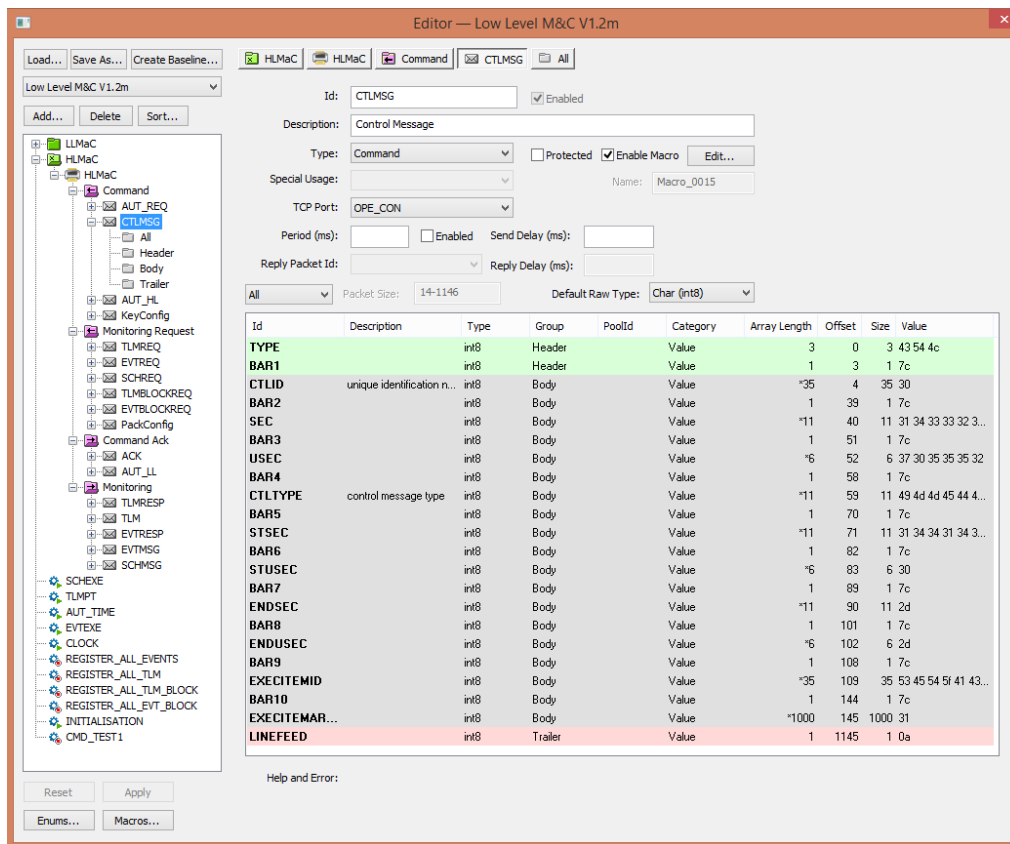


Figure 82. Device Simulator Editor

The main effort for the development of this simulator was to implement the macros. They can be divided into periodic macros and packet-triggered macros. The former are executed only once, with a specified initial delay, or regularly with a specified time interval. When disabled, these macros can be executed manually at run-time. Periodic macros implemented for this simulator are reported in Table 28.

**Table 28. Simulator periodic macros**

| <b>ID</b>              | <b>Activation</b>                     | <b>Description</b>   |
|------------------------|---------------------------------------|--|
| CLOCK                  | initial delay: 1s<br>period: 1s       | Updates the current UNIX time displayed in the JAVA GUI.   |
| AUT_TIME               | initial delay: 10s<br>period: 10s     | Checks if the HL M&C authenticates within 10s from the connection to the CON port. If not, reset the connection. |
| INITIALISATION         | initial delay: 0s<br>period: run once | Performs all initialisation tasks for both HL and LL M&C, reading from XML configuration files.                  |
| REGISTER_ALL_TLM       | manual                                | Sends TM requests for all parameters known by the HL M&C.  |
| REGISTER_ALL_EVT       | manual                                | Sends EVT requests for all events known by the HL M&C.   |
| REGISTER_ALL_TLM_BLOCK | manual                                | Similar to the REGISTER_ALL_TLM but multiple requests are packed in a single TCP call.                           |
| REGISTER_ALL_TLM_BLOCK | manual                                | Similar to the REGISTER_ALL_EVT but multiple requests are packed in a single TCP call.                           |
| SCHEXE                 | initial delay: 0s<br>period: 10s      | Simulates the dynamics of the LL M&C schedule: checks the exe time of items and changes the status accordingly.  |
| EVTEXE                 | initial delay: 10s<br>period: 10s     | Simulates the execution of events in the LL M&C: a random event happens every period.                            |
| TLMPT                  | initial delay: 10s<br>period: 10s     | Simulates the change of a random TM point in the LL M&C.   |
| CMD_TEST1              | manual                                | Sends a set of different types of CTLMSG to test the simulator.  |

The packet-triggered macros are executed at the reception and/or at the sending of a packet and they are listed in Table 29.

Telemetry parameters, events, commands and initial values are defined in XML values at both LL and HL M&C side. Therefore, we implemented XML parsing operations (reading, creating and modifying) using the Java DOM parser. This parser comes with the JDK distribution and it is simple and intuitive to use. Other parsers are faster for reading operations (e.g. StAX or XPath) but DOM is recommended for creating and modifying XML files. The implemented code relies on the corresponding XSD files, which defines the legal building blocks of an XML document (e.g. elements, child elements, optional elements, etc.). For a detailed description of the implemented code and the use case scenarios, please refer to [46].

**Table 29. Simulator packet-triggered macros**

| <b>Triggered by</b> | <b>Executed at</b> | <b>Description</b>  |
|---------------------|--------------------|---|
| AUT_REQ reception   | LL M&C             | sends the AUT_LL  |
| CTLMSG reception    | LL M&C             | validates and executes the command and sends the ACK                          |
| AUT_HL reception    | LL M&C             | checks the authentication keys and sends the AUT_LL                           |
| TLMREQ reception    | LL M&C             | checks the request, registers the parameter and sends the TLMRESP and the TLM |
| SCHREQ reception    | LL M&C             | reads the schedule content and sends the SCHMSG                               |
| EVTREQ reception    | LL M&C             | checks the request, registers the event and sends the EVTRESP                 |
| TLM sending         | LL M&C             | replaces the space char with the “?” char                                     |
| CTLMSG sending      | HL M&C             | sets sending time and automatically filled fields                             |
| ACK reception       | HL M&C             | reads and displays the packet fields  |
| AUT_LL reception    | HL M&C             | checks the authentication keys and sends the AUT_HL                           |
| TLMRESP reception   | HL M&C             | reads and displays the packet fields  |
| TLM reception       | HL M&C             | reads and displays the packet fields  |
| EVTRESP reception   | HL M&C             | reads and displays the packet fields  |
| EVTMSG reception    | HL M&C             | reads and displays the packet fields  |
| SCHMSG reception    | HL M&C             | reads and displays the packet fields  |

#### **4.3.4 Testing**

Before delivering the simulator and its user guide to the developer of the ground station M&C system for the MTG programme, it has been extensively tested in all its functionalities. DS offers a runtime configuration window, which allows the user to set the fields of a packet and sends the packet by pressing a button (Figure 83). This is useful to set and send commands, telemetry, event and schedule requests and initiate the authentication process.

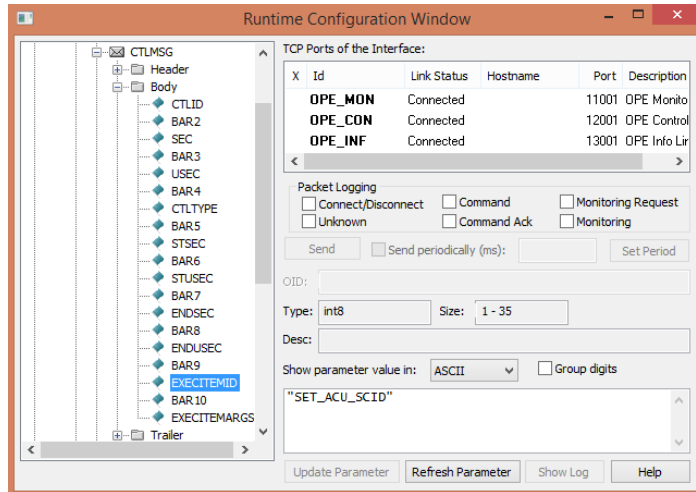


**Figure 83. Device Simulator Runtime Configuration window**

The DS status window (Figure 84) allows the user to check that the number of sent and received packets is as expected. It shows the CPU load, and some error, warning and info messages useful for debugging and display the values of the packet fields. In particular, Figure 84 shows in the log window, the messages exchanged between the HL and LL M&C during the authentication process.

For testing purposes, we also implemented a GUI to display the messages received by the HL M&C. This GUI shows the current UNIX time in the menu bar and it consists of four different tabs for each type of received message: telemetry (Figure 85), events (Figure 86), schedule (Figure 87) and acknowledgements (Figure 88). These messages are inserted into a table composed of several columns, one for each field. We used different row background colours to highlight particular messages (e.g. OOL telemetry values; warning, error and alarm events, executed or failed commands, completed, suspended or pending time-tagged commands).

For these tests, we used the telemetry, events and commands of the BRGS, which counts 1907 telemetry parameters. The simulator has been successfully tested and it has been delivered to CGI Space for the development of the M&C.

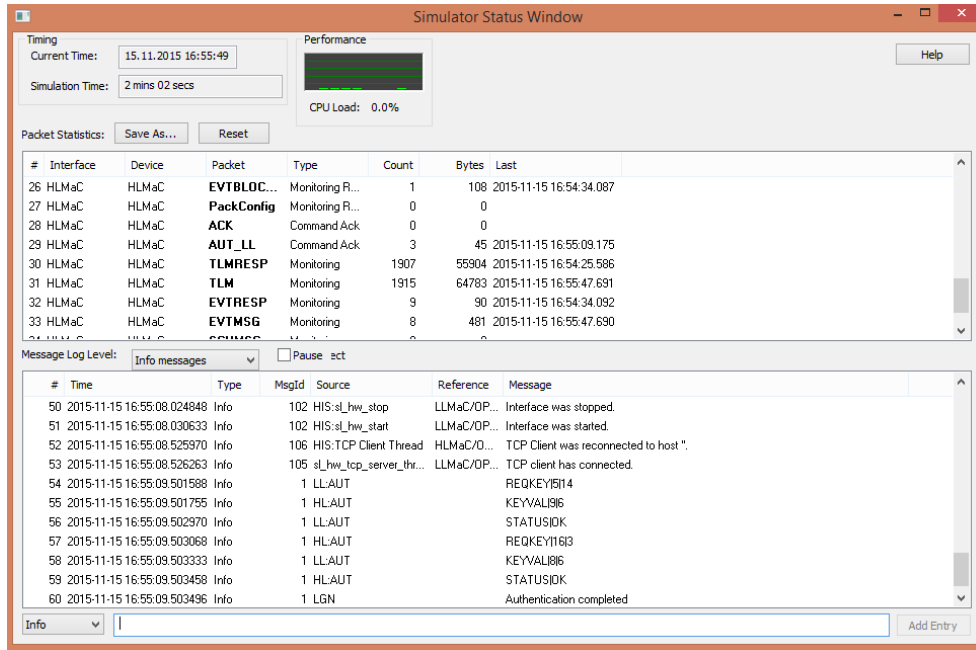


Figure 84. Device Simulator Status window

| Index | ExecItemID | MNEMONIC           | Type                | Raw             | EU           | units | State                 | Sec        | USec   | Statu... |
|-------|------------|--------------------|---------------------|-----------------|--------------|-------|-----------------------|------------|--------|----------|
| 1149  |            | BRGS:TTC1:TTCMAA1  | Real(Single)        | 1.0001e+04      | 1.0001e+04   | Hz    | -                     | 1444214563 | 625000 | 0x40     |
| 1742  |            | BRGS:TTC2:TTCMTE5M | Enumerated          | 0               | -            | -     | -                     | -          | -      | 0x20     |
| 570   |            | BRGS:ACU1:APSD4E49 | Real(Double)        | 1.443750e-01    | 1.443750e-01 | -     | -                     | -          | -      | 0x20     |
| 569   |            | BRGS:ACU1:APSD4E48 | Real(Double)        | 1.443750e-01    | 1.443750e-01 | -     | -                     | -          | -      | 0x20     |
| 568   |            | BRGS:ACU1:APSD4E47 | Real(Double)        | 1.443750e-01    | 1.443750e-01 | -     | -                     | -          | -      | 0x20     |
| 567   |            | BRGS:ACU1:APSD4E46 | Real(Double)        | 1.443750e-01    | 1.443750e-01 | -     | -                     | -          | -      | 0x20     |
| 566   |            | BRGS:ACU1:APSD4E45 | Real(Double)        | 1.443750e-01    | 1.443750e-01 | -     | -                     | -          | -      | 0x20     |
| 1747  |            | BRGS:TTC1:TTCMTIAM | Enumerated          | 0               | -            | -     | -                     | -          | -      | 0x20     |
| 565   |            | BRGS:ACU1:APSD4E44 | Real(Double)        | 1.443750e-01    | 1.443750e-01 | -     | -                     | -          | -      | 0x20     |
| 564   |            | BRGS:ACU1:APSD4E43 | Real(Double)        | 1.443750e-01    | 1.443750e-01 | -     | -                     | -          | -      | 0x20     |
| 563   |            | BRGS:ACU1:APSD4E42 | Real(Double)        | 1.443750e-01    | 1.443750e-01 | -     | -                     | -          | -      | 0x20     |
| 562   |            | BRGS:ACU1:APSD4E41 | Real(Double)        | 1.443750e-01    | 1.443750e-01 | -     | -                     | -          | -      | 0x20     |
| 561   |            | BRGS:ACU1:APSD4E40 | Real(Double)        | 1.443750e-01    | 1.443750e-01 | -     | -                     | -          | -      | 0x20     |
| 560   |            | BRGS:ACU1:APSD4E39 | Real(Double)        | 1.443750e-01    | 1.443750e-01 | -     | -                     | -          | -      | 0x20     |
| 559   |            | BRGS:ACU1:APSD4E38 | Real(Double)        | 1.443750e-01    | 1.443750e-01 | -     | -                     | -          | -      | 0x20     |
| 558   |            | BRGS:ACU1:APSD4E37 | Real(Double)        | 1.443750e-01    | 1.443750e-01 | -     | -                     | -          | -      | 0x20     |
| 557   |            | BRGS:ACU1:APSD4E36 | Real(Double)        | 1.443750e-01    | 1.443750e-01 | -     | -                     | -          | -      | 0x20     |
| 556   |            | BRGS:ACU1:APSD4E35 | Real(Double)        | 1.443750e-01    | 1.443750e-01 | -     | -                     | -          | -      | 0x20     |
| 555   |            | BRGS:ACU1:APSD4E34 | Real(Double)        | 1.443750e-01    | 1.443750e-01 | -     | -                     | -          | -      | 0x20     |
| 1018  |            | BRGS:ACU1:SCNMELST | Enumerated          | 0               | -            | -     | -                     | -          | -      | 0x20     |
| 1904  |            | BRGS:RFQ1:UCSMOPMO | Enumerated          | 0               | -            | -     | -                     | -          | -      | 0x20     |
| 1514  |            | BRGS:TTC2:TTCMMINM | Real(Single)        | 1.75e+05        | 1.75e+05     | RAD   | -                     | -          | -      | 0x20     |
| 984   |            | BRGS:RFQ1:PTI15000 | Time(Abs)-CDS Short | 1500010123.1... | -            | -     | 2017-195-05:28:43.123 | -          | -      | 0x20     |
| 1040  |            | BRGS:RFQ1:SIPMSW2C | Enumerated          | 0               | -            | -     | -                     | -          | -      | 0x20     |
| 554   |            | BRGS:ACU1:APSD4E33 | Real(Double)        | 1.443750e-01    | 1.443750e-01 | -     | -                     | -          | -      | 0x20     |
| 553   |            | BRGS:ACU1:APSD4E32 | Real(Double)        | 1.443750e-01    | 1.443750e-01 | -     | -                     | -          | -      | 0x20     |
| 1234  |            | BRGS:TTC2:TTCMDOU3 | Enumerated          | 0               | -            | -     | -                     | -          | -      | 0x20     |
| 552   |            | BRGS:ACU1:APSD4E31 | Real(Double)        | 1.443750e-01    | 1.443750e-01 | -     | -                     | -          | -      | 0x20     |
| 898   |            | BRGS:RFQ1:HPAMEIRP | Real(Single)        | 1.75e+05        | 1.75e+05     | dBW   | -                     | -          | -      | 0x20     |
| 551   |            | BRGS:ACU1:APSD4E30 | Real(Double)        | 1.443750e-01    | 1.443750e-01 | -     | -                     | -          | -      | 0x20     |
| 700   |            | BRGS:ACU1:APSDST49 | Time(Abs)-CDS Short | 1500010123.1... | -            | -     | 2017-195-05:28:43.123 | -          | -      | 0x20     |
| 697   |            | BRGS:ACU1:APSDST46 | Time(Abs)-CDS Short | 1500010123.1... | -            | -     | 2017-195-05:28:43.123 | -          | -      | 0x20     |
| 696   |            | BRGS:ACU1:APSDST45 | Time(Abs)-CDS Short | 1500010123.1... | -            | -     | 2017-195-05:28:43.123 | -          | -      | 0x20     |
| 1031  |            | BRGS:ACU1:SCNMSIAC | Enumerated          | 0               | -            | -     | -                     | -          | -      | 0x20     |
| 699   |            | BRGS:ACU1:APSDST48 | Time(Abs)-CDS Short | 1500010123.1... | -            | -     | 2017-195-05:28:43.123 | -          | -      | 0x20     |
| 698   |            | BRGS:ACU1:APSDST47 | Time(Abs)-CDS Short | 1500010123.1... | -            | -     | 2017-195-05:28:43.123 | -          | -      | 0x20     |
| 1232  |            | BRGS:TTC2:TTCMDOU1 | Enumerated          | 0               | -            | -     | -                     | -          | -      | 0x20     |
| 850   |            | BRGS:RFQ1:DCSMALSU | Enumerated          | 0               | -            | -     | -                     | -          | -      | 0x20     |
| 55    |            | BRGS:ACU1:ACUMSTAT | Enumerated          | 0               | -            | -     | -                     | -          | -      | 0x20     |
| 1064  |            | BRGS:SYS15003      | Enumerated          | 0               | -            | -     | -                     | -          | -      | 0x20     |
| 1063  |            | BRGS:SYS15002      | Enumerated          | 0               | -            | -     | -                     | -          | -      | 0x20     |
| 1062  |            | BRGS:SYS15001      | Enumerated          | 0               | -            | -     | -                     | -          | -      | 0x20     |
| 1039  |            | BRGS:RFQ1:SIPMSWTC | Enumerated          | 0               | -            | -     | -                     | -          | -      | 0x20     |
| 37    |            | BRGS:ACU1:ACUMINTE | Integer(Insignd)    | 10              | -            | sec   | -                     | -          | -      | 0x20     |

Figure 85. Telemetry points messages table

| Event ID | Sec        | USec   | Source | Severity | Message                   |
|----------|------------|--------|--------|----------|---------------------------|
| 124      | 1443191836 | 796000 | ACU2   | DEBUG    | Antenna mode changed      |
| 124      | 1443191826 | 796000 | ACU2   | ALARM    | Antenna mode changed      |
| 126      | 1443191816 | 796000 | SDC3   | ERROR    | Connection lost with unit |
| 123      | 1443191806 | 796000 | TTC1   | INFO     | Ranging started           |
| 123      | 1443191796 | 796000 | TTC1   | WARNING  | Ranging started           |
| 124      | 1443191786 | 812000 | ACU2   | INFO     | Antenna mode changed      |
| 124      | 1443191776 | 812000 | ACU2   | WARNING  | Antenna mode changed      |
| 123      | 1443191766 | 812000 | TTC1   | ALARM    | Ranging started           |
| 126      | 1443191756 | 812000 | SDC3   | ALARM    | Connection lost with unit |
| 123      | 1443191746 | 812000 | TTC1   | DEBUG    | Ranging started           |
| 124      | 1443191736 | 812000 | ACU2   | ALARM    | Antenna mode changed      |
| 124      | 1443191726 | 828000 | ACU2   | DEBUG    | Antenna mode changed      |
| 123      | 1443191716 | 828000 | TTC1   | WARNING  | Ranging started           |
| 123      | 1443191706 | 828000 | TTC1   | INFO     | Ranging started           |
| 126      | 1443191696 | 828000 | SDC3   | ALARM    | Connection lost with unit |
| 123      | 1443191686 | 828000 | TTC1   | ERROR    | Ranging started           |
| 124      | 1443191676 | 828000 | ACU2   | ALARM    | Antenna mode changed      |
| 123      | 1443191666 | 828000 | TTC1   | ERROR    | Ranging started           |
| 126      | 1443191656 | 843000 | SDC3   | ERROR    | Connection lost with unit |
| 124      | 1443191646 | 843000 | ACU2   | WARNING  | Antenna mode changed      |
| 125      | 1443191636 | 843000 | SDC3   | INFO     | Connection lost with unit |
| 125      | 1443191626 | 843000 | SDC3   | DEBUG    | Connection lost with unit |
| 124      | 1443191616 | 843000 | ACU2   | DEBUG    | Antenna mode changed      |

Figure 86. Events messages history

| Sched ID | Start Sec  | Start USec | Stop Sec   | Stop USec | Exec Item ID | Exec Item Args | Status    | Info     |
|----------|------------|------------|------------|-----------|--------------|----------------|-----------|----------|
| 1        | 1443191178 | 0          | 1443191188 | -         | PROC12345    | 1,1,10         | COMPLETED | ANY INFO |
| 2        | 1443192178 | 0          | -          | -         | PROC12345    | 1,1,9          | PENDING   | ANY INFO |
| 0        | 1541422178 | 0          | 1541422188 | -         | PROC12345    | 1,1,10         | PENDING   | ANY INFO |

Figure 87. Time-tagged commands inserted in the schedule

| Ctl ID | Ctl Type   | ExecItem ID  | ExecItem Args | Sec        | USec   | Ack Type | Fail Reason    |
|--------|------------|--------------|---------------|------------|--------|----------|----------------|
| 12     | TIMETAGGED | PROC12345    | 1,1,9         | 1443191673 | 109000 | 5        | -              |
| 11     | TIMETAGGED | PROC12345    | 1,1,9         | 1443191624 | 468000 | 6        | IT             |
| 10     | TIMETAGGED | PROC12345    | 1,1,10        | 1443190977 | 468000 | 5        | -              |
| 9      | TIMETAGGED | PROC12345    | 1,1,10        | 1443190927 | 653000 | 6        | CT             |
| 8      | TIMETAGGED | PROC12345    | 1,1,10        | 1443190910 | 937000 | 6        | IT             |
| 7      | TIMETAGGED | PROC12345    | 1,1           | 1443190885 | 734000 | 2        | FEEXECITEMARGS |
| 6      | TIMETAGGED | PROC125      | 1,1           | 1443190887 | 15000  | 2        | UC             |
| 5      | IMMEDIATE  | PROC12345    | 1,1           | 1443190851 | 808000 | 2        | FCTLTYPE       |
| 4      | TIMETAGGED | PROC12345    | 1,1           | 1443190834 | 265000 | 2        | FEEXECITEMARGS |
| 3      | TIMETAGGED | PROC12345    | 1,1,10        | 1443190816 | 921000 | 5        | -              |
| 2      | IMMEDIATE  | SET_ACU_SCID | 1             | 1443190698 | 640000 | 5        | -              |
| 1      | IMMEDIATE  | SET_ACU_SCID | 1             | 1443190455 | 187000 | 2        | NLI            |

Figure 88. Acknowledgement messages history

## 5. Conclusions

The work presented in this thesis focused on the design and implementation of software solutions for the ground segment of satellite missions, with application to the ESEO project. The project started at the same time of the PhD course in January 2013 and it is currently in Phase D after successfully passing the preliminary and critical design reviews. For this purpose, we first had to define the requirements for a ground segment suitable to the ESEO mission and then design the components of the ground segment to cover all the required functionalities. We started from our experience with operations of ALMASat-1 micro-satellite launched in February 2012 and we greatly improved the ground systems for a more complex mission like ESEO. One of the most important improvement in the ground systems was the introduction of a software defined radio (SDR) in our ground station which required first the study of this new device and then the implementation of a proper software application to have a transceiver capable of communicating with the on-board transceiver at the registered frequencies and using the defined communication protocol and modulation scheme. Moreover, during the satellite operations, ground operators will greatly benefit from displaying the received signal in frequency and time domain and registering the acquired signal for post-processing in case of issues. The spacecraft monitoring and control system and the telemetry data visualisation and display tool have been designed keeping in mind the high number of subsystems and payloads that are hosted in the satellite, the possibility to re-use the same software for future missions with the minimum effort and the low experience of people which will control the spacecraft. The introduction of a connection to a database is essential considering the high number of spacecraft and mission data. The work done during the phase B and C of the ESEO mission has been also the object of some students' thesis and scientific papers presented in different workshops [6], [24] and [47].

This thesis also presented the software solutions designed for the ground stations used by EUMETSAT to operate LEO and GEO weather satellites. This was the result of a six-month internship within the realtime services and system operations (RSO) division. The Ground Station Analysis and Reporting (GSAR) tool is now used by the ground station operations and maintenance engineers to check the performance of two ground stations in Svalbard used to operate Metop and NOAA satellites. It was implemented with the goal to generate period reports containing ground station data in tables and graphs to spot possible issues. The Satellite Passes and Conflicts Engine (SPACE) is now used by the ground

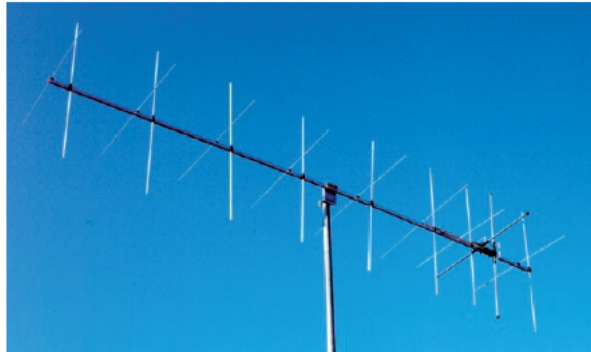
station operations team to support the schedule of Metop and NOAA satellite passes over Svalbard ground station especially when one of the two antennas is under maintenance or upgrade. However, it is a general tool which can be used to compute passes and resolve conflicts of multiple satellites over multiple ground stations based on the propagation of the TLEs. Finally a ground station centralised monitoring and control simulator has been implemented and fully tested and will now be used as the reference for the procurement of the monitoring and control system for the ground stations used to operate the satellites of Meteosat Third Generation programme.

# Appendix A

## 2x9 elements Yagi antenna

144 to 146 MHz

Part Nr. 220818



### Electrical data

#### Radiation at 144.5 MHz

|                                   |                   |
|-----------------------------------|-------------------|
| Effective electrical length ..... | : 1.65 $\lambda$  |
| Isotropic gain .....              | : 13.1 dBi        |
| Aperture angle @ -3 dB            |                   |
| - E-plane .....                   | : 2 x 20.2°       |
| - H-plane .....                   | : 2 x 23.0°       |
| First side lobe set               |                   |
| - E-plane .....                   | : - 20.5 dB @ 54° |
| - H-plane .....                   | : - 13.6 dB @ 58° |
| Rear protection .....             | : - 19 dB         |
| Average stray radiation           |                   |
| - E-plane .....                   | : - 35 dB         |
| - H-plane .....                   | : - 24 dB         |

### Bandwidth

|  |                      |
|--|----------------------|
| Gain @ -1 dB .....   |                      |
| Nominal impedance .....  | : 140 to 148 MHz     |
| Impedance match bandwidth @ SWR <1.3/1.....                              | : 50 $\Omega$        |
| Acceptable RF power (continuous duty) .....                              | : 143.4 to 146.2 MHz |
| Required phase delay between frontmost and rearmost driven element ..... | : 1000 W             |

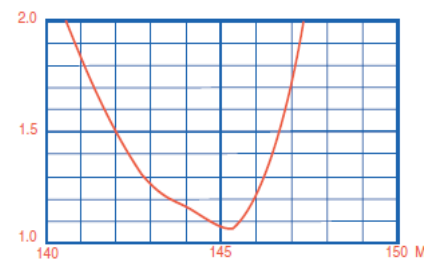
### Array of 2 or 4 antennas

|   |                  |
|---|------------------|
| .....   | : 72°            |
| (optimized stacking distance. from center to center of elements. for minimal side lobe radiation) |                  |
| - Electrical distance .....   | : 1.33 $\lambda$ |
| - Pratical distance .....   | : 2.77 m         |

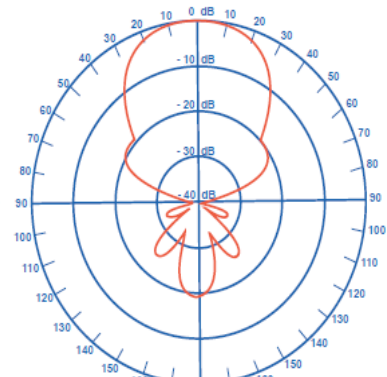
### Mechanical data

|  |                       |
|--|-----------------------|
| Connector .....                                | : N                   |
| Overall length .....                           | : 3.57 m              |
| Mass .....                                     | : 3.3 kg              |
| Effective wind load.....                       | : 0.15 m <sup>2</sup> |
| Approximate wind load (25 m/s - 55 mph) .....  | : 5.6 daN             |
| Approximate wind load (45 m/s - 100 mph) ..... | : 18.2 daN            |

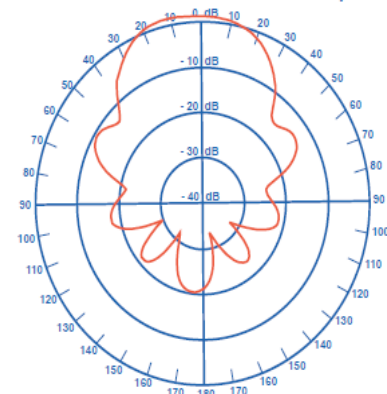
### SWR curve



### Radiation patterns



E plane



H plane

# 2x19 elements crossed yagi antenna

430 to 440 MHz

Part Nr. 220938



## Electrical data

### Radiation at 432 MHz

|                                   |                   |
|-----------------------------------|-------------------|
| Effective electrical length ..... | : 4.02 $\lambda$  |
| Isotropic gain .....              | : 16.0 dBi        |
| Aperture angle @ -3 dB            |                   |
| - E-plane .....                   | : 2 x 14.8°       |
| - H-plane .....                   | : 2 x 14.7°       |
| First side lobe set               |                   |
| - E-plane .....                   | : - 16.0 dB @ 38° |
| - H-plane .....                   | : - 12.9 dB @ 38° |
| Rear protection .....             | : - 23.6 dB       |
| Average stray radiation           |                   |
| - E-plane .....                   | : - 36 dB         |
| - H-plane .....                   | : - 28 dB         |

### Bandwidth

|   |                  |
|---|------------------|
| Gain @ -1 dB .....  | : 416 to 442 MHz |
| Nominal impedance .....   | : 50 $\Omega$    |
| Impedance match bandwidth @ SWR <1.3/1.....                                 | : 431 to 439 MHz |
| Acceptable RF power (continuous duty) .....                                 | : 1000 W         |
| Required phase delay between frontmost and<br>rearmost driven element ..... | : 14°            |

### Array of 2 or 4 antennas

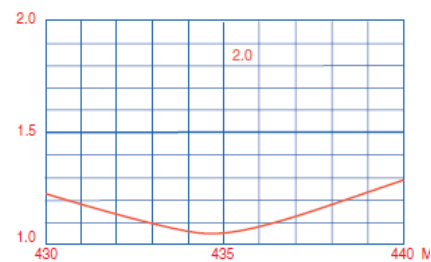
(optimized stacking distance. from center to center of elements. for minimal side lobe radiation)

|                                       |                  |
|---------------------------------------|------------------|
| - E plane - Electrical distance ..... | : 1.80 $\lambda$ |
| - Pratical distance .....             | : 1.25 m         |
| - H plane - Electrical distance ..... | : 1.80 $\lambda$ |
| - Pratical distance .....             | : 1.25 m         |

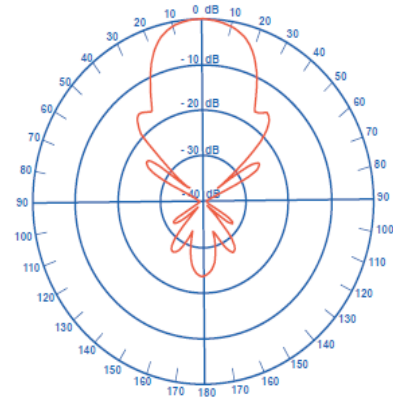
## Mechanical data

|  |                       |
|--|-----------------------|
| Connector .....                                | : N                   |
| Overall length .....                           | : 3.25 m              |
| Mass .....                                     | : 2.2 kg              |
| Effective wind load .....                      | : 0.09 m <sup>2</sup> |
| Approximate wind load (25 m/s - 55 mph) .....  | : 3.5 daN             |
| Approximate wind load (45 m/s - 100 mph) ..... | : 11.3 daN            |

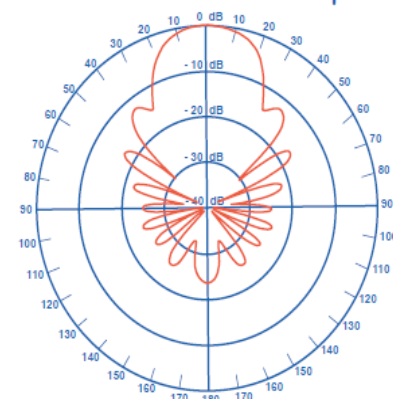
## SWR curve



## Radiation patterns



E plane



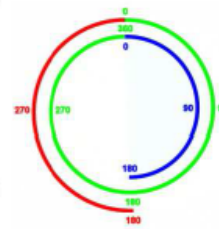
H plane

## Appendix B

### **SPID Azimuth & Elevation antenna rotator** **Type: RAS**



Normal 360  
- 180  
or  
+540 from  
North 0  
for  
total of 720



| <b>Specifications:<br/>SPID RAS Azimuth and<br/>Elevation Rotator</b> | <b>RAS @ 12V</b>                            | <b>RAS @ 18V</b>    |
|---|---|---------------------|
| Turning torque in-lbs/Nm  | >1,328 in lb/150 Nm                         | >2,734 in lb/309 Nm |
| Brake Torque in lbs/Nm  | 13985 in lb/1580 Nm                         | 13985 in lb/1580 Nm |
| Brake Construction  | Double Worm Gears                           | Double Worm Gears   |
| Vertical Load lbs/Kg  | >550 lbs/250 Kg                             | >550 lbs/250 Kg     |
| Rotation Speed (360 Deg)  | +/- 150 sec                                 | +/- 120 sec         |
| Resolution  | 1 deg                                       | 1 deg               |
| Rotation Range Az/El  | 360/180 deg                                 | 360/180 deg         |
| Weight lbs / Mass Kg  | 31 lbs/14 Kg                                | 31 lbs/14 Kg        |
| Position Sensor   | Reed Switch                                 | Reed switch         |
| Mast size inches/mm Bottom<br>mount                                   | 2.6 in/66 mm                                | 2.6 in/66 mm        |
| Mast size inches/mm<br>Elevation                                      | 2.0 in/50 mm                                | 2.0 in/50 mm        |
| Environment   | Ground / Mobile free air and / or Sheltered |                     |
| MTBF  | 12500 hours @ -20 to +55°C                  |                     |
| Control cable core  | 8   | 8                   |

| <b>Specifications Controller:</b> |   |          |  |
|-----------------------------------|---|----------|--|
| Supply voltage                    | 12 Volts  | 18 Volts |  |
| Current consumption               | 6 ...10 A   | 6...11 A |  |
| Supplied with                     | Digital controller, build in PC track interface (serial), software, mouse, PC-cable |          |  |
| Dimensions                        | 245x235x40mm  |          |  |
| Weight:                           | 1.6 Kg  |          |  |
| Case                              | Aluminium / steel   |          |  |
| Environment                       | Ground / Mobile Sheltered   |          |  |
| MTBF                              | 15000 hours @ -5 to +40°C   |          |  |
| Display                           | 2* 4 digit (green)  |          |  |
| Control cable 8-core              | Connection inc. 2* 4 pin-DIN connector  |          |  |

## Appendix C

- ✓ This 3 Meter Prime Focus MESH DISH KIT is specially designed to use with prime focus dish feeds.
- ✓ RF HAMDESIGN can offer you a wide range of Dish feeds, Linear (H or V) or circular (LHCP or RHCP) polarized. Multiband linear dish feeds up to 5 band are also available.
- ✓ We can supply you several dish feeds clamps to fit a dish feed.
- ✓ Built up notes of each Mesh Dish are in the delivered user manual described step by step with lot of pictures.
- ✓ All delivered mounting parts are made of stainless steel and or aluminum.
- ✓ To assemble RF HAMDESIGN's DISH KIT you only need some small hand tools, a little hand driller, a metal saw, a fine liner, a small metal hand cutter, a open end spanner No. 10 and 13 and a Hand riveter
- ✓ Assembly time is about 7...8 hours.



### Specifications 3 Meter Prime Focus Mesh Dish

|                                    |  |
|------------------------------------|--|
| Mesh useable up to                 | 6 GHz / Option 11GHz 2.8mm mesh          |
| Weight 3M dish (ex dish feed)      | 27 Kg / 31.5 Kg (6mm / 2.8mm mesh)       |
| Wind load 120 Km/h                 | 771 N / 1046 N (6mm / 2.8mm mesh)        |
| DISH Surface area:                 | 7.07 M2                                  |
| Supplied including Mast clamp      | No: Available Option                     |
| 2 pcs CNC Milled center            | Aluminum, 20cm diameter / 10mm thickness |
| 20mm assembled ribs ready to place | 12 pcs                                   |
| Inner rings to secure mesh         | 5 pcs                                    |
| Easy to place outer RIM            | 1 pcs                                    |
| Feed support including             | 3 or 4 leg 15 or 20mm/sq                 |
| Available F/D                      | 0.4 and 0.45                             |

### Gain calculation

(Surface quality factor ( $\eta$ ) 0.65)

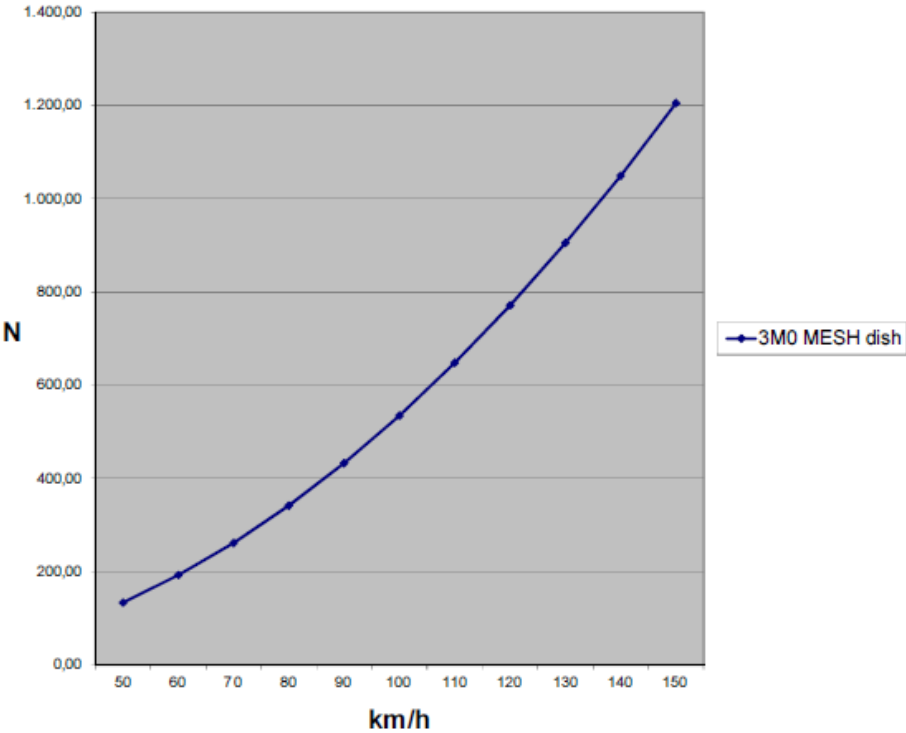
| Frequency MHz            | Gain dBd | 1/2-power (3 dB) beam widths Degree |
|--------------------------|----------|-------------------------------------|
| 1296                     | 30.3     | 5.7                                 |
| 2320                     | 35.4     | 3.2                                 |
| 3456                     | 38.8     | 2.1                                 |
| 5760 (option 2.8mm mesh) | 43.3     | 1.3                                 |
| 10368 (2.8mm mesh)       | N.A.     | N.A.                                |

### Focal length

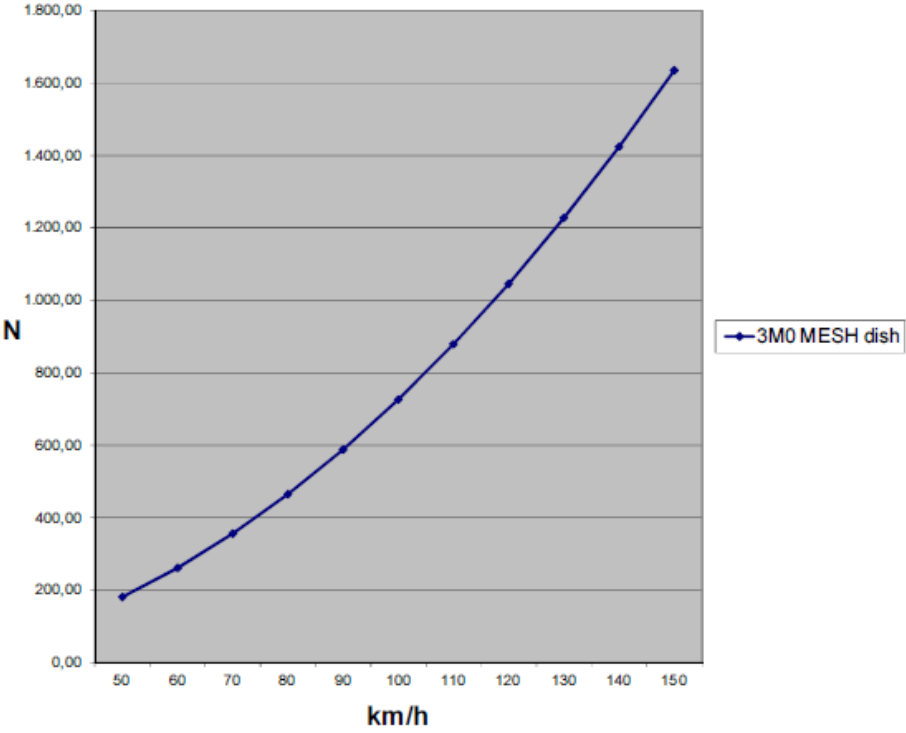
(Focal length: the distance from the center of the dish to the front of the dish feed.)

| DISH SIZE | F/D=0.40 | F/D=0.45 |
|-----------|----------|----------|
| 3 meter   | 120 cm   | 135 cm   |

**RF HAMDESIGN  
WIND LOAD 3M0 MESH DISH 6mm Mesh**



**RF HAMDESIGN  
WIND LOAD 3M0 MESH DISH 2.8mm Mesh**



# Appendix D

## Coaxial High Power Amplifier

**ZHL-50W-52+**  
**ZHL-50W-52**

50Ω 50W 50 to 500 MHz

### Features

- High power, 50 Watt
- Excellent IP3, +55 dBm typ.
- Class A amplifier, usable up to 75W
- Shuts off when base plate temperature exceeds +100°C
- Good gain flatness, ±1.0 dB typ.
- Internal power regulator (current remains constant over 22 to 28V)
- Over voltage protection, shut off above 29V
- Protected by US Patent 7,348,854

### Applications

- VHF/UHF transmitters
- Defense
- Amateur radio, FM, TV
- Laboratory use



|              |                     |                               |
|--------------|---------------------|-------------------------------|
| Model No.    | ZHL-50W-52-S(+)     | ZHL-50W-52X-S(+) <sup>▲</sup> |
| Case Style   | BT1165              |                               |
| Connectors   | SMA                 |                               |
| Price (Qty.) | \$1395.00 ea. (1-9) | \$1320.00 ea. (1-9)           |

### Electrical Specifications<sup>1</sup> at 25°C

| Parameter                                 | Frequency (MHz) | ZHL-50W-52(+) |      |      | ZHL-30W-50W-52X(+) <sup>▲</sup> |      |      | Units |
|---|-----------------|---------------|------|------|---------------------------------|------|------|-------|
|   |                 | Min.          | Typ. | Max. | Min.                            | Typ. | Max. |       |
| Frequency Range                           |                 | 50            |      | 500  | 50                              |      | 500  | MHz   |
| Gain                                      | 100             | 47            | 50   |      | 47                              | 50   |      | dB    |
|   | 500             | 46            | 50   |      | 46                              | 50   |      |       |
| Gain Flatness                             |                 |               | ±2.0 | ±2.8 |                                 | ±2.0 | ±2.8 | dB    |
| Output Power at 1dB compression           | 120-260         | +45.5         | +48  |      | +45.5                           | +48  |      | dBm   |
|   | 50-500          | +43           | +45  |      | +43                             | +45  |      |       |
| Saturated Output Power at 3dB compression | 120-260         | +47           | +48  |      | +47                             | +48  |      | dBm   |
|   | 50-500          | +45           | +48  |      | +45                             | +48  |      |       |
| Noise Figure                              |                 |               | 6.0  | 8.0  |                                 | 6.0  | 8.0  | dB    |
| Output third order intercept point        |                 |               | +55  |      |                                 | +55  |      | dBm   |
| Input VSWR                                |                 |               | 1.6  |      |                                 | 1.6  |      | :1    |
| Output VSWR                               |                 |               | 2.0  |      |                                 | 2.0  |      | :1    |
| DC Supply Voltage                         |                 |               | 24   | 25   |                                 | 24   | 25   | V     |
| Supply Current                            |                 |               |      | 9.3  |                                 |      | 9.0  | A     |

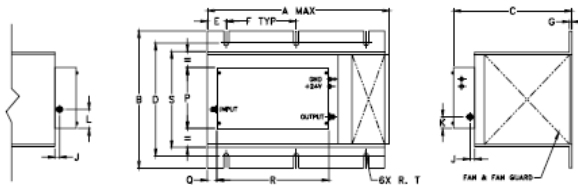
1. All specifications are for a single input CW signal.

At nominal output load, 24V nominal supply voltage.

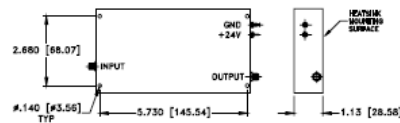
An open or a short load is not recommended potentially can cause damage.

<sup>▲</sup> Heat sink and fan not included. Alternative heat sinking and heat removal must be provided by the user to limit maximum base-plate temperature to 85°C, in order to ensure proper performance. For reference, this requires thermal resistance of user's external heat sink to be 0.08°C/W max.

### Outline Drawing



#### MOUNTING INFORMATION FOR MODELS WITHOUT HEATSINK



### Maximum Ratings

| Parameter                  | Rating         |
|----------------------------|----------------|
| Operating Temperature      | -20°C to 85°C  |
| Storage Temperature        | -55°C to 100°C |
| Base Plate Temperature     | 85°C           |
| Input RF Power (no damage) | 0 dBm          |

Permanent damage may occur if any of these limits are exceeded.

### Outline Dimensions (inch/mm)

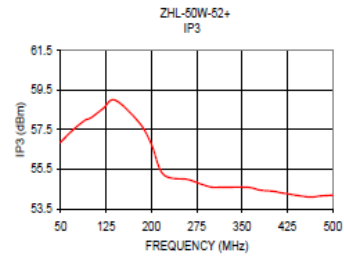
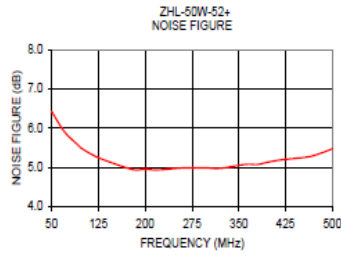
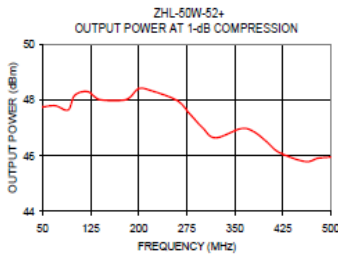
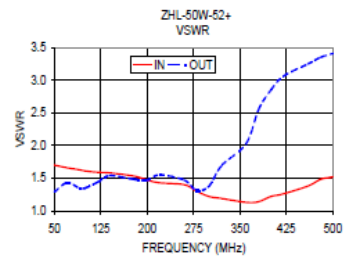
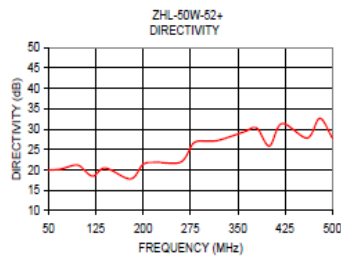
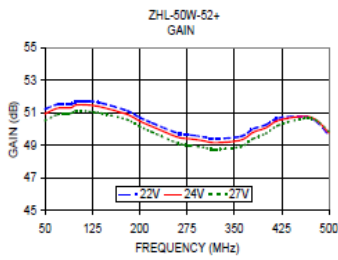
| A    | B      | C      | D      | E     | F     | G    | H | J    | K     | L     | M | N | P     | Q     | R      | S      | T    | wt                 |
|------|--------|--------|--------|-------|-------|------|---|------|-------|-------|---|---|-------|-------|--------|--------|------|--------------------|
| 0.85 | 7.3    | 6.3    | 6.00   | 1.00  | 3.75  | 1.18 | — | .25  | .63   | 1.00  | — | — | 3.25  | .5    | 6.00   | 5.1    | 1.35 | grams <sup>*</sup> |
| 25.0 | 186.42 | 160.02 | 152.40 | 25.40 | 95.25 | 3.30 | — | 6.35 | 16.00 | 25.16 | — | — | 82.55 | 12.70 | 152.40 | 129.54 | 3.43 | 4186               |

<sup>\*</sup>500 grams without heatsink

# Typical Performance Data/Curves

## ZHL-50W-52+ ZHL-50W-52

| FREQUENCY (MHz) | GAIN (dB) |       |       | DIRECTIVITY (dB) | VSWR (:1) |      | NOISE FIGURE (dB) | POUT at 1 dB COMP. (dBm) | IP3 (dBm) |
|-----------------|-----------|-------|-------|------------------|-----------|------|-------------------|--------------------------|-----------|
|                 | 22V       | 24V   | 27V   | 24V              | IN        | OUT  | 24V               | 24V                      | 24V       |
| 50.00           | 51.23     | 50.95 | 50.53 | 19.96            | 1.70      | 1.29 | 6.43              | 47.75                    | 56.86     |
| 70.00           | 51.53     | 51.29 | 50.90 | 20.24            | 1.66      | 1.43 | 5.92              | 47.79                    | 57.47     |
| 90.00           | 51.53     | 51.31 | 50.97 | 21.16            | 1.63      | 1.35 | 5.60              | 47.64                    | 57.96     |
| 100.00          | 51.69     | 51.49 | 51.14 | 20.95            | 1.61      | 1.35 | 5.46              | 48.16                    | 58.09     |
| 120.00          | 51.71     | 51.48 | 51.09 | 18.47            | 1.59      | 1.44 | 5.28              | 48.30                    | 58.55     |
| 140.00          | 51.60     | 51.35 | 50.98 | 20.47            | 1.58      | 1.54 | 5.15              | 48.01                    | 58.98     |
| 180.00          | 51.13     | 50.91 | 50.58 | 17.81            | 1.53      | 1.48 | 4.94              | 48.01                    | 57.84     |
| 200.00          | 50.72     | 50.50 | 50.17 | 21.37            | 1.47      | 1.47 | 4.95              | 48.40                    | 56.76     |
| 220.00          | 50.38     | 50.16 | 49.82 | 21.89            | 1.43      | 1.55 | 4.93              | 48.33                    | 55.23     |
| 260.00          | 49.76     | 49.52 | 49.14 | 21.96            | 1.40      | 1.47 | 4.98              | 47.98                    | 54.98     |
| 280.00          | 49.65     | 49.41 | 49.01 | 26.60            | 1.30      | 1.31 | 4.98              | 47.50                    | 54.77     |
| 300.00          | 49.54     | 49.30 | 48.89 | 27.07            | 1.22      | 1.38 | 4.98              | 47.00                    | 54.59     |
| 320.00          | 49.42     | 49.17 | 48.76 | 27.29            | 1.19      | 1.69 | 4.97              | 46.64                    | 54.59     |
| 360.00          | 49.56     | 49.33 | 48.93 | 29.37            | 1.13      | 2.03 | 5.07              | 46.97                    | 54.58     |
| 380.00          | 50.02     | 49.81 | 49.42 | 30.28            | 1.14      | 2.55 | 5.07              | 46.86                    | 54.44     |
| 400.00          | 50.27     | 50.09 | 49.74 | 25.88            | 1.22      | 2.85 | 5.14              | 46.50                    | 54.39     |
| 420.00          | 50.68     | 50.54 | 50.24 | 31.38            | 1.26      | 3.06 | 5.19              | 46.11                    | 54.28     |
| 460.00          | 50.79     | 50.79 | 50.66 | 27.85            | 1.38      | 3.25 | 5.26              | 45.79                    | 54.10     |
| 480.00          | 50.47     | 50.55 | 50.54 | 32.67            | 1.48      | 3.35 | 5.35              | 45.91                    | 54.15     |
| 500.00          | 49.62     | 49.77 | 49.84 | 27.81            | 1.52      | 3.41 | 5.47              | 45.95                    | 54.19     |



## Appendix E

### KU LNA 222 AH, Super Low Noise Amplifier 2200 ... 2400 MHz



#### Features

- Low noise figure
- High IP3
- Reverse polarity protection
- Solder pin for direct power supply
- Small mechanical dimensions
- Remote power supply via output connector

#### Applications

- Analog and digital transmission systems
- Measurement and laboratory equipment

#### Important notes

- Amplifier does not contain a coaxial relay!
- Maximum input power 1 mW

#### Technical specifications:

|                              |                             |
|------------------------------|-----------------------------|
| Frequency range              | 2200..2400 MHz              |
| Noise figure @ 18 °C         | typ. 0.5 dB, max. 0.6 dB NF |
| Gain                         | typ. 30 dB                  |
| Maximum input power          | 1 mW                        |
| Output IP3                   | typ. +27 dBm                |
| Supply voltage               | +9 ... 15 V DC              |
| Current consumption          | typ. 80 mA                  |
| Ambient temperature          | -20 ... +65 °C              |
| Input connector / impedance  | SMA-female, 50 ohms         |
| Output connector / impedance | SMA-female, 50 ohms         |
| Case                         | milled aluminium            |
| Dimensions (mm)              | 73 x 30 x 20                |
| Weight                       | 90 g (typ.)                 |

## Bibliography

- [1] E. S. Agency, "ESA Bulletin 111," August 2002. [Online]. Available: <http://esamultimedia.esa.int/multimedia/publications/ESA-Bulletin-111>. [Accessed 2015].
- [2] ESA, "Statement of Work for Phase C/D/E1 of the European Student Earth Orbiter (ESEO) Project," Noordwijk, 2012.
- [3] T. Uhlig, *Spacecraft Operations*, Wien: Springer, 2015.
- [4] ECSS-E-ST-70C *Space engineering: Ground systems and operations*, Noordwijk, The Netherlands: ESA - ESTEC Requirements and Standard Division, 2008.
- [5] M. D. D. Staff, "Small Spacecraft Technology State of the Art Ames Research Center," Moffett Field, 2014.
- [6] D. Modenini, M. Bosco, A. Locarini and P. Tortora, "Space Engineering and Small Satellites Educational Activities at University of Bologna," in *1st Symposium on Space Educational Activities*, Padua, 2015.
- [7] V. Fabbri and D. Bruzzi, "ESEO Consolidated Report on Mission Analysis," ALMASpace, Forlì, 2015.
- [8] W. Beech, D. Nielsen and J. Taylor, "AX.25 Amateur Packet-Radio Link-Layer Protocol," July 1998. [Online]. Available: [http://www.tapr.org/pub\\_ax25.html](http://www.tapr.org/pub_ax25.html). [Accessed 2015].
- [9] M. Bosco, "ESEO TM/TC Communication protocol," ALMASpace, Forlì, 2015.
- [10] A. Avanzi, "ESEO OBDH TMTC communication protocol," ALMASpace, Forlì, 2015.
- [11] O. Koudelka, "BRITE Constellation - A case study," in *ITU Symposium and Workshop on small satellite regulation and communication systems*, Prague, 2015.
- [12] F. Agaudo, D. Nodar and A. Gonzalez, "Preliminary noise measurements campaign carried out by HUMSAT-D during 2014," in *ITU Symposium and Workshop on small satellite regulation and communication systems*, Prague, 2015.
- [13] S. Busch, P. Bangert, S. Dombrovski and K. Schilling, "UWE-3, In-Orbit Performance and Lessons Learned of a Modular and Flexible Satellite Bus for Future Picosatellite Formations," in *65th International Astronautical Congress*, Toronto, 2014.
- [14] ECSS-E-ST-50-01C *Space data links - Telemetry synchronization and channel coding*, Noordwijk, The Netherlands: ESA - ESTEC Requirements and Standard Division, 2008.
- [15] ECSS-E-ST-50-03C *Space data links - Telemetry transfer frame protocol*, Noordwijk, The Netherlands: ESA - ESTEC Requirements and Standard Division, 2008.
- [16] B. Sklar, *Digital Communications: Fundamentals and Applications*, Tarzania, California: Prentice Hall, Second Edition.
- [17] M. Bosco and D. Cinarelli, "ESEO Space to Ground Interface Control Document," ALMASpace, Forlì, 2015.

- [18] R. Tubio-Pardavilla, A. Vazquez-Alvarez and J. Puig-Suari, "The SatNet Network: Open Source for sharing CubeSat Ground Stations," in *Small Satellite Systems and Services Symposium*, Majorca, Spain, 2014.
- [19] M. Bosco, "Ground Segment & Operations Requirements Document," ALMASpace, Forlì, 2015.
- [20] R. L. Buffington, C. J. Kief and R. S. Erwin, "GENSO, SPA, SDR, and GNURadio: The Pathway Ahead for Space Dial Tone," *American Institute of Aeronautics and Astronautics*, pp. 1-10.
- [21] A. Gulati and S. Chavan, "IITMSAT Communications System - A LeanSat Design Approach," in *3rd IAA Conference on University Satellite Missions and CubeSat Workshop*, Rome, 2015.
- [22] "GNURadio," [Online]. Available: <http://gnuradio.org/redmine/projects/gnuradio/wiki>. [Accessed 2015].
- [23] F. Ge, C. J. Chiang, Y. M. Gottlieb and R. Chadha, "GNU Radio-based digital communications: computational analysis of a GMSK transceiver," in *Global Telecommunications Conference (GLOBECOM)*, 2011.
- [24] M. Bosco, D. Cinarelli and P. Tortora, "Alma Mater Ground Station Transceiver: a Software Defined Radio for Satellite Communications," in *1st IEEE Workshop on Metrology for Aerospace*, Benevento, Italy, 2014.
- [25] N. Instruments, "An Introduction to Software Defined Radio," 2013. [Online]. Available: [ftp://ftp.ni.com/pub/events/campus\\_workshop/niusrp\\_hands\\_on\\_sp\\_manual.pdf](ftp://ftp.ni.com/pub/events/campus_workshop/niusrp_hands_on_sp_manual.pdf). [Accessed 2015].
- [26] T. Instruments, "CC1020 Low-Power RF Transceiver for Narrowband Systems," 2015. [Online]. Available: <http://www.ti.com/lit/ds/swrs046h/swrs046h.pdf>. [Accessed 2015].
- [27] D. Cinarelli, "ESEO TMTC Subsystem Design Definition File," ALMASpace, Forlì, 2015.
- [28] A. Avanzi and V. Fabbri, "ESEO OBDH HK and TC description," ALMASpace, Forlì, 2015.
- [29] M. Bosco, "ESEO Ground Segment Database," ALMASpace, Forlì, 2015.
- [30] M. Bosco, "ESEO Satellite Operations Handbook," ALMASpace, Forlì, 2015.
- [31] "EUTELSAT Procedure Style Guide," Cloudbridge Engineers Ltd., England, 2002.
- [32] A. Lucci, "Design and Implementation of the ESEO Spacecraft Simulator," University of Bologna, Forlì, 2015.
- [33] A. Lucci, "Design and implementation of the ESEO spacecraft simulator," University of Bologna, Forlì, 2015.
- [34] M. Elson, "CHART-core Design Document," EUMETSAT, Darmstadt, 2014.
- [35] M. Elson, "GSAR Initial Design and Planning," EUMETSAT, Darmstadt, 2014.
- [36] C. Peat, "Satmon Client User Guide," EUMETSAT, Darmstadt, 2013.
- [37] M. Bosco, "GSAR Reports Development Guide," EUMETSAT, Darmstadt, 2015.

- [38] B. Rhodes, “PyEphem,” [Online]. Available: <http://rhodesmill.org/pyephem>. [Accessed 2015].
- [39] M. Raspaud, “pyorbital,” [Online]. Available: <http://github.com/pytroll/pyorbital>. [Accessed 2015].
- [40] R. T. Pardavilla, “SATNet - Satellites Network,” [Online]. Available: <https://github.com/satnet-project>. [Accessed 2015].
- [41] I. Charitopoulos, “SatNOGS,” [Online]. Available: <https://satnogs.org/>. [Accessed 2015].
- [42] T. S. Kelso, “CelesTrack,” [Online]. Available: <https://celestrak.com>. [Accessed 2015].
- [43] EUMETSAT, “Metop-A and Metop-B Two Line Elements,” [Online]. Available: <http://oiswww.eumetsat.org/metopTLEs/html/index.htm>. [Accessed 2015].
- [44] M. Smith, “Ground Station Centralised High Level M&C ICD,” EUMETSAT, Darmstadt, 2015.
- [45] M. Smith, “Device Simulator Requirements,” EUMETSAT, Darmstadt, 2013.
- [46] M. Bosco, “Ground Station Centralised M&C Simulator User Guide,” EUMETSAT, Darmstadt, 2015.
- [47] M. Bosco and P. Tortora, “ESEO Ground Segment Software Solutions: Design, Implementation and Testing,” in *3rd IAA Conference on University Satellite Missions and Cubesat Workshop*, Rome, 2015.

## Acknowledgments

At the end of my PhD thesis, I would like to thank all those people who made this work possible and a learning experience of great value.

Foremost, I would like to express my sincere gratitude to my supervisor Prof. Paolo Tortora for giving me the chance to attend this PhD course and be fully involved in a very exciting microsatellite project (ESEO). The importance of this international project helped me to gain experience and improve my knowledge in space engineering. I also really appreciate the opportunity he gave me to attend some interesting workshops and to do two internships which greatly contributed to my professional growth.

My very sincere thanks also goes to my supervisor at EUMETSAT Dr. Thomas Sheasby and Iñigo Madurga for following me during the internship and giving me the opportunity to work on ground station operations. In the framework of the internship, I would also thank Sean Burns, head of Realtime Services and System Operations Division, Chiara Cocchiara for having made the internship possible and all my other colleagues at EUMETSAT.

I would also thank Etienne Tilmans, PROBA mission operations engineer, and Daniele Galardini, head of ESA Redu Centre for giving me the opportunity to study the PROBA mission control centre and take inspiration for the design of the ESEO mission control centre.

I thank my fellow labmates Dr. Dario Modenini and Alfredo Locarini and the SITAEEL personnel for the fruitful collaboration within the ESEO project.

Last but not least, I would like to thank my parents for supporting me during these years of study and my girlfriend Francesca Paolini for the nice moments we have been spending.